FLEXURAL PROPERTIES AND CHARACTERIZATION OF GEOPOLYMER

BASED SANDWICH COMPOSITE STRUCTURES AT ROOM AND ELEVATED

TEMPERATURES

by

MILAN SIMONOVIC

A thesis submitted to the

Graduate School - New Brunswick

Rutgers, The State University of New Jersey

in partial fulfillment of the requirements

for the degree of

Master of Science

Graduate Program in Mechanical and Aerospace Engineering

written under the direction of

Professor Assimina A. Pelegri

and approved by

_____

_____

_____

New Brunswick, New Jersey

May, 2007

ABSTRACT OF THE THESIS

Flexural Properties and Characterization of Geopolymer Based Sandwich Composite

Structures at Room and Elevated Temperatures

by MILAN SIMONOVIC

Thesis Director:

Professor Assimina A. Pelegri

This thesis is an experimental study on structural changes and change of the
mechanical properties of geopolymer-based sandwich structures. Specimens were
prepared combining a potassium aluminosilicate geopolymer base, perlite filler and three
different mass ratios of cenosphere material. Prepared specimens were left to age for
four weeks at room temperature, before a reinforcing skin layer was added. The
reinforcing layer was produced with one or two tows of ceramic or carbon fibers.
Samples were divided into several groups and exposed to different temperatures: from
room to one-hour exposure at 750°C. After temperature treatments, the samples were
subjected to a three-point bending test and flexural properties were determined. SEM
microscopy was used to examine the following features: contact properties between the
geopolymer base and fillers, adhesion between the reinforcement fibers and core and
micro structural changes in material caused by high temperature and loading conditions.

It was determined that adhesion among the geopolymer material, fillers and fibers was very good. Cracks, which appeared after temperature treatment and flexural tests, usually progressed through lower-density areas (like undamaged perlite particles, voids or other imperfections) and higher-porosity areas of the geopolymer cenosphere mixture. The flexural strength of unreinforced samples was low (between 1-12 MPa). It was determined that thermally treated samples show a drastic decrease (60-65%) in residual flexural properties. After temperature treatment, significant sample deformation was observed. The SEM revealed that micro structural changes were significant, including increase in pore size, volume expansion, cracking and perlite and geopolymer material expansion. It was noticed that the maximum strength of sandwich structures falls with an increase of cenosphere mass ratio, but flexibility and material toughness increase. Tensile failure of the bottom reinforcing layer was the primary failing mechanism for the majority of tested samples. During thermal exposure, some samples experienced severe cracking and deformation, which caused premature (tensile) failures and other failure types (like core shear). It was concluded that the thermal stability of the tested material and structures was inadequate, that structural applications would not be recommended and that refractory applications would be limited.

ACKNOWLEDGMENTS

friendliness, sense of humor, understanding and support. Vasilije, Marcis, Jeffrey, Lucian, Kemal … thanks guys.

Most of all I would like to thank my family for their patience and continuous support. Especially, I want to thank my wife Jelena for having an unbelievable amount of support, patience and positive energy that kept me going through good and bad. На крају пар речи за моје најближе: Јелена, Исидора, Растко ви сте моје све на свету. Много вас воли тата.

I am dedicating this thesis to my family: Isidora, Rastko and Jelena.

TABLE OF CONTENTS

LIST OF TABLES

LIST OF ILLUSTRATIONS

CHAPTER 1 - INTRODUCTION

1.1 Problem statement

Sandwich structures are generally constructed out of weaker core material and two stronger, reinforcing "skin" layers on the top and bottom surfaces. That type of structure combines good mechanical properties and high stiffness with low weight ratios. The advantage of sandwich structures (as of any composite material) is that they can be specially engineered to give the best performance for specific kind of loads and applications. Today, the majority of sandwich composites are manufactured out of organic polymers (epoxy, polyester, vinyl ester, phenolic and other organic resins) that can provide excellent mechanical properties; have great applicability and are easy to manufacture, but their usage can be limited by inadequate performance at high temperatures and flame-exposed conditions [1]. Organic materials are susceptible to combustion and mechanical properties of average organic composites rapidly deteriorate at higher temperatures (sometimes as low as 100°C), which limits their applicability as structural carrying members in cases of high temperature or flame conditions [2]. When exposed to carbohydrate fire, organic polymer composites can light up easily and quickly; they can burn vigorously, generating additional heat and toxic fumes and finally, as a result of high temperature exposure, they can fail mechanically [3]. These properties of organic composites can be very dangerous when fire occurs in confined spaces such as tall buildings, airplanes, cars, trains and ships [4]. In cases of high-intensity hydrocarbon flames, temperature changes very quickly and inadequately designed composite materials

and structures can ignite very quickly. The amount of toxic fumes and the speed of fire progression can severely decrease an occupant's probability of survival [5]. Knowledge of the thermo-mechanical performances of materials is essential for the optimum design of protection and evacuation systems. When organic composites are exposed to the high temperature or flame conditions the initial temperature increase occurs due to transient heat conduction [6]. During this period the material does not experience any chemical reactions. But when temperatures reach 200-300°C, depending on heating rate and material composition, a chemical reaction called pyrolysis may start. At this point, material goes through chemical decomposition and various residues and gaseous products such as carbon monoxide, carbon dioxide, hydrogen, nitrogen or methane are formed. In a few minutes the heat release rate reaches its highest levels. As pyrolysis advances deeper, material properties decline and they will lead to mechanical failure [7]. This problem can be avoided or minimized by using different structural design or usage of different types of composite fibers or matrices. Application of novel inorganic matrices can improve material or structural fire resistance and increase the survivability rate in confined areas. Flexural mechanical properties will be examined and the influence of temperature on general properties and material microstructure will be tested.

1.2 Introduction to geopolymer

In the late seventies scientist J. Davidovits focused his research on a new type of inorganic polymers. The term "geopolymer" was used because the new synthetic materials were similar to minerals that are formed in the Earth's crust [8]. Similarities in

synthesis conditions between zeolite and feldspathoide minerals and new geopolymeric materials were noted, but the new aluminosilicate materials had an amorphous structure, in contrast to crystalline structure of zeolite and feldspathoides. These amorphous polymeric materials are named polysialates and can be represented with the empirical formula:

$$M_n \{-(S_iO_2)_z - AlO_2\}_n \, wH_2O$$
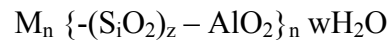
In the previous formula M is a cation (such as potassium, sodium or calcium); n is a degree of polycondensation; z is 1, 2 or 3 (number of Si/Al ratios). The sialate network consists of SiO_4 and AlO_4 tetrahedra linked and alternately sharing all the oxygen. Positive ions (Na^+, K^+, Ca^{++} etc.) have to be present in the framework cavity to balance the negative charge of Al_3^+ in IV-fold coordination [9]. The governing mechanism that defines geopolymers is the process of gel-sol transformation or the hardening process of silicate solution. When aluminosilicate (silica-alumina oxide mixture) mineral is immersed in silicate (alkali silicates) solution, a reaction of dissolution and copolymerization forms: polysialates -MPS- (-Si-O-Al-O-), polysialate-siloxo -MPSS- (-Si-O-Al-O-Si-O-) and polysialate-disiloxo -MPSDS- (-Si-O-Al-O-Si-O-Si-O-). Polysialates are chain and ring polymers with Si^{4+} and Al^{3+} in IV-fold coordination with oxygen and range from amorphous to semicristaline [10]. Certain geopolymer resins comprise a geopolymeric network made of polysialate-disiloxo associated with the molecular silicon oxide SiO_2 embedded within the matrix. The trapped molecular SiO_2 yields a low-porosity, highly packed microstructure with higher density. Physical

properties of geopolymers, such as fusion temperature and CTE, are a function of the Si/Al ratio. CTE values measured for geopolymers are those of resins, without any additional filler. In the case of PSDS formulations, CTE values increase with the amount of the molecular silicon oxide SiO_2 packed inside the geopolymeric tri-dimensional network. The exact chemical process behind dissolution and gel formation reactions in geopolymeric systems is still not completely explained, so several different authors have presented their view of this geopolymerization process [11], [12]. Geopolymers are amorphous polymers, but because of their mineral (inorganic) origin, they are hard and weather-resistant and can sustain being exposed to high temperatures [13]. Experiments on geopolymers' thermal properties by Davidovits et al. [9] and by Barbosa and MacKenzie [14] concluded that geopolymers can show very high thermal stability up to 1200-1400°C. In these experiments, materials were prepared using sodium silicate, potassium silicate and metacaolin.

An interesting property of geopolymers is that by using the process of alkaline activation, certain waste materials or byproducts can be used for geopolymer manufacturing [15]. By using adequate chemical process conditions, these waste materials can be transformed from glassy structures (partially or totally amorphous) into very compact, well-cemented composites [16], [17]. That opens the possibility of using various inorganic waste materials like fly ash, cenospheres or (granulated) furnace blast slag [18].

1.3 Why fly ash

Fly ash is a byproduct of coal burning in power plants. This fine powder is made out of hollow spherical particles, whose chemical composition (Mullite, Crystalline Silica - Quartz and Glass Oxide) provides good chemical stability and promising high temperature properties, including low expansion and good insulating capabilities [19]. Huge amounts of fly ash are generated every day as a result of energy demand and usually that material is disposed into landfills. Disposing such a huge amount of waste into the landfills represents an environmental hazard and big problem for the future. Landfills are not endless and possibility of pollution is also emerging: some types of fly ash contain heavy metals like nickel, vanadium, cadmium, molybdenum, arsenic, lead, and radium) [20]. Ways have to be found to properly utilize this type of material [21]. In the last twenty years, several countries started to utilize fly ash as additive to cement and concrete in civil industry. Special types of lightweight, high-strength concrete were manufactured and in general it is determined that using fly ash (or fly ash components like cenospheres) as a fine aggregate can decrease the density of concrete with minor or no loss in strength [22]. Thermal and sound insulating properties were usually connected to the concrete density and they can be improved by using a certain ratio of fly ash [23]. The correlation between mechanical properties of concrete manufactured with cenospheres and loss of water and humidity changes were analyzed in [24]. Civil industry is still the largest user of fly ash products since there are a wide number of applications where fly ash can be used. But there is a fundamental difference between fly ash use in geopolymeric materials and in lightweight concrete. In geopolymers, cenospheres are among the active components that are a part of the complicated chemical

reaction that transforms glassy structure into cementitious material [25]. In concrete applications, fly ash is used as supplementary cementitious material and as a substitutefor other fine aggregates [26].

1.4 Fly ash application in new geopolymer based composites

The majority of research on the aggregates for geopolymer usage is based on the usage of fly ash, usually class F, a byproduct of Lignite coal burning. Several authors performed detailed experiments with geopolymer fly ash combination to determine and explain: the effect of using different types of fly ash [27], [28], different curing techniques and to test properties of new material in harsh conditions (such as high temperature and chemically aggressive environment) [29]. Preliminary data showed that the chemical composition of fly ash in combination with the proper agent could produce materials that are thermally stable, have a low coefficient of thermal expansion and have good insulating capabilities [30]. But due to an absence of precise manufacturing standards and varying quality of used components, general properties of manufactured materials were different. In some cases, properties, values and conclusions were almost completely opposite [31] [28]. Small differences in the quality of used components will cause huge differences in the properties of the final product. This presents a potential problem: since manufacturing technology is not standardized yet, repeatability and reproducibility of obtained results is low. But if standardized manufacturing procedure is followed and chemical components of equal quality are used, it would be possible to produce material that will, if exposed to certain conditions, react in an expected, adequate

way. By following standardized procedures and establishing a manufacturing model to develop generic base material, products with specific properties can be manufactured just by optimizing the base mix [32], [33].

One of the most exciting properties of geopolymeric composites is their inability to burn. If exposed to flame, geopolymers will not burn; they will not generate excess heat [34]; they will not generate almost any smoke and when certain levels of temperature are reached, they will usually just melt [14]. Geopolymeric materials are also pretty good heat and sound insulators in comparison to concrete based structures [30]. These properties make usage of geopolymer composites very interesting, especially when compared to modern organic polymer-based composites, which are very susceptible to flame [35]. But in comparison to the modern organic composites, geopolymeric materials don't have very good mechanical properties.

1.5 Research objective

Previous research has revealed that mechanical properties of geopolymeric materials (at this level of manufacturing technology) are inconsistent and are not reliable or good enough for modern structural application [31]. Gain from refractory and fire resistance, cheap component materials and a relatively simple manufacturing process still cannot outweigh the low strength and inconsistency problems [27]. Because of that, sandwich structures are produced. It has to be determined if an engineered geopolymer sandwich structure can provide level of strength and results that are consistent and good enough for structural applications.

The basic idea behind this research is to prepare a composite sandwich structure that has a geopolymer core and fibrous reinforcing skin. The geopolymer core will be manufactured using cenospheres as active component and reinforced with two types of inorganic, fire-resistant fibers to improve structure mechanical properties. By adding skin reinforcements, general mechanical, flexural properties are expected to improve, with only minor structural weight increase. We need to investigate flexural and mechanical properties of geopolymeric samples before and after exposure to high temperatures.

The objectives of this research are:

- To prepare several series of geopolymer base material made with different cenosphere mass ratios.

- Look for micro structural and mechanical difference between different cenosphere mass ratio groups.

- Evaluate the influence of different curing methods on sample general material properties. Determine any aging effects on material properties.

- Prepare sandwich structures by adding fibrous reinforcing skin.

- Expose selected samples to open flame conditions for 30 minutes and analyze the effects of flame on material structure.

- Expose selected samples to high temperature oven cycles and analyze temperature effects.

- Perform three-point bending flexural test, for all samples and compare results for the thermally treated and untreated sample groups.

- Evaluate the influence of high temperature and open flame conditions on the material inner structure and mechanical properties of sandwich structures.

- Using SEM, examine the material microstructure and changes caused by high temperature cycles, flame exposure and loading conditions.

- Determine the effects of flame exposure and temperature cycles on interaction between the geopolymer core and reinforcing skin.

- Observe the reaction between the fiber and geopolymer protective layer during and after high temperature treatment and analyze the effects of the geopolymer bonding agent.

- Analyze the collected data and give an opinion on possible structural, thermal insulating or fire-refractory applications.

CHAPTER 2 – MATERIALS

All samples used in this study are manufactured from geopolymeric composite material used as a core and fiber-geopolymer combination as reinforcing skin. The following materials were used:

- Geopolymer - Two component chemical system that consists of amber-colored potassium silicate solution (component A) and very fine white silica powder (component B).

- Cenospheres - Obtained from Sphere Services Inc. The Cenosphere Company Type SG-300 Recyclospheres^{TM}.

- Granulated expanded Perlite.

- Alkaline activator or curing agent.

- 3M^{TM} - NEXTEL^{TM} 610 ceramic fibers 10,000 denier tows.

- MITSUBISHI CHEMICALS DIALEAD® Carbon fibers 12,000 denier tows.

- 3M^{TM} - Zeeosphere^{TM} W-210 White Ceramic Microspheres.

2.1 Geopolymer

Geopolymer materials are described as inorganic polymer, a polysialate, derived from the natural geological materials silica and alumina, hence the name *geo-polymer* [36]. Geopolymerization is a geosynthesis (a reaction that chemically integrates minerals) that involves naturally occurring silica-aluminates. The silicon (Si) and

aluminum (Al) atoms react to form molecules that are chemically and structurally comparable to those binding natural rock. From the chemical point of view, the most important factor is the silica content [37]. Silica is the main constituent of the structural skeleton of the reaction product formed in the alkaline activation of the ashes. The reactive silicates of the ashes are dissolved under highly alkaline conditions, yielding polymeric Si–O–Al bonds. This main reaction product is an aluminosilicate gel that can be considered a zeolite precursor. It is the main factor responsible for the mechanical properties of this type of binder. It means that high reactive silica content involves the formation of a high amount of alkaline aluminosilicate gel and consequently a high mechanical strength is developed in the resulting material. In our case, a two-component chemical system is used as a basic material for the preparation of all geopolymer samples:

- Amber colored potassium silicate solution (component A).
- A very fine amorphous silica powder (component B).

When mixed together, the components make highly alkaline slurry. Later various ratios of cenospheres and perlite filler are added, mixed and poured in molds.

2.2 Cenospheres

The cenosphres used in research are Recyclospheres™, product of Sphere Services Inc. Cenospheres are lightweight, strong, hollow, inert spheres mainly composed of silica and alumina and filled with air, carbon dioxide and nitrogen gases. Cenospheres are naturally occurring by-product of the coal burning process at power

plants. The process of burning coal in thermal power plants produces fly ash containing ceramic particles made largely out of alumina and silica. These particles form only part of the total fly ash quantity produced in the burning process. They are produced through a complicated chemical and physical transformation at high temperatures between 1500 and 1750°C. The color of cenospheres varies from gray to almost white and their density is (due to the hollow structure) about 0.4 to 0.8 [g/cm^3], which gives them a great buoyancy. When waste fly ash is disposed of by means of settlement pools, cenospheres float and gather on the surface and are known as "floaters" [38]. Their chemical composition and structure varies considerably depending on the composition of coal from which they were generated. The ceramic particles in fly ash have three types of structures. The first type of particles are solid and called the precipitator. The second type is hollow particles called cenospheres. The third type is called plerospheres, which are hollow particles of large diameter filled with smaller precipitator and cenosphere particles [20], [39].

2.2.1 Using cenospheres - benefits

The spherical shape of cenospheres improves the flowability of the cementitious base in most applications and provides a more even distribution of the filler material (if we look at concrete or similar materials). The natural properties of cenospheres make it possible to use them either in dry or wet slurry form. Cenospheres are easy to handle and provide a low surface area-to-volume ratio. Cenospheres are 75% lighter than other minerals currently used as a filler or extender and are 30% lighter than most resins. They

are strong enough to be used as a substitute or additive to other fillers. Since they are by-products, utilization of cenospheres reduces the cost of raw materials.

The savings may be recognized in one or more of the following benefits:

- Reduced resin demand

- Resistance to resin absorption.

- Improved flowability.

- Reduction in the weight of the finished product.

- Improved thermal and acoustic insulation values.

Cenospheres can improve finished products by improving strength, durability and by reducing weight. Cenospheres also provide added buoyancy and better thermal and sound-insulating properties. Their spherical shape may improve product stability and increase resistance to impact. Used in the production of insulating materials, cenospheres better control both sound values and thermal conductivity. Cenospheres are hard and rigid, light, waterproof, safe and insulative. This makes them highly useful in a variety of products, notably fillers. Cenospheres are now used as fillers in the cement and concrete industry to produce low-density concrete. Usage of cenospheres can also decrease pressure on landfills, since material that used to be dumped in landfills now can be recycled and used for beneficial purposes. The chemically inert properties of cenospheres make them 100% recyclable [40]. The chemical composition of cenospheres makes them a good candidate for usage as active ingredients in other applications like geopolymerization.

2.2.2 Cenospheres - material data sheet

- Silica as SiO_2 : 55-65%

- Aluminium as Al_2O_3 : 25-35%

- Iron Oxide as Fe_2O_3 : 1-5%

- Potassium as K_2O : 0.5-2%

- Calcium as CaO : 0-2%

- Magnesium as MgO : 0-2%

- Titanium as TiO_2 : 0-2%

- Sodium as Na_2O : 0-2%

- Trapped Gas: Carbon Dioxide : 65-75% and Nitrogen : 25-35%

Physical properties:

- Particle size: 10 - 300μm; mean particle size 140 [μm] (micrometers or microns)

- Average particle density: 0.6 - 0.85 [g/cm^3]

- Bulk density: 0.30 - 0.40 [g/cm^3]

- Appearance: odorless, low density fine powder; color: light gray / off white

- Softening temperature: 1470°C

- Loss on ignition: < 2%

- Moisture content: 1.0% max.

- Crush strength: 24.1317 - 34.4748 [MPa] (3500 - 5000 psi)

- Average wall thickness: 10% diameter

- pH in water: 6.5 - 7.5

- Thermal conductivity (general data): 0.08 - 0.3 [W/mK]

- Hardness (general data): ~5 (Moh scale)

2.3 Perlite

Perlite is an amorphous form of siliceous volcanic glass that has relatively high water content. Since perlite is a form of natural glass, it is classified as chemically inert and has a pH of approximately 7. Due to its glassy structure and high SiO_2 and Al_2O_3 contents, perlite is a pozzolan [41]. Pozzolana is a siliceous and aluminous material, which reacts with calcium hydroxide in the presence of water to form compounds possessing cementitious properties at room temperature (cementitious materials set and harden in the presence of water). Perlite is available in different forms: coarse, crushed, expanded, fine etc. Due to its high water content, when the coarse form is heated to a temperature of about 900°C, trapped water vaporizes, creating small bubbles in glassy particles causing the structure volume increase of 7 to 15 times. The expanded material is white due to the reflectivity of the trapped bubbles; bulk density of expanded perlite can range from 30 to 240 $[kg/m^3]$. By further processing, expanded perlite particles can be crushed into glass flake form with an interlocking three-dimensional structure. This 3-D structure can help reduce shrinking or dimensional changes caused by drying or curing [42]. These perlite forms are mainly used in water-based construction compounds, concrete, plaster or resin-based systems. Perlite is soluble in certain environments (such as highly alkaline solutions) and this property can increase the level of chemical interaction and connection between the filler and base component (pozzolanic effect).

2.3.1 Perlite - benefits

Because of its excellent insulating characteristics and low weight, it is widely used as loose-fill insulation in masonry construction. In addition to providing thermal

insulation, perlite enhances fire ratings and reduces noise transmission [42]. Perlite is also ideal for insulating low-temperature and cryogenic vessels. This same heat resistant property is taken advantage of when perlite is used in the manufacturing of refractory bricks, mortars, and pipe insulation. When perlite is used as an aggregate in concrete, a lightweight, fire resistant, insulating concrete is produced that is ideal for roof decks and other applications [43]. Perlite can also be used as an aggregate in Portland cement and gypsum plasters for exterior applications and for the fire-protection of beams and columns. Industrial applications for perlite are the most diverse, ranging from high-performance fillers for plastics to cement for petroleum, water and geothermal wells. In our case perlite was chosen as volume filler. Good thermal properties, low density and chemical compatibility were ideal to combine with a geopolymer core.

2.3.2 Perlite - material data sheet

Perlite crystals - typical chemical composition:

- Silicon dioxide SiO_2 : 70-75%

- Aluminium oxide Al_2O_3 : 12-15%

- Sodium oxide: Na_2O : 3-4%

- Potassium oxide: K_2O : 3-5%

- Iron oxide: Fe_2O_3 : 0.5-2%

- Magnesium oxide MgO : 0.2-0.7%

- Calcium oxide: CaO : 0.5-1.5%

Physical properties:

- Color: white

- Free moisture: 0.5% max.

- Loss on ignition (chemical / combined water): 3-5%

- pH: 6.5-8

- Bulk density: 30 – 250 [kg/ m^3]

- Softening point: 880 - 1100°C

- Fusion point: 1260 - 1350°C

- Specific heat: 387 [J/kgK]

- Thermal conductivity (at room temperature): 0.04 – 0.06 [W/mK]

- Solubility:

  - Soluble in hot concentrated alkali and HF (hydrofluoric) acid

  - Moderately soluble (<10%) in NaOH (sodium hydroxide)

  - Slightly soluble (<3%) in mineral acids, water or weak acids (<1%)

2.4 3M^{TM} - NEXTEL^{TM} 610 ceramic fibers (10K denier tow)

NEXTEL^{TM} 610 ceramic fibers are noted for their outstanding single filament tensile properties. The family of Nextel™ Fibers 312, 440 and 550 are designed for non-structural applications where their primary purpose is to insulate or to act as a flame barrier. Nextel™ Fibers 610 (and 720) are composite grade fibers designed for load-bearing applications in metal, ceramic, and polymer matrices. Some industrial fibers, (Nextel™ Fiber 312 and 440) are made from Al_2O_3, SiO_2, and B_2O_3 at varying percentages. These fibers have both crystalline and glassy phases. The glassy phase helps the fiber retain strength after exposure to high temperatures. However, the glassy

phase also weakens the fiber when stressed at high temperatures. Composite grade fibers, Nextel™ Fibers 610 have more refined crystal structures based on alpha-Al_2O_3 and do not contain any glassy phases. This allows them to retain strength in higher temperatures than other industrial fibers [44] - Figure 1. The Nextel™ Fiber 610 has essentially a single-phase composition of alpha - Al_2O_3.
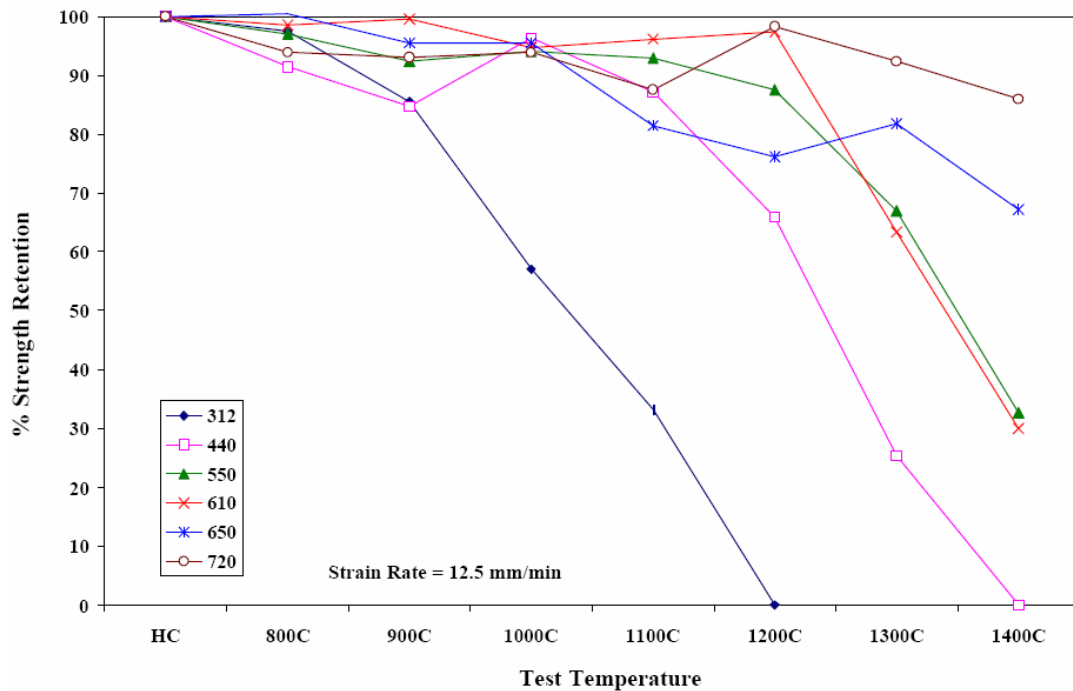
Figure 1: Comparison of relative tensile strength retention of multi-filament strands at elevated temperature

The Nextel™ Fiber 720, which is alpha-Al_2O_3 with SiO_2 added (forming alpha-Al_2O_3/mullite), has better strength retention and lower creep. 3M™ Nextel™ Fabric 610 is >99% alumina and offers the highest strength of all Nextel™ fibers [45] - Figure 2. High strength makes Nextel™ Fibers and Fabric 610 ideal for polymer, metal and lower-

temperature ceramic matrix composites used in industrial, aerospace and automotive applications.
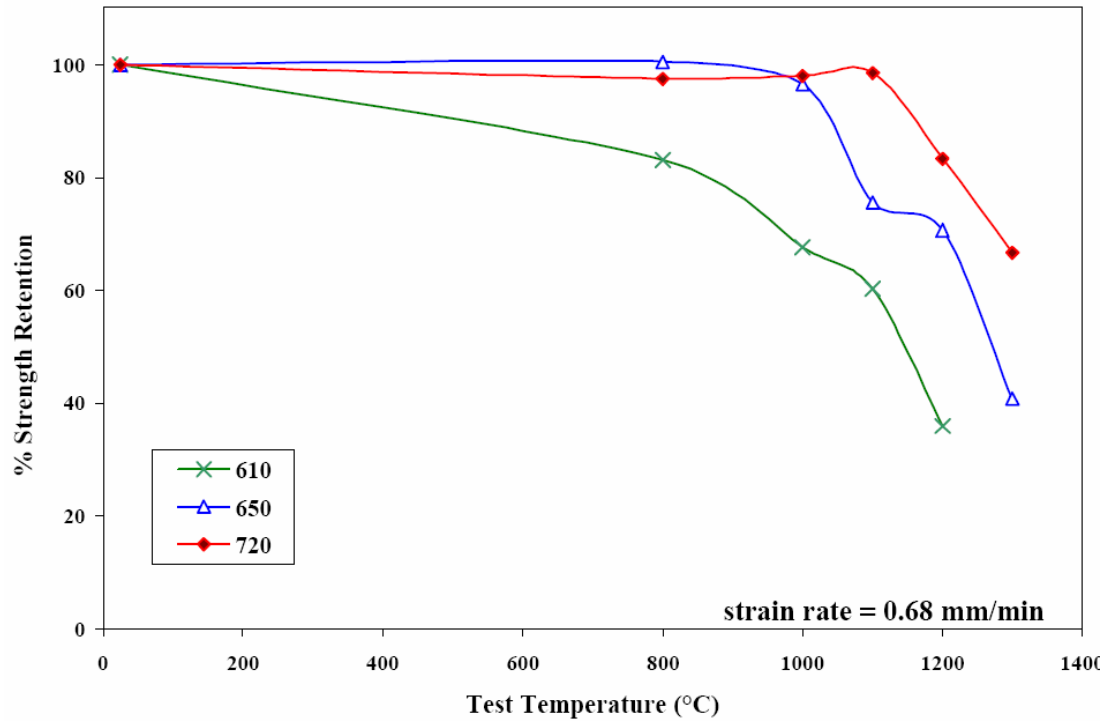
Figure 2: Comparison of relative tensile strength retention of single filaments of Nextel 610, 650 and 720 fibers at elevated temperature

A possible alternative to 610 was fiber type composed of 85% alumina and 15% silica, which offers the lowest creep of any Nextel™ Fiber at temperatures up to 1150°C (2102°F) [44]. This makes the fiber or fabric suited for load-bearing ceramic matrix composites used in industrial, aerospace and automotive applications. Ceramic oxide fibers should have excellent thermal shock resistance, due to their ability to move relative to one another and by doing so, relieve thermo mechanical stress. The Nextel 610 fiber has high strength (3.3 GPa,) Weibull modulus (m=11) and excellent thermo chemical

stability provided by its ultra-fine grained, single-phase a-Al_2O_3 microstructure. It maintains excellent high-temperature strength and resists creep temperatures up to 1000°C. The fiber surface is smooth and non-porous so water absorption is very low. Roving denier: filament count 10K denier has 2600 filaments. Fibers have low shrinkage, less than 3% after 15 hours at 1200°C [46].

2.4.1 NEXTEL 610 fibers - material data sheet

- Filament Tensile Strength: 2930 [MPa].

- Filament Tensile Modulus: 373 [GPa].

- Density: 3.88 [g/cm^3].

- Number of filaments: 2600 (10K denier).

- Filament diameter: 11 [μm].

- Thermal expansion (100-1100°C): 7.9 [ppm/°C]

- Composition:

    ➢ Al_2O_3 >99%

    ➢ SiO_2 0.2-0.3%

    ➢ Fe_2O_3 0.4-0.7%

2.5 MITSUBISHI CHEMICALS DIALEAD® carbon fibers (12K denier tow)

DIALEAD® fibers are high performance, coal tar pitch-based carbon fibers and in this research type: K63712, 12K denier tow with no chemical sizing (no coating) was used. A "carbon fiber" is a carbon-based fibrous material that has a micro graphite

crystal structure. It is made by fibrillation of acrylic resin or from oil or coal pitch by applying a special heat treatment. Carbon fibers are classified into three groups: PAN-based, pitch-based and rayon-based group. PAN Type carbon fibers are produced by carbonization of PAN precursor (Polyacrylonitrile). PAN type fibers have a high tensile strength and high elastic modulus and can be extensively used for the manufacturing of structural composites in aerospace and industrial fields. They can also be used for sport equipments manufacturing or in any field where high strength-to-weight ratios are required [47]. Pitch Type carbon fibers are produced by carbonization of oil or coal pitch precursor. They can be specialty engineered to have wide range of properties from low to ultra high elastic modulus. Fibers with ultra high elastic modulus are specially used in high stiffness components; others can be used in such way to utilize some of the other particular properties like high thermal or electric conductivity.

In general, carbon fibers are: lightweight, strong, durable, have high specific tensile strength and elastic modulus, etc. They have attractive properties like heat resistance, electric conductivity, high heat conductivity, low thermal expansion coefficient and good dimensional stability and mechanical properties, even at high temperatures. Carbon fibers are chemically stable; they don't react with any agent except with strong oxidizers. They are not susceptible to ignition (no flash point) and when exposed to temperatures higher than 400°C, they oxidize or burn (but only in the presence of external fuel) [48].

2.5.1 DIALEAD® type K63712 fibers - material data sheet:

- Tensile strength: 2600 [MPa] (380 Ksi).

- Tensile modulus: 640 [GPa] (92 Msi)

- Ultimate elongation: 0.4%.

- Yield: 2000 g/1000m (250 yard/lb).

- Density: 2.12 [g/cm^3].

- Thermal conductivity: 140 [W/mK]

- Number of filaments: 10K (12 K denier tow)

- Filament Diameter: 11 [μm]

- Carbon Content: over 99%

2.6 3M^{TM} Zeeospheres^{TM} - Ceramic Micro Spheres type W-210

Zeeospheres are strong, hard, thick walled, hollow white spheres with particle size in range between 0.3 and 12 [μm]. This kind of material is usually used as additive or filler and in our case we will use this material to prepare geopolimeric bond or glue for fibrous skin reinforcement. This material offers a variety of benefits to various applications:

- As filler it can increase the viscosity and flow of basic material.

- It can improve chemical inertness, corrosion resistance and stability.

- It can also improve hardness, abrasion and temperature resistance.

Typical material properties follow:

- Composition: alkali aluminosilicate ceramic

- True density: 2.4 [g/cm^3]

- Bulk density: 1.5 [g/ cm^3]

- pH value: 9-12

- Hardness: 6 (Moh's scale)

- Softening point: 1020°C

CHAPTER 3 - SPECIMEN PREPARATION

3.1 Sandwich core preparation

Since there is no standard that specifically deals with this kind of experiment, specimen geometry and size was chosen in accordance with ASTM standards: C393, C1341 and C1211. The core for all samples was prepared out of a two-component geopolymer system, cenospheres and granulated perlite particles. Reinforcing skin for the sandwich was prepared out of one or two tows of reinforcing fibers and a geopolymer bonding agent. Three basic groups of samples, with different relative mass ratios of cenospheres to geopolymer components, were prepared. The mixing mass ratio for each component is given in Table 1:

Cenosphere mass ratio	30%	40%	50%
Geopolymer Component A (liquid)	200	200	200
Geopolymer Component B (powder)	250	250	250
Curing Agent (alkaline activator)	15	15	15
Cenospheres	135	180	225
Perlite	31.5	31.5	31.5

Table 1: Core preparation material mixing ratios (mass in grams)

Preparation process started with the following steps: using an analytical scale (0.1[g] precision) we measured 200[g] of the liquid geopolymer component (component A) and 250[g] of the powder component (component B) and added them into the food processor; on top of that, 15[g] of alkaline activator/curing agent was added and components were mixed for thirty seconds or until we got gray, viscous, homogenous

slurry. In that mixture different cenosphere mass ratios (135, 180 and 225[g]) were added and the mass was mixed until the mixture was completely homogenous (for approximately one minute). At that point a measured quantity of expanded perlite was added and the material was mixed until it became homogenous (for about one minute). It was noticed that material viscosity changes with different cenosphere mass ratios: samples made with a 30, 40% relative mass ratio had good flowability but some mixing problems and some additional aggregating and bubble presence were noticed. The 50% group was more dense and viscous, but it was mixed more homogenously and had fewer aggregating problems than the previous two. After the mixing was over, we could feel heat being generated due to the ongoing chemical reaction, since the geopolymerization process is exothermic. This process was repeated for each mass ratio group. This viscous, sticky slurry is then poured into prepared mold - Figure 3.

Figure 3: Wooden molds cowered with Teflon® film

Molds were prepared out of wood and wrapped in Teflon® foil to avoid and minimize geopolymer-to-wood bonding. Molds were designed to form beams of the following size: 548x65x10 [mm]. Picking the size, we kept in mind that we would have to cut the beams to appropriate standardized size (180x30x10 [mm]). After the material was poured into the mold, it was noticed that due to low viscosity, air bubbles are being trapped in the material. So the material had to be compacted by hand, with a plunger and a comb, to get rid of the trapped bubbles. Samples also had to be leveled with the upper surface of the mold (10[mm] thickness). After that, material was left unsealed at room temperature (20-22°C) to age for 4 weeks; relative humidity conditions could not be controlled, but they were monitored and changed between 25 and 35%.

3.2 Curing and drying procedures

After the room temperature aging period was over, one group of beams was removed from the mold and placed in the ESPEC-ESX-3CA environmental chamber for the elevated temperature curing process. Samples treated with this high temperature curing cycle, were marked with additional "cured" sign. Several different authors used different curing procedures: various curing temperatures (from 40 to 150°C), different curing times (from a few hours to a few days), and different environmental conditions (controlled humidity, controlled pressure etc.) [35], [49]. In general, geopolymer samples were cured at temperatures of 70-85°C, from 15 to 24 hours. In this case, our "cured" group was exposed to 100°C, at 15% relative humidity, for 48 hours - Figure 4. We wanted to determine how the following curing conditions would affect sample strength:

would free water loss affect the material mechanical properties and would higher curing temperature be beneficial to the geopolymerization process. Using a tile cutter saw, specimens were cut (according to C1341) to a predetermined, standardized size of 180x30x10 [mm] and then subjected to the appropriate curing cycle [50].

High TemperatureCuring Cycle Temperature vs Humidity
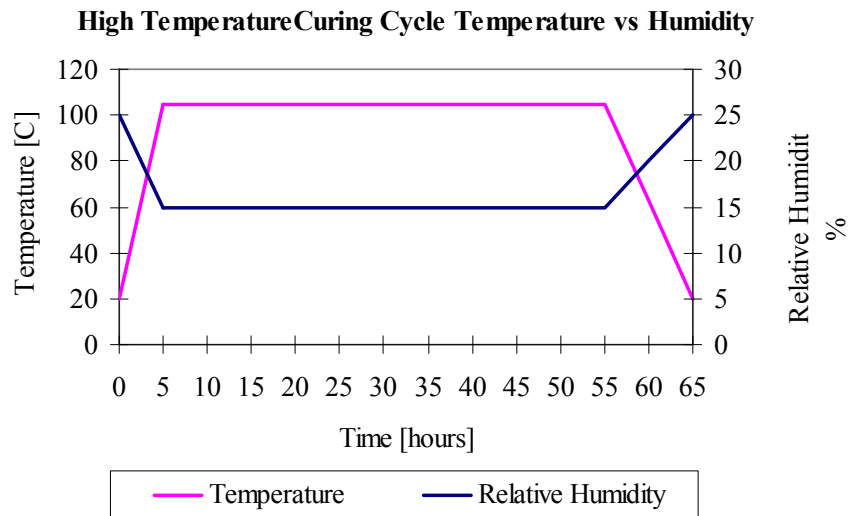
Figure 4: High temperature curing cycle (used for "cured" group)

It was noticed that the curing cycle dried out the samples significantly and they seemed to have lost some of their strength. Because of those reasons second, a standard curing cycle was also used - Figure 5. Other samples were exposed to that regular curing/drying cycle for 12 hours at 80°C, with 75% relative humidity. After curing samples were left at room conditions for two hours; thickness, length, width and mass were measured by calipers and an analytical scale. These bulk dimensions were used to calculate volume and sample density.

Regular Curing Cycle Temperature vs Humidity
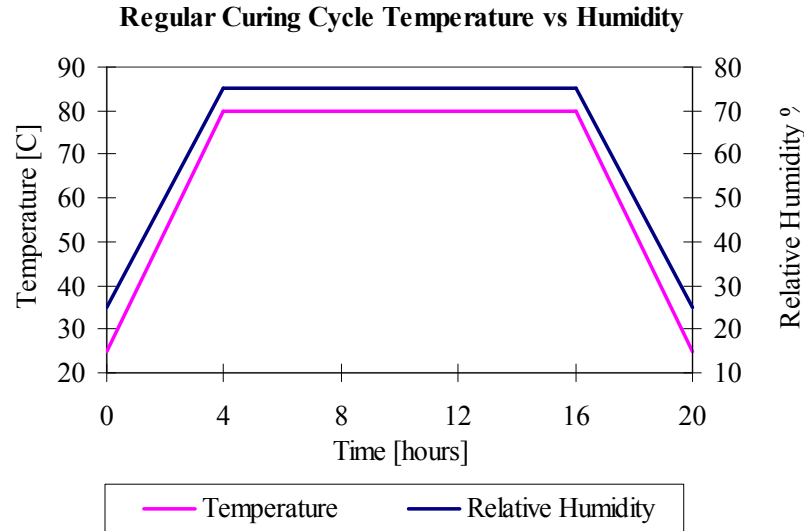
Figure 5: Regular curing cycle (used for the rest of the specimens)

3.3 Manufacturing and application of reinforcement layers

At this point the reinforcing layer is added to prepared specimens. Two different types of reinforcing fibers were used: carbon MITSUBISHI DIALEAD® and ceramic aluminum NEXTEL® 610 fibers. The bonding agent, used to saturate the fibers and connect them to the core, was geopolymer glue that was prepared in following steps: 100[g] of the liquid geopolymer component was mixed with 125[g] of the powder geopolymer component for thirty seconds in a food processor. After that, 65[g] of W-210 zeeospheres was added and mixed for about 2 minutes. The milky, viscous mixture was then by fine brush applied onto the core surface; fibers were laid onto that thin layer of bonding agent and carefully, using a small roller, pressed and spread until they were completely wetted and uniformly distributed over the sample surface. After one side was prepared, the geopolymer glue had to harden, so the samples were left at room

temperature for 24 hours and the process was repeated for the other side. After we had reinforced both sides, samples were dried in the regular oven for 12 hours at 60°C (with no humidity control). This drying was necessary to remove all additional humidity that was connected to the samples after reinforcement.

3.4 Sample categorization

Manufactured samples were categorized in several groups according to different factors:

According to curing cycle:

- Samples with regular curing cycle

- "Cured" samples that have been exposed to high temperature low humidity cycle.

From a reinforcement point of view we had 5 major groups:

- Reference samples that have no reinforcement

- 1TC sample group, reinforced with one tow of carbon fibers

- 2TC sample group, reinforced with two tow of carbon fibers

- 1TN sample group, reinforced with one tow of alumina fibers

- 2TN sample group, reinforced with two tow of alumina fibers

According to mass ratio percentage of cenosphere particles to geopolymeric components, we have three groups: 30, 40 and 50% mass ratio groups. During the manufacturing process, all precautions were taken and protective glasses, gloves and breathing masks were used. Geopolymer bonding agent is highly alkaline very sticky and adheres very

well to surfaces like cotton textile, wood, paper. [34]. It was noticed that it also sticks to

and reacts with aluminum foil (chemical connection).

Specimen classification is given in the following table:

No.	Reinforced	Serial	Exposed to flame	Oven cycle	No temp. treatment	SEM
1	REF	30-A-1				
2	2TN	30-A-2		X		
3	2TC	30-A-3		X		
4	1TN	30-A-4			X	
5	2TN	30-A-5			X	X
6	1TC	30-A-6	X		X	
7	2TN	30-B-7			X	
8	2TC	30-B-8		X		
9	2TC	30-B-9			X	
10	2TN	30-B-10		X		
11	2TC	30-B-11			X	
12	1TN	30-B-12	X		X	
19	1TC	30-D-19		X		
20	REF	30-D-20				
21	1TN	30-D-21		X		
22	1TC	30-D-22			X	
23	1TN	30-D-23	X	X		
24	1TC	30-D-24		X		
25	2TC	30-CURED-1			X	X
26	2TC	30-CURED-2		X		
27	2TN	30-CURED-3		X		
28	REF	30-CURED-4				
30	1TN	30-CURED-6		X		
31	2TN	30-CURED-7			X	
32	1TN	30-CURED-8			X	
33	1TC	30-CURED-9		X		
34	1TC	30-CURED-10			X	

35	REF	40-A-1				
36	2TC	40-A-2			X	
38	1TC	40-A-4	X		X	
39	2TC	40-A-5	X	X		
40	1TC	40-A-6		X		
41	1TN	40-B-7			X	
44	2TN	40-B-10			X	
45	1TC	40-B-11			X	
47	2TN	40-C-13		X		
49	1TC	40-C-15		X		
50	2TC	40-C-16		X		

52	REF	40-C-18				
54	2TC	40-D-20	X		X	
55	2TN	40-D-21			X	X
57	2TN	40-D-23		X		
58	1TN	40-D-24			X	
59	1TN	40-E-25				
60	1TN	40-E-26		X		
61	2TN	40-CURED-25	X		X	X
62	REF	40-CURED-26				
65	1TC	40-CURED-29		X		
67	1TN	40-CURED-31			X	X
68	1TC	40-CURED-32			X	
69	2TC	40-CURED-33		X		
70	1TN	40-CURED-34		X		
71	2TN	40-CURED-35		X		
72	2TC	40-CURED-36			X	

73	2TC	50-A-1			X	
74	2TC	50-A-2		X		
75	1TC	50-A-3	X		X	X
76	2TN	50-A-4	X			
77	2TN	50-A-5	X		X	
78	1TN	50-A-6			X	
79	1TC	50-B-7			X	
80	1TC	50-B-8		X		
83	2TN	50-B-11		X		
84	1TN	50-B-12		X		
85	REF	50-C-13				
87	1TC	50-C-15		X		
91	REF	50-D-19				
93	2TN	50-D-21			X	
94	1TC	50-D-22		X		
95	2TN	50-D-23		X		
96	1TN	50-D-24		X		
98	1TN	50-E-26	X		X	
99	2TC	50-E-27			X	
100	2TN	50-E-28	X			
102	2TC	50-E-30		X		
103	2TN	50-CURED-31		X		
104	1TN	50-CURED-32		X		
105	2TC	50-CURED-33			X	
106	1TN	50-CURED-34			X	
107	2TC	50-CURED-35		X		
108	REF	50-CURED-36				
111	2TN	50-CURED-39			X	X
112	1TC	50-CURED-40			X	

Table 2: Specimen classification

3.5 Some observations noticed during manufacturing process

During the four-week aging period, it was noticed that the material was not drying equally on all sides, since the plates were covered by coated wood on three sides and the plate top surface was exposed to environment. That uneven drying was a probable cause for the slight deforming and warping of the beams. Deformation was not significant, but it was a good indicator that some additional stress was developing as a result of the uneven drying/aging process. At this stage of manufacturing process stress concentrations should be avoided as much as possible. It was concluded that samples should be properly protected and coated so that water evaporation would be more controlled and even. Some authors made more serious steps ([27], [51] and others) to isolate samples from surroundings (vacuum bagging etc.) to minimize uneven water evaporation. By doing that, unwanted contact and possible chemical reactions between contaminants or other active elements (Oxygen) from the atmosphere and geopolymer components are minimized. However, vacuum bagging is not standardized procedure, and in other studied cases, samples were not sealed and they were in contact with atmosphere.

During the sample manufacturing process, it was noticed that, with higher mass ratios of cenospheres (40 and 50%), the mixture was denser and more difficult to mix, but after mixing it was more homogenous than lower percentages. It was also observed that 50% samples had some problems with bigger voids and releasing trapped bubbles. That was obvious when the room aging process was over and samples were taken out of the mold - Figure 6. With low mass ratio samples (30%) the mixture was less viscous and easier to mix but, had fewer bubbles, but it had a serious problem with perlite

aggregating. As perlite particles are much bigger and are lighter than the mixture perlite was collected on the surface of 30% samples. This can cause nonuniform material properties and inconsistent testing results.
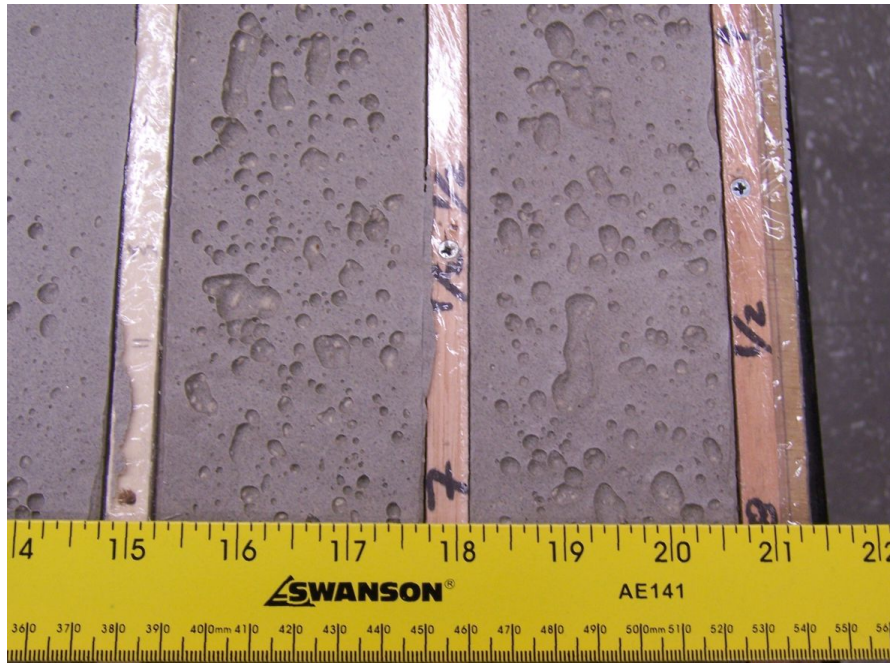
Figure 6: Pitting problems (caused by big bubbles) with 50% group

There were some problems with the fiber handling and wetting process: fibers would often get caught and tangled with the rolling cylinder. For appropriate wetting, a larger amount of geopolymer glue was needed, but a larger amount of bonding agent between fibers and the core could affect the mechanical properties of the reinforcing layer and induce some premature failures due to debonding between the fibers and glue or delamination between the reinforcements and core. Since some of the specimens will be exposed to open flame conditions, possible changes or the reaction of that extra layer of geopolymeric glue and it affect on sandwich structure behavior has to be considered.

The curing process (high temperature curing cycle) caused some level of material drying and cracking. The material had lost a lot of it original strength and became brittle and flaky. "Cured" samples were in general lighter than uncured samples cut from the same beam. After fiber reinforcement and a short drying cycle, some samples developed different type of cracks: horizontal longitudinal, short vertical etc. The possible effect of these imperfections on structure properties will be analyzed later in text. The explanation for the mentioned changes can be found in water evaporation. Due to increased pore pressure and the escape of free water that had been trapped, the material microstructure was probably stressed or damaged.

CHAPTER 4 - TESTING CONDITIONS AND EQUIPMENT

To determine the possible flammability of geopolymer material or reinforcing fibers, flexural properties and possible structural changes, four different testing setups were used. Testing properties and conditions were in accordance with adequate ASTM standards. All instruments used in this experiment and described in this chapter were previously tested and calibrated.

4.1 Flame exposure and temperature measurement

To determine material and sandwich behavior in flame conditions, certain samples with and without reinforcing skin were exposed to open flame for 30 minutes. In this case, samples were not subjected to any loading; top and bottom surface temperatures were measured and material reaction to flame was monitored. As a flame and heat source, propane gas-powered micro-Bunsen burner was used. Samples were carefully positioned at the top of the flame cone peak, in the area of highest temperatures. The temperature heating curve was controlled and in accordance with the ASTM E-119 standard - Figure 7. Maximal generated temperatures were in a range of 850°C. For surface temperature measurement the noncontact infrared thermometer "RealTemp Pyrometer" (manufactured by The Pyrometer Instrument Company) was used. The measuring head was positioned 16 inches away from the surface and several preliminary temperature readings were performed in order to find the highest emissivity position.

After this step, all other samples were positioned in the same way; temperature was measured and data collected with 0.5 [Hz] frequencies. Instrument features are:

- Temperature measurement range: 500°C - 1300°C

- Temperature measurement accuracy: ±3°C

- Target distance 30-46 [cm] (12-18 [in])

- Focal length: 40 [cm] (16 [in])

- Spot size diameter: from 6.5 [mm] (0.25 [in]) at focal length and larger
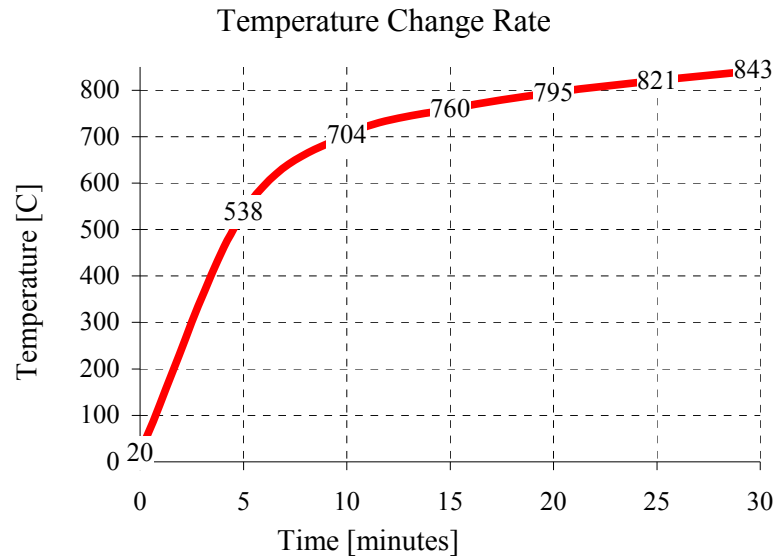

Figure 7: Standard temperature change rate during fire exposure (ASTM E119)

4.2 Flexural testing system, fixtures and procedures

To determine flexural properties of geopolymer based structures, a three-point bending test was performed on an INSTRON 8821S servo-hydraulic testing system. All samples were tested on a nonarticulating three point bending fixture. The distance

between fixture supports was set according to the ASTM C1341 standard and it was 160mm. For crosshead motion and deformation measurement, an onboard LVDT (linear variable differential transformer) instrument, positioned inside the INSTRON servo-hydraulic actuator, was used. Usually, for this type of experiment, external LVDT is used to avoid system yielding generated by high tensile or compressive forces. The reason for choosing the onboard unit instead of an independently mounted LVDT was that in our case expected loads would not top 1 [KN] of force and for that level of loading, machine compliance is low and total system deformations are negligible [52]. But to obtain good levels of precision, calibrating measurement was done, using material with known geometry and modulus of elasticity. After data were analyzed, a linear law that connects load levels and system deformation was generated. System deformations were subtracted from the total deformations measured by the LVDT unit. Following standardized testing procedures is necessary to provide required level of repeatability and reproducibility and it allows us to analyze and compare values obtained from different experiments and different sources.

Tests were performed according to these standards: ASTM C393, C1341 and D790. According to standards C393 and C1341, crosshead displacement rate of 0.5 [mm/min] was used. In some cases, higher displacement rates are used to avoid possible creep effects that can occur especially at higher testing temperatures, but since our material was expected to be very brittle and tests were performed at room temperature, a lower feed rate was used.

4.3 High temperature oven cycles

To test the behavior of sandwich samples at elevated temperatures and residual flexural properties, samples were divided into two groups and one group was exposed to a high temperature oven cycle. The temperature cycle went as follows:

- The temperature was increased from room to 750°C in 60 minutes.

- Samples were kept at 750°C for 60 minutes.

- Then power was turned off and samples were left to cool down to room temperature (it took about 6 hours for samples to cool down).

This group was used to determine sandwich residual flexural properties and reaction to oven high temperature conditions. Temperature influence on sample structural changes and on interaction between core and reinforcement was also closely monitored. Residual flexural properties of heat treated samples were measured and compared to the group that was not exposed to high temperature. For high temperature exposure cycles an NEY M-525 Series III (maximum temperature 1100°C) furnace was used and onboard thermocouple was used as temperature monitoring device.

4.4 SEM analysis

After each experimental step all used samples were visually inspected, measured and analyzed, so possible structural changes could be observed and failure modes detected. An AMRAY 1830 I, SEM (scanning electron microscope) was used to inspect the microstructure of prepared samples and changes caused by high temperature, flame exposure and material aging.

Figure 8: AMRAY 1830 I, SEM (scanning electron microscope)

SEM samples were cut by a high speed rotary tool, from representative areas of donor samples. Specimen areas that were exposed to the influence of temperature, flame or tensile and compressive loads we marked and pieces used for the SEM analysis were cut out. We were especially interested to investigate crack surfaces, areas that were directly affected by load, flame or temperature. Areas exposed to open flame could give us insight on flame-caused micro structural material changes, so they were also closely monitored. Another area of interest was interface among the reinforcing fibers, geopolymer glue and core material, so those areas were examined also. All SEM tested samples were prepared from tensile, bottom sides of the samples since major failure modes were happening in those areas.

An SEM works on the principle of electron emission and it was necessary for tested samples to conduct electricity. To make material conductive, the samples had to be coated with $20\text{-}25\times10^{-9}$ [m] thick gold-palladium coating. Coating was done on a

BALZERS SCD-004 Sputter Coating unit. Since we were interested in micro structural material changes and the properties of failure surfaces, standard surface preparation techniques (like cleaning and polishing) were not used, since that would probably damage delicate failure surfaces. The SEM was used with operating voltage of 20 [KV].

CHAPTER 5 - RESULTS AND DISCUSSION

5.1 Samples exposed to flame conditions and high temperature oven cycles

5.1.1 Samples exposed to flame conditions

To determine material reaction to the flame conditions, several samples (with and without reinforcing fibers) were positioned on two supports and in the middle they were exposed to propane flame for 30 minutes; temperatures generated on the exposed surface were in a range of 850°C. Temperature change rate was based on the ASTM E 119 standard (refer to Figure 7) and the temperature-increasing function used internationally [30], [53]. The specimens were not under any physical load during this part of the experiment. Though specimen thickness was 10±2 [mm], temperatures on the opposite side were lower than 600°C.

When exposed to flame, due to the uneven one-sided point heating, thermal shock and other thermodynamic effects, severe specimen deformation appeared almost instantly. The first thing noticed was that the flame-flushed area started changing color to milky white. Samples started to swell and bend toward the flame, which was expected since material was expanding noticeably in contact with heat, but it was not expected that samples would deform at such a high rate. Reinforcement played a small role in sample endurance and every tested sample showed some level of deformation and swelling. It was noticed that the geopolymeric glue used to prepare reinforcing layers was especially susceptible to expansion and swelling - Figure 9.

Figure 9: Swelling of the geopolymer glue
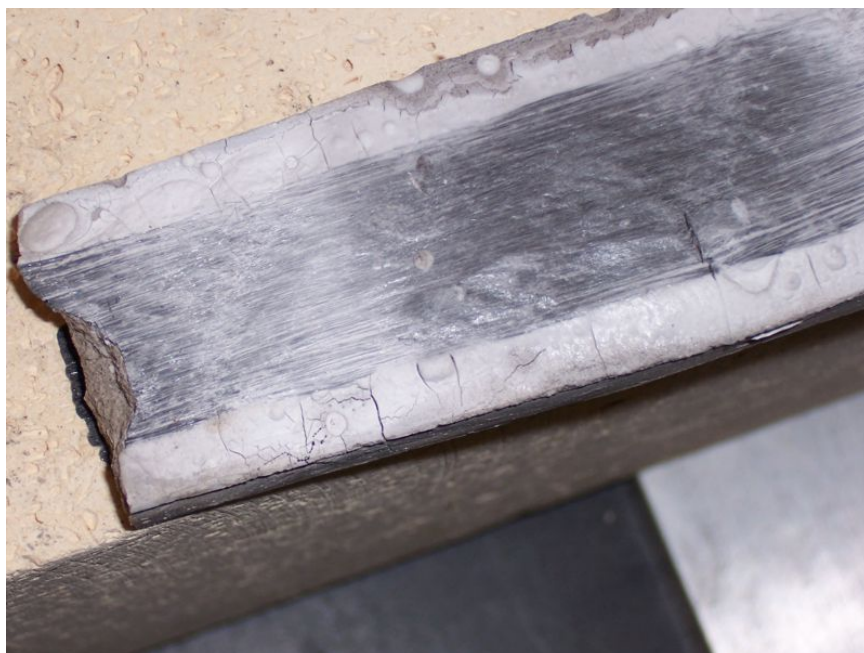
Figure 10: After flame exposure, material glassy surface and fiber breaking

If a larger amount of glue (like droplet) was in the flame zone, it was swelling intensively, but that effect was not easy visible in areas rich in fibers. Some fiber breaking (both carbon and alumina) was caused by glue swelling and the fiber's inability to adapt to such high strain rates. It was noticed that due to local geopolymer melting, surface that was exposed to the flame had a glassy look - Figure 10. Another problem noticed with flame-exposed reinforcing specimens was that on the edges of fibrous material, some delamination between the core and reinforcements appeared; this was noticed in all specimens exposed to flame. The delamination level ranged from small surface cracking (between reinforcement fibers) and cracking between the reinforcement and core - Figure 11, up to serious longitudinal cracking formed deeper in the core, beneath reinforcing layer - Figure 12.

Figure 11: Delamination between the reinforcing layer and core (50A3)

Figure 12: Longitudinal cracks formed underneath the reinforcing layer (40D20)

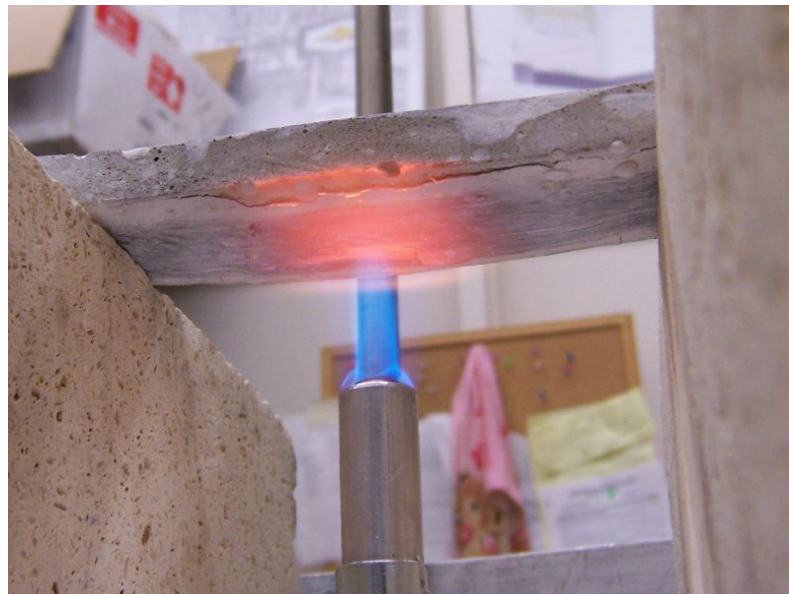During fire exposure, material was continuously reacted to the flame, deforming until somewhat stable thermal conditions were obtained. After about 20 minutes, material changes became less obvious, slower and fewer. It was noticed that samples made with a high percentage of cenospheres (50%) reacted better to the flame conditions: temperature-caused deformations were slower and damage was less severe than in other groups. After thermally stable conditions had been reached, some of the samples had tendency to return approximately to the same shape they have had at the beginning of test. After thirty minutes of exposure, the flame was turned off and samples were left at room temperature to cool down. Since decrease in temperature also represented thermal shock, several samples, while cooling down, produced cracking sounds and in some cases the crack forming and progression process were easy to monitor. Some samples broke by themselves without any load application and only due to thermal stresses. It was evident that this newly prepared material had a very high coefficient of thermal expansion,

although this was not measured directly. There are several possible explanations for this type of behavior:

- Cracks forming can be explained by the high level of deformation that the material is experiencing. This material is very brittle, probably even more brittle at elevated temperatures, and it cannot support this type of dimensional change.

- Another possible explanation for this material swelling can be seen in the content of free water that is trapped inside of material pores. As material gets heated water starts evaporating, increasing pore pressure, rupturing material's inner structure and diminishing the material's mechanical properties. This effect has to be taken into consideration since pre-cured samples deformed significantly less than non-cured ones.

- Other authors [27], [54] have explained this effect with properties of geopolymer mixture. Certain levels of silica (silicon dioxide) in combination with potassium and sodium can form structures that are either expanding (expansion of uncombined silica) or contracting (due to water evaporation and pore collapse) when exposed to higher temperatures - over 800°C. These effects are not yet fully explained.

After this test phase had ended, samples were visually examined. Different types of surface cracking were noticed on both sides (bottom and upper) in the majority of tested samples; also some alligator skin cracks and swelling were present. Surface cracks can be explained by water loss and the drying-out of the surface layer. In some cases, fusion between fibers and the core was noticed, along with the appearance of glass-like surface which happened as a result of surface material melting - Figure 13. Some

samples exhibited severe cross-section swelling and bubbling of the core material. It was noticed that all samples became very brittle after fire exposure.

Figure 13: Cracks and melting of material surface area (50E28)

5.1.2 Oven heating treatment

Though we could not observe samples during oven cycles, reactions similar to those from flame exposure were observed after oven heating treatments were over. The difference is that changes were spread across the entire sample surface, in contrast to the limited flame exposed area. Surface cracking, which in some cases was followed by deep structural cracks, appeared in some samples with lower cenosphere percentages. Significant cracking was also observed close to the ends of samples since that area has no structural support from reinforcing fibers - Figure 14, 15.

Figure 14: End cracking 1TC (30D19)

Figure 15: End cracking 2TC (30A3)

A similar phenomenon is also observed in composite laminates as the interlaminar stress problem and it is usually solved by application of reinforcement or a patch in the affected area. Since DIALEAD and NEXTEL 610 fibers have coefficients of thermal expansion

lower than the core material, additional stress concentrations were caused by core material to fiber expansion and longitudinal cracks parallel to reinforcement layers were noticed in several samples (usually carbon reinforced ones) - Figure 16.

Figure 16: Longitudinal cracks 1TC (40cured29)

Figure 17: Structural failure caused by expanding geopolymer droplet

As before, it was noticed that excess geopolymer bonding glue material swells significantly when exposed to high temperatures. In some cases, swelling of geopolymer binder has caused fiber breaking - Figure 10 and premature structural failures during high

temperature oven cycles - Figure 17. Real-time development of swelling and deformations could not be monitored during oven heating cycles.

Several conclusions can be drawn from this part of the experiment:

- Reinforced material does not burn, generating no visible smoke or fumes, but significantly deforms when exposed to higher temperatures.

- Lower mass ratios of the cenospheres mixture (30 and 40%) were very susceptible to cracking, drying, flaking and other changes during and after heat treatments.

- Sample inner structure is affected by material swelling and bubbling and free water evaporation is affects and damages material micro structure.

- As a result of the different thermal expansion coefficients of the core and skin reinforcements, internal stresses were generated and some cracks were formed during heating cycles.

- The bond between the reinforcement layers and core was good even after exposure to high temperatures. In some cases, samples were structurally damaged during high temperature exposures and those situations were connected to the expansion of perlite particles and to excessive swelling of the geopolymer bonding agent.

5.2 Flexural Testing

Selected specimens were subjected to a flexural three point bending test, with a cross head feeding rate of 0.05 [mm/min]. Each sample was monitored and analyzed during and after the flexural test to determine failure mode and detect any other effects or

problems that may have happened during the test. Load and deflection values were acquired with adequate sampling frequency and stored in a computer. Although this type of testing does not reveal the true mechanical properties of component materials, the observations and results were a good foundation for the understanding of the general mechanical properties of a newly formed sandwich structures. Tests were performed and data are organized at three major levels: reference samples, samples unexposed to high temperature treatments and samples exposed to high temperatures. Collected data were correlated at several different levels in order to more easily recognize some properties that are not obvious enough on general load deflection (stress/strain graphs).

5.2.1 Flexural test - reference group samples

A group of reference samples was tested to obtain a general idea about the flexural properties of composite geopolymer material alone without any reinforcements. Three groups with different mass ratios of fly ash were tested and load deformation properties are represented in Figure 18. All samples had failed in a brittle manner on a tensile-loaded bottom surface. A crack was usually formed close to the mid span and was perpendicular to the tensile plane; other failure modes such as pitting (due to compression) or surface crushing damages were not detected.

Results showed that the material is extremely brittle and maximum stress (calculated for three-point bending) is low, in a range from 0.91 to 11.87 [MPa]. The obtained results were highly inconsistent and it was difficult to draw a strong conclusion about material flexural properties. In spite of inconsistent results it was concluded that samples with higher density sustained higher stress conditions - refer to Table 3.
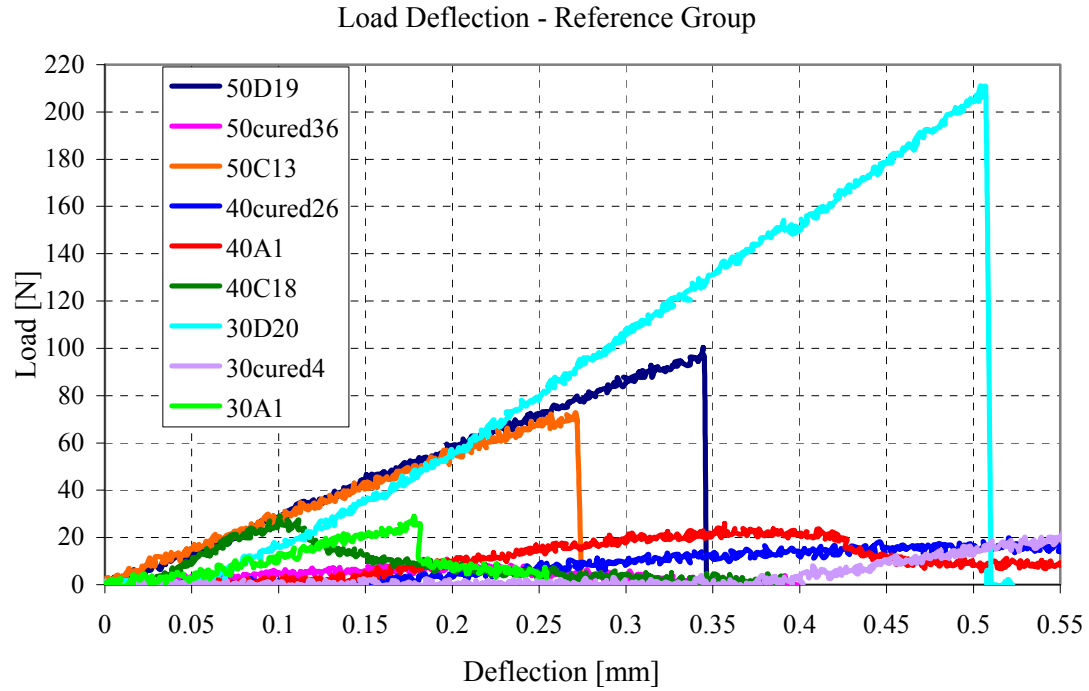
Load Deflection - Reference Group

Figure 18: Load deflection graph for reference sample group

Specimen	Width [mm]	Thick [mm]	Specimen Density [kg/m3]	Maximum Deflection [mm]	Maximum Load [N]	Flexural Strength [MPa]	Flexural Strain	Failure Mode
30-A-1	32	11.68	1192.95	0.176497824	28.99915	1.594266228	0.000483163	TB
30-D-20	32.22	11.51	1323.58	0.493910932	210.69646	11.84656106	0.001332402	TB
30-cured-4	32.35	11.32	1122.3	0.673702027	27.734041	1.605673561	0.001787416	TB
40-A-1	31.38	12.04	1102.05	0.355458368	26.008487	1.372209486	0.001003059	TB
40-C-18	31.61	11.96	1169.88	0.099254878	28.820336	1.529760442	0.000278224	TB
40-cured-26	30.52	11.69	1126.78	0.51927994	19.855797	1.142575781	0.001422746	TB
50-C-13	30.25	9.8	1102.72	0.267303709	72.774291	6.011899257	0.000613963	TB
50-D-19	29.25	10.17	1103.28	0.339493315	100.39806	7.96468834	0.000809214	TB
50-cured-36	31.58	9.53	1029.78	0.19619803	10.837615	0.906874173	0.000438227	TB
Average	31.24	11.0778	1141.48					
Standard Deviation	1.0308	0.9708	82.3053	Test speed:	Span:	Displacement control mode		TB= Tensile bottom
Test Method	ASTM C1341			0.5 mm/min	160 [mm]			

Table 3: Reference sample group properties

Samples from the 50% group produced the most consistent results, probably due to good mixed material and even dispersion of filler particles. The 40% group had a good particle distribution and the cross-section looked "healthy", but it gave us poor results and it is unclear why this happened. After the crack surfaces were examined, it was noticed that, although the sample preparation process was very meticulous, there were some aggregating and particles grouping across the sample cross section - Figures 19, 20 and 21. Larger particles and smaller bubbles were usually closer to the one side of the sample and that problem was observed with the 30% group; the 40 and 50% groups were mixed in good manner.

The main observation, in this part of experiment, is that this type of geopolymer cenosphere mixture (without any reinforcements) is extremely brittle and weak. The material fails after only minor loads are applied, but in some cases specimen performed very well (the density of this specimen was highest of all measured samples). Specimen properties were very inconsistent and it was difficult to draw a proper conclusion from this group. Specimens with lower fly ash mass ratios generated higher flexural forces, but at that point it was difficult to connect other material properties, like fly ash mass ratio or density, directly to mechanical properties. The "cured" samples from the reference group very dry and flaky and had even weaker flexural capabilities.
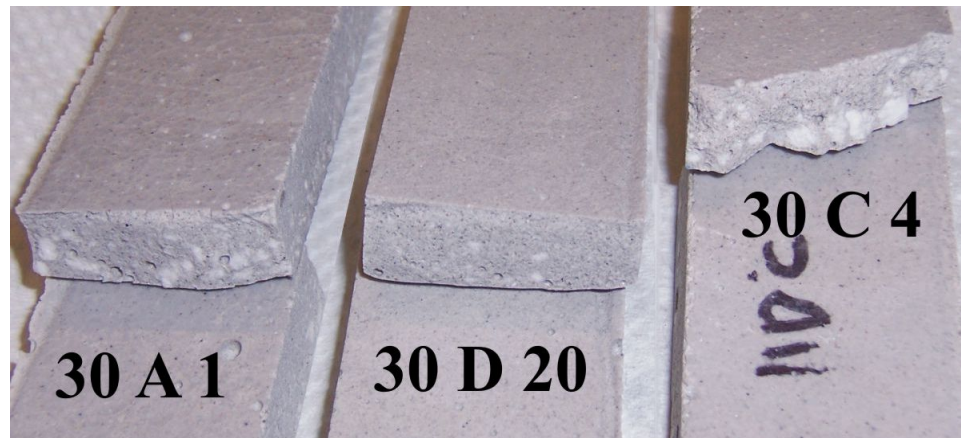
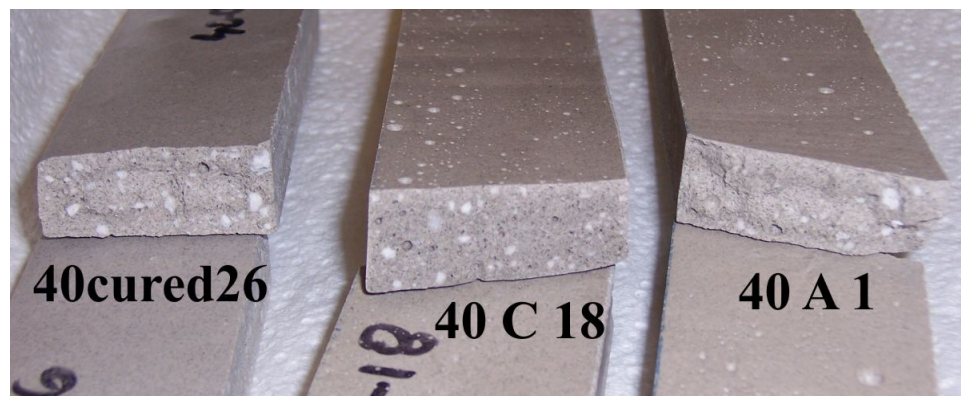Figure 19: Break cross section and aggregating in the 30% sample group

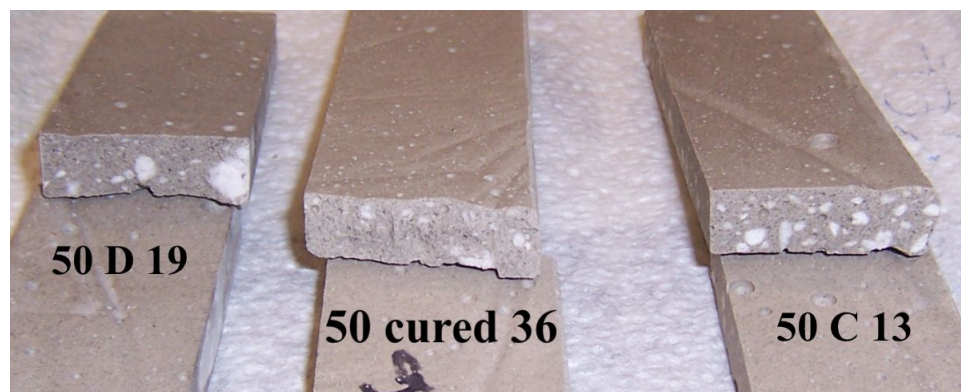Figure 20: Break cross section and aggregating in the 40% sample group

Figure 21: Break cross section and aggregating in the 50% sample group

5.2.2 Flexural test - reinforced samples without temperature treatment

The flexural test (with the same test conditions as for reference group) was performed on randomly selected reinforced samples. The samples were visually checked and analyzed after every test. It was noticed that material consistency and homogeneity plays a very important role in the mechanical properties of the sandwich panel. It was noted that samples that had generated higher levels of flexural force usually had a clean cracking surface with no flakes, bubbles, perlite particles or chips of broken material. A cross section of those samples usually looked homogeneous without serious aggregating effects. The failure mode in the majority of cases was skin tensile failure. Pitting, buckling, debonding effects or any other damages caused by fixture pressing points were not noticed. In the majority of samples, failure was brittle (low energy), without any explosive effects, but several samples that had generated higher flexural forces experienced some fiber pullout and splitting.

Samples reinforced with NEXTEL 610 fibers produced more consistent results but generated lower peaks of flexural force than carbon-reinforced samples. Aluminum samples rarely showed any gradual fiber failure or fiber pullout and when the sample failed it was brittle with no warning affects. This failure trend can be linked to a very good connection between geopolymer glue, saturated fibers and core. Carbon fibers gave us higher flexural force peaks and samples also showed some additional partial fiber failure and stress relaxation prior to total sample failure. This may be connected to the higher stiffness of carbon fibers and ability to move to redistribute load across the fiber tow. DIALEAD fibers did not have any sizing on them, so the contact between geopolymer and fibers looked healthy but some local failures and stress relaxation defects

were detected on the load deformation graphs. Additional conclusions about failure mechanisms and mechanical properties of our samples can be drawn from the following load deflection graphs (Figures 22 to 25). Graphical data was organized and presented according to the type of reinforcing fiber layer.
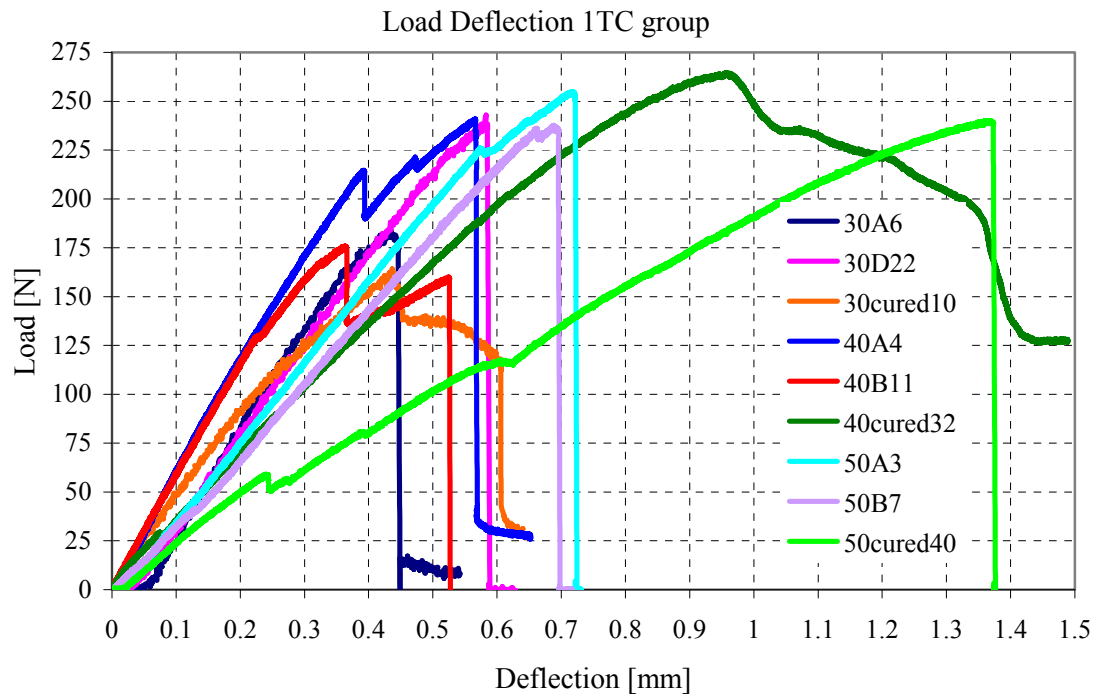

Figure 22: Load deflection graph for 1TC group of samples

From the graphs it was noticed that the flexural energy used in some "cured" samples was higher than in other samples from same group, even thou "cured" samples showed poor mechanical properties, especially very high brittleness and low strength. Moment-carrying capabilities were tested and it was determined that, after applying fiber reinforcements, the increase in flexural moment is significant (around 300%). From the

graph it is easy to determine that carbon reinforced specimens experienced some gradual

fiber failing that was occurring before the total failure of the specimen.
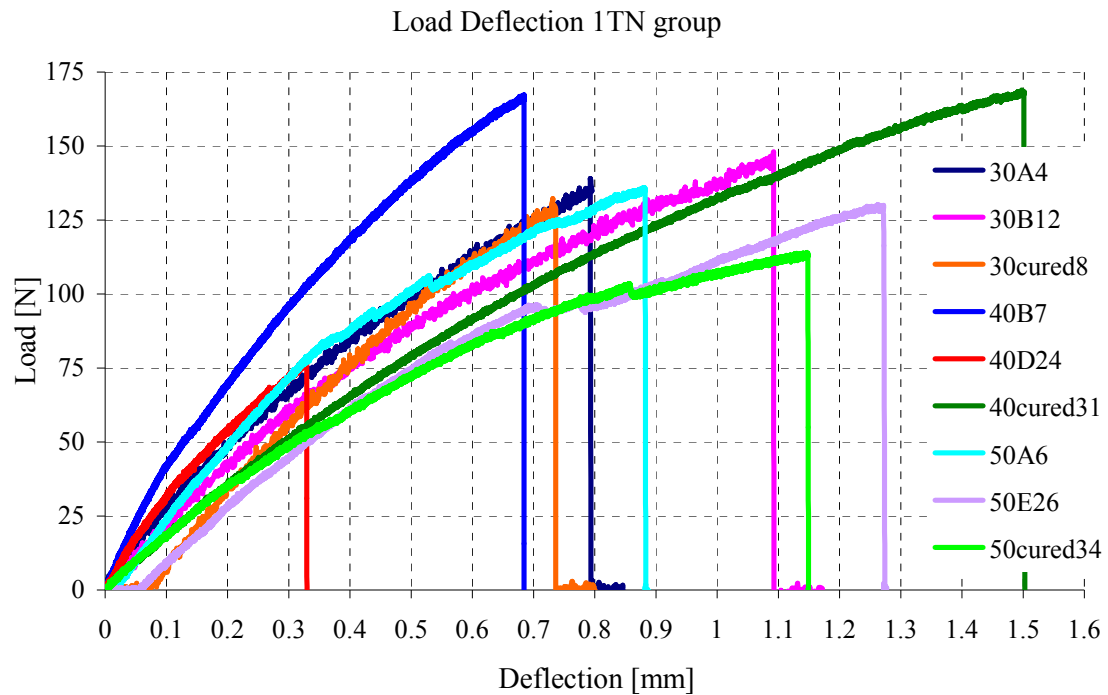
Load Deflection 1TN group

Figure 23: Load deflection graph for 1TN group

No obvious differences among flexural properties of samples made with different

cenosphere mass ratio were determined, but samples made with a higher percentage of

cenosphere gave us more consistent results.   Graphical data showed that carbon

reinforced samples, though very brittle, show properties of linear elastic material.

Samples prepared with aluminum fibers exhibit somewhat non-linear elasto-plastic
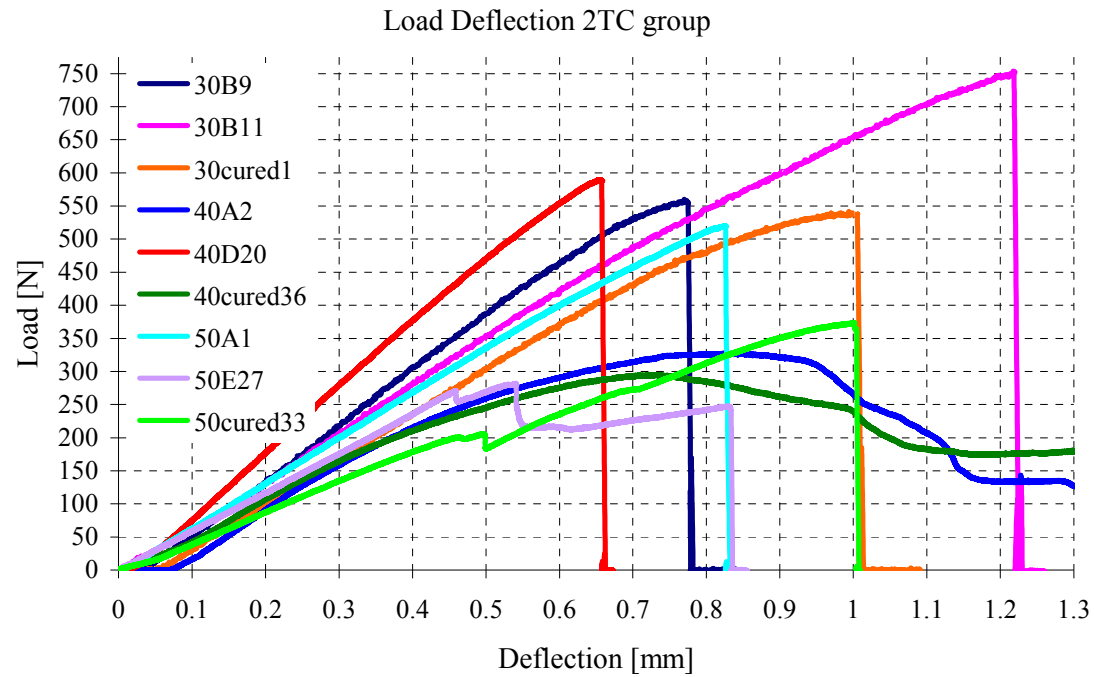
behavior.

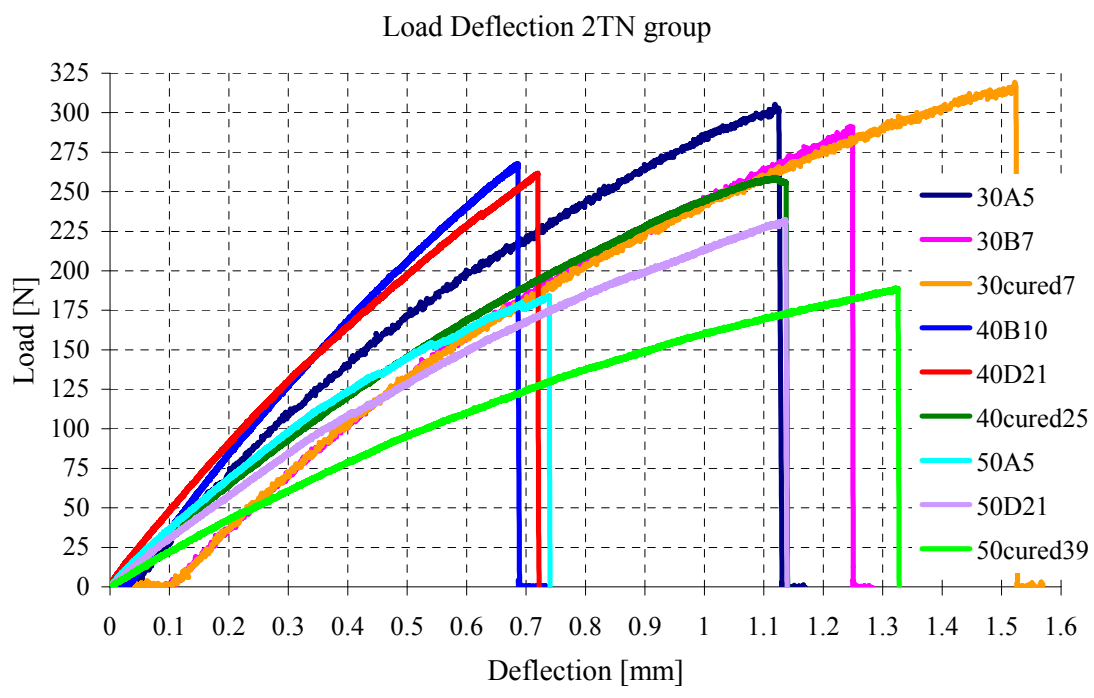Figure 24: Load deflection graphs for 2TC group

Figure 25: Load deflection graphs for 2TN group

5.2.3 Flexural test - reinforced samples after high temperature treatment

This group of specimens was exposed to 750°C for one hour; humidity was not controlled. The specimens were tested under the same conditions as previous groups and residual flexural properties of sandwich structures were monitored. After the high temperature cycle, each sample was weighted and it was determined that samples lost between 5.5 and 8.9% of their mass (on average 6.85, st. dev. 1.09), which is consistent with values from other researchers [35]. Further calculations and analysis of sandwich structure mechanical properties will be done later.

Visual examination and characterization (as mentioned in 3.1) revealed that all the samples exposed to a heating cycle were deformed to some degree, so for calculation purposes we used dimensions that were taken before the temperature exposure. Most of deformations occurred close to sample ends where uneven coefficients of thermal expansion and stress between the core and reinforcements caused significant cracking and deformation. The outer sample surfaces changed from smooth to rough, dry and milky white. It was also noticed that samples with more uniform fiber distribution were less deformed and that the previously cured group sustained least amount of deformation but developed some longitudinal cracking. In general, the surface layer of the geopolymer binder was swollen, dried out and started cracking and chipping off. Samples and reinforcing layers (saturated with geopolymer glue) were swollen and dried out. In some cases, binder swelling caused structural defects like fiber breaking, deformation and sample failure. An increase in bubble pits' presence and a significant increase in surface cracking were also observed; in some samples, surface cracks expanded deeper into the core. Specimen ends were specially affected by cracking,

delamination and deformation (this happened in all three sample groups). In general, the shape and condition of the rest of the samples was satisfactory.

After temperature exposure samples from the 50% group had become flakier, samples that were rich in geopolymer binder showed significant swelling. After flexural testing was finished, it was noticed that <u>aluminum</u> fiber reinforced samples, both one and two tows, showed very brittle behavior. According to manufacturer specifications, NEXTEL^{TM} 610 ceramic fibers should retain about 80% of their strength after 750°C, but the samples had retained on average 36% of their residual flexural force. Aluminum fiber samples generally failed in the brittle mode, with a cracking plane that was perpendicular to the tensile surface. In most specimens, the crack did not extend all the way through the specimen thickness. Aluminum samples had very good fibber saturation and the reinforcing layer did not looked dried out. <u>Carbon</u> samples were in some cases visibly dry and in some cases had experienced longitudinal fiber tow splitting due to the thermal expansion of the core material and binder. Fibers splitting affected the method of failure in some samples; by that I mean that at some point during the test, there was a relative motion along the fibers. If reinforcing fibers were not wet enough, the usual failing mode was bottom surface tensile failure with some level of fiber pullout or fiber layer delimitation (only through reinforcing layer thickness); this occurred in several cases. When looking at the crack surface, it was noticed that if there were any perlite particles present the crack would always go through the particle rather than cause particle pullout or cracking along the contact line between the matrix and particle. That means that bonds (supported by chemical compatibility [55]) among perlite, geopolymer and cenospheres were strong, stronger than perlite crystal itself.

The 40% group showed changes similar to those of the 50% group. Deformations were noticeable and "cured" group specimens deformed least. Cracks, delamination, deformations and debonding were significant and obvious, close to the samples' edges. In this group some horizontal cracks started to appear at sample ends (close to the neutral line). Bubble presence and surface layer cracking were significantly increased in comparison to samples not exposed to temperature cycles. As in the 50% group, the surface layer cracked and peeled off. In several samples, longitudinal cracks appeared close to the neutral line - Figure 26.

Figure 26: Longitudinal cracks appeared after the oven cycle (40cured33)

Several carbon samples (40A5-2TC) failed in the brittle mode with higher generated flexural force, with some delamination through the reinforcement layer thickness (this delamination was limited on the inner volume of the fiber reinforcement) and fiber pullout on the tensile surface. This reaction can be explained by an incomplete saturation

of the reinforcing fibers, which can lead to possible fiber-to-fiber sliding and stress redistribution. Other samples failed as expected, without any unexpected effects.

The 30% group samples sustained the most deformation and cracking during the heat treatment. The samples were significantly deformed; edges were dried out, cracked and deformed with obvious delamination and debonding of the fiber reinforcement in affected areas. There was also a noticeable presence of longitudinal, shear like, cracks along the length of the samples (on all sides), a significantly higher visibility of bubbles and surface cracks and also several cracks that were generated by perlite and/or geopolymer binder expansion. The samples look dried out; in some places carbon fibers were broken (torn) due to different thermal expansion of the reinforcing fibers and core, and to excess thermal expansion of the geopolymer binder. "Alligator skin" was present in several samples with both types of reinforcement. The presence of the mentioned imperfections did not significantly influence the flexural test and the majority of samples failed in expected manner.

At this point, it was noticed that the majority of longitudinal cracking was occurring in "cured" group and the cracking was more severe than in other sample groups. This type of cracking occurred in both types of reinforcements. In several cases these cracks (which were usually formed close to the bending neutral line) resulted in core shear failure. Specimens that failed in the core shear mode felt very flaky and dry.

Load deflection graphs of temperature-treated specimens and specimens that were not temperature-treated will be presented. To provide easier data analysis, each graph will include six measurements of oven and room temperature samples. A total of twelve

graphs (Figure 27 to 38); one for each type of reinforcing skin (oven and room temperature for each cenosphere mass ratio and fiber type) will be presented.
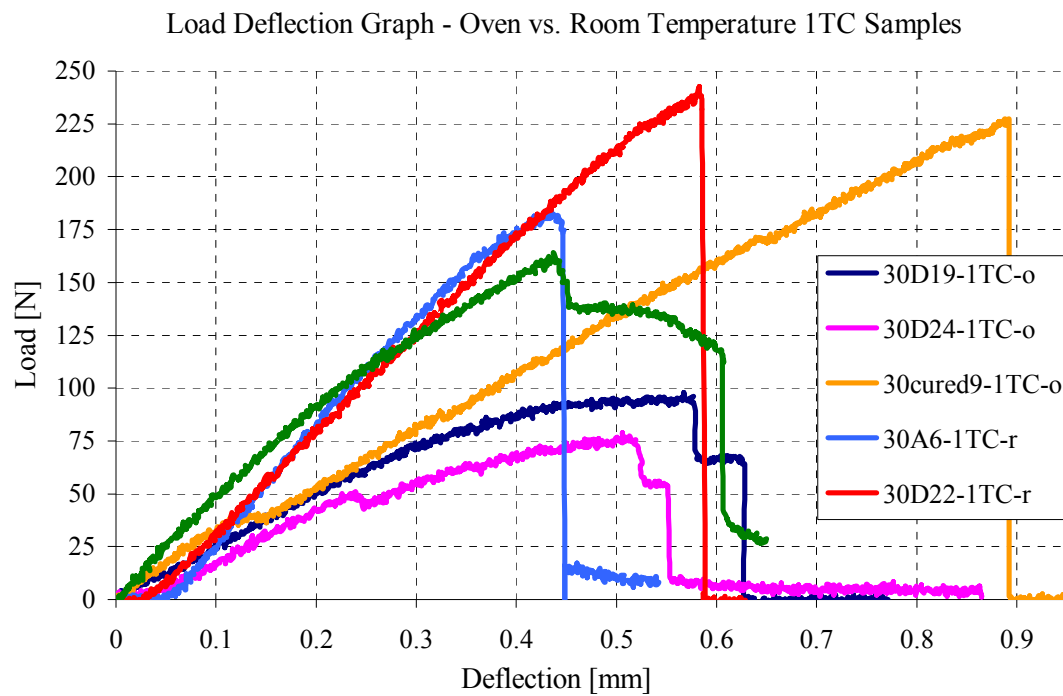

Figure 27: Load deflection for oven vs. room temperature treated 30% 1TC samples
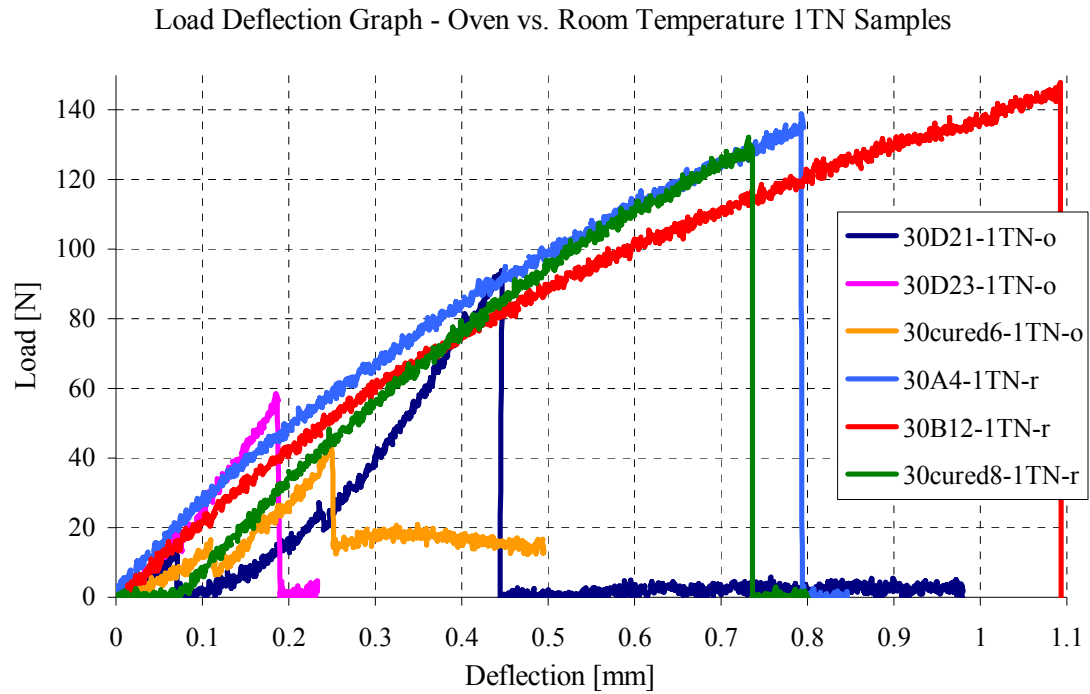
Load Deflection Graph - Oven vs. Room Temperature 1TN Samples

Figure 28: Load deflection for oven vs. room temperature treated 30% 1TN samples

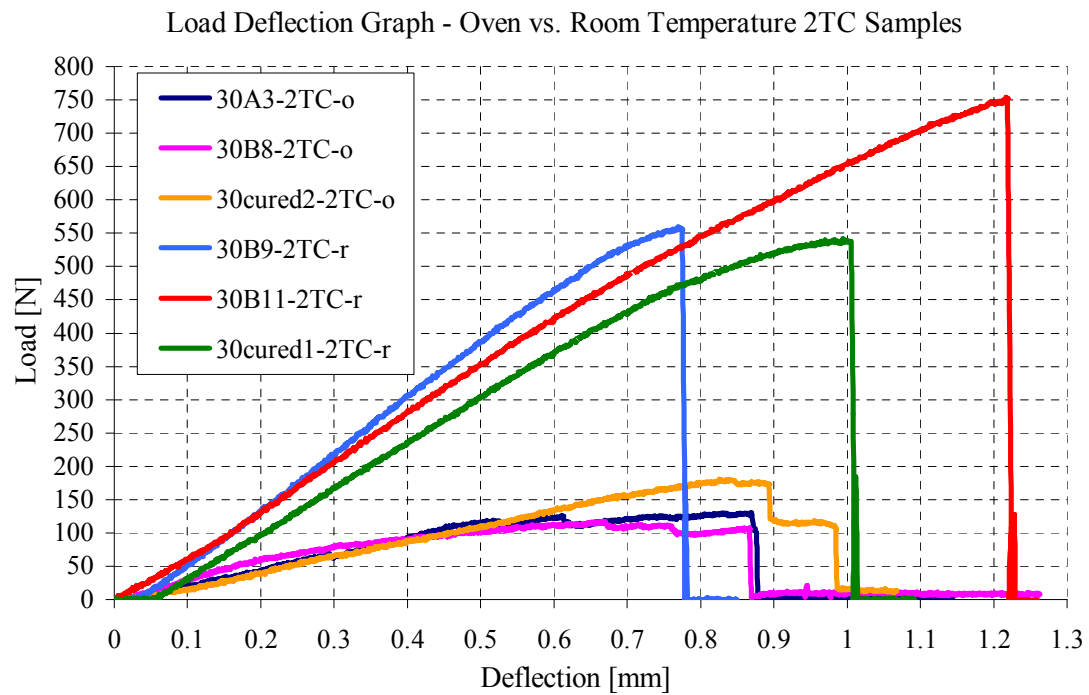Load Deflection Graph - Oven vs. Room Temperature 2TC Samples

Figure 29: Load deflection for oven vs. room temperature treated 30% 2TC samples

Figure 30: Load deflection for oven vs. room temperature treated 30% 2TN samples

Figure 31: Load deflection for oven vs. room temperature treated 40% 1TC samples

Figure 32: Load deflection for oven vs. room temperature treated 40% 1TN samples

Figure 33: Load deflection for oven vs. room temperature treated 40% 2TC samples
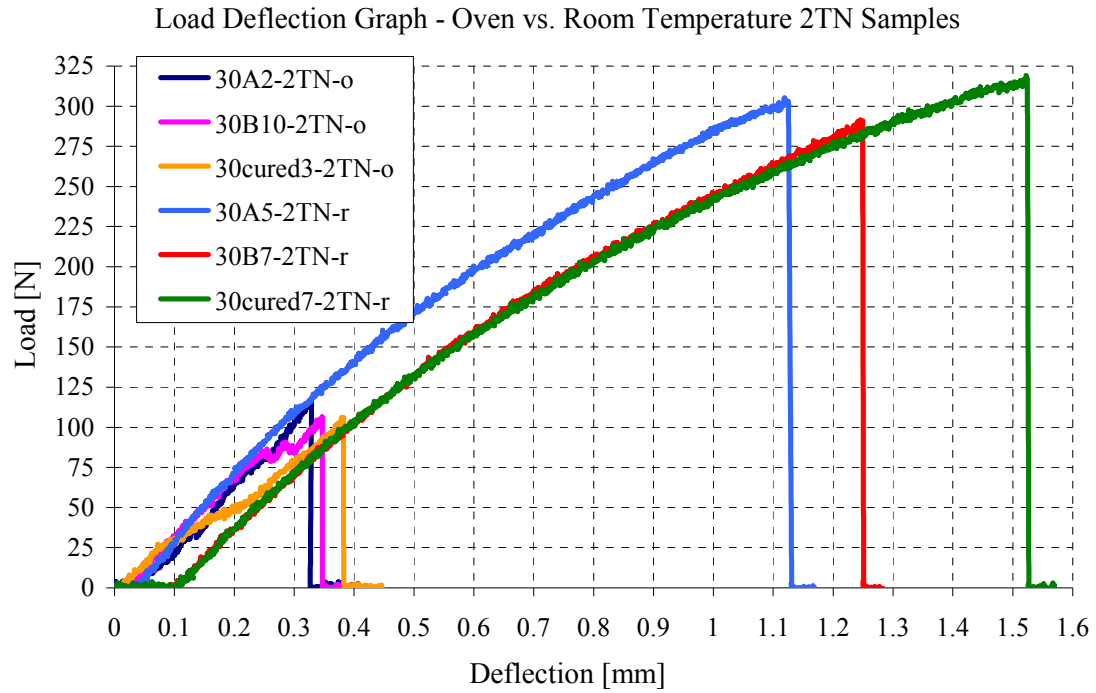
Figure 34: Load deflection for oven vs. room temperature treated 40% 2TN samples
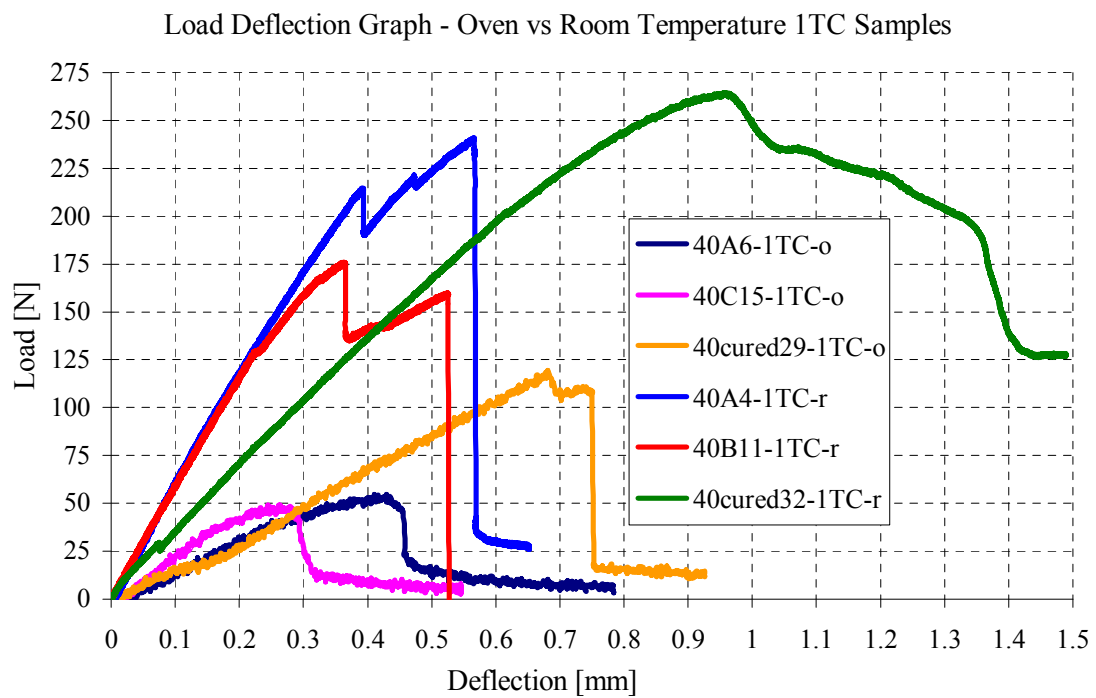

Figure 35: Load deflection for oven vs. room temperature treated 50% 1TC samples
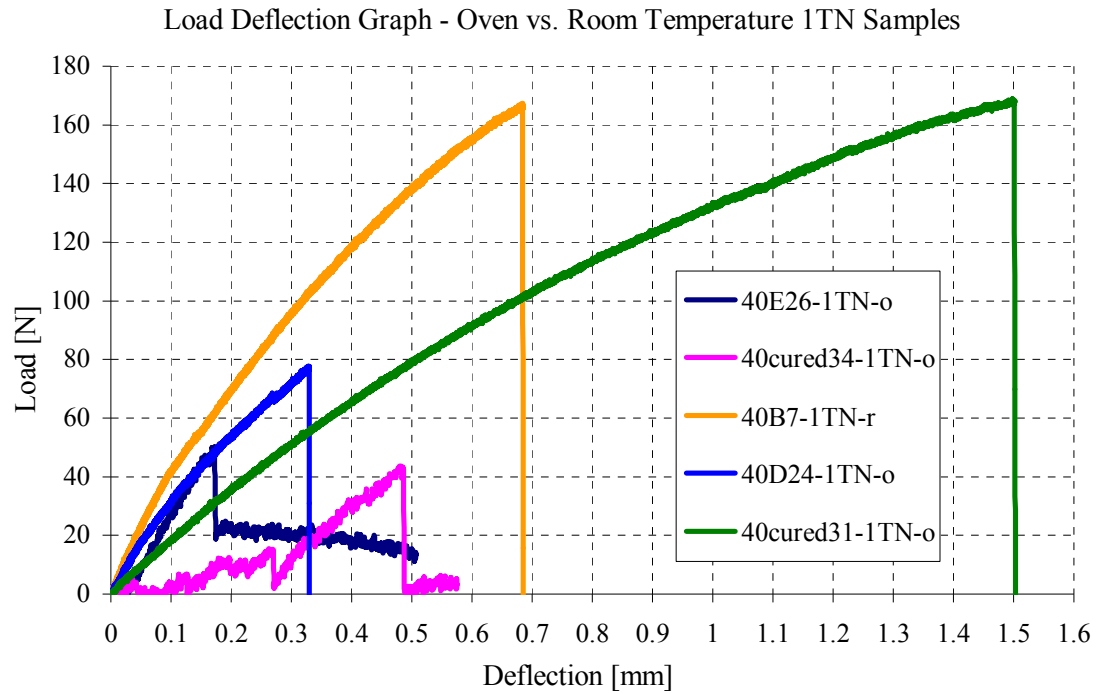
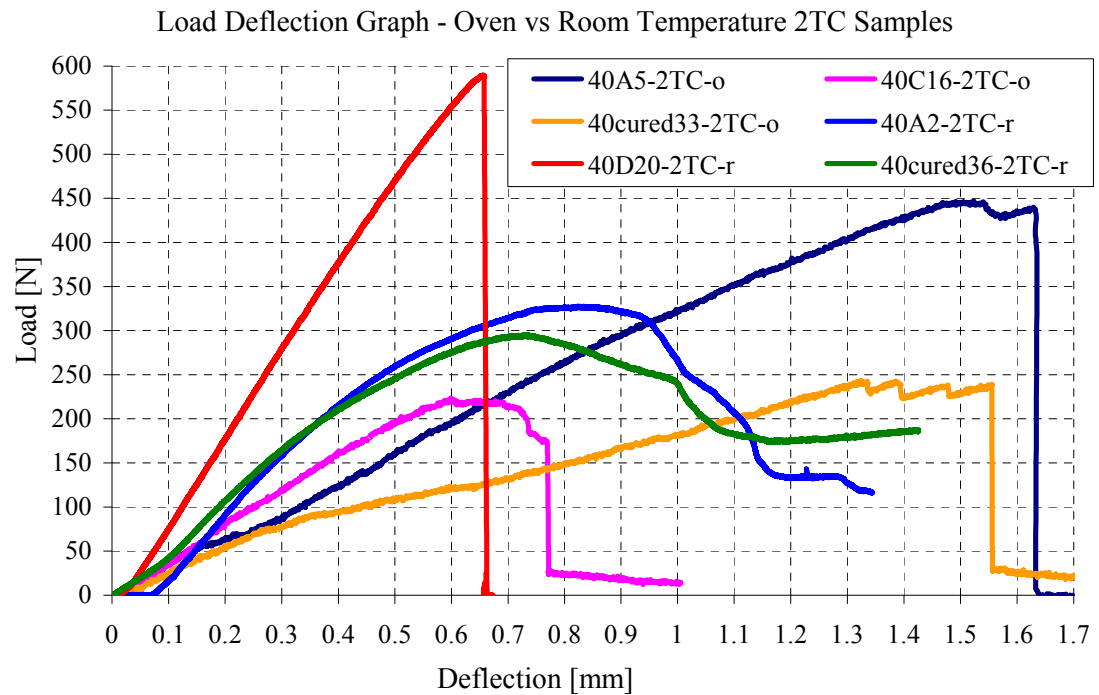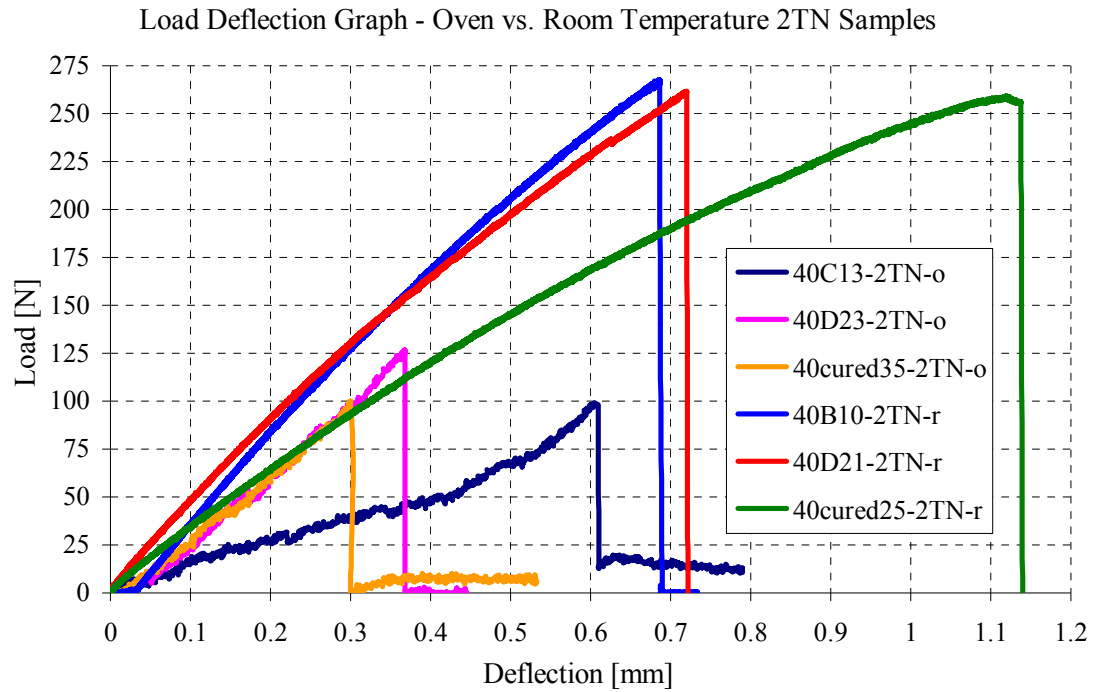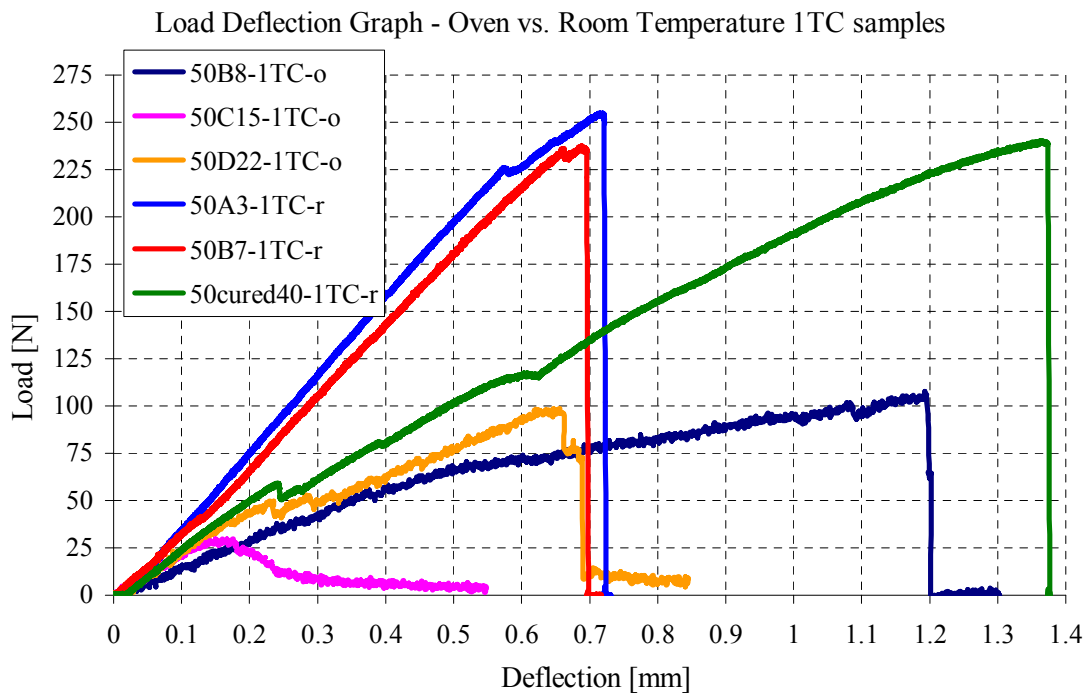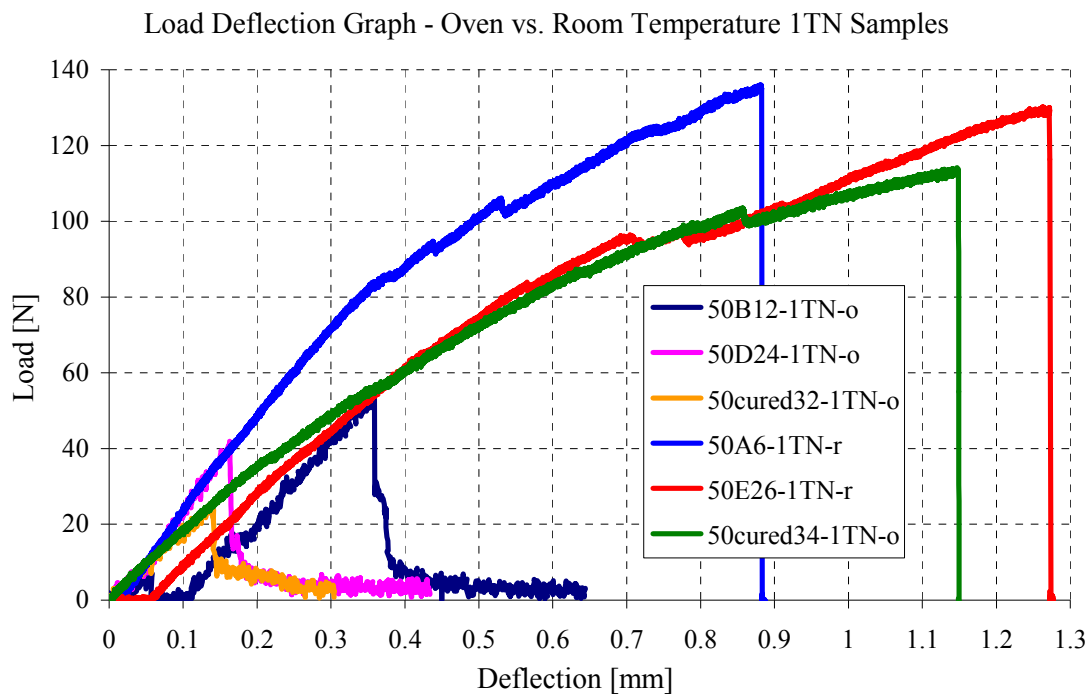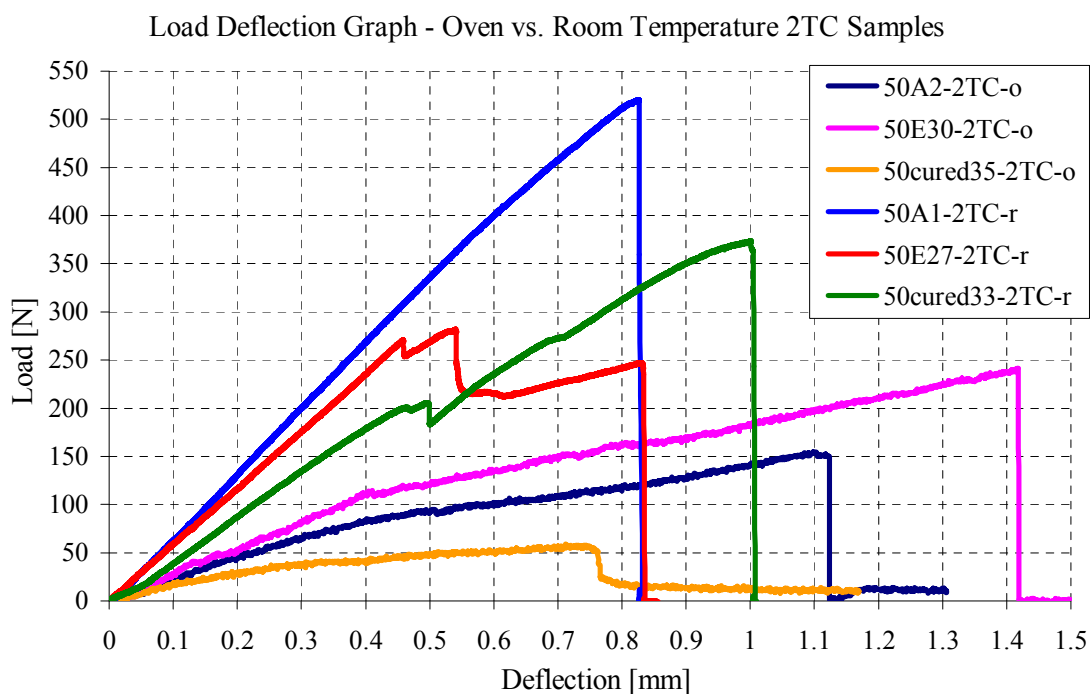Figure 36: Load deflection for oven vs. room temperature treated 50% 1TN samples

Figure 37: Load deflection for oven vs. room temperature treated 50% 2TC samples

Load Deflection Graph - Oven vs. Room Temperature 2TN samples
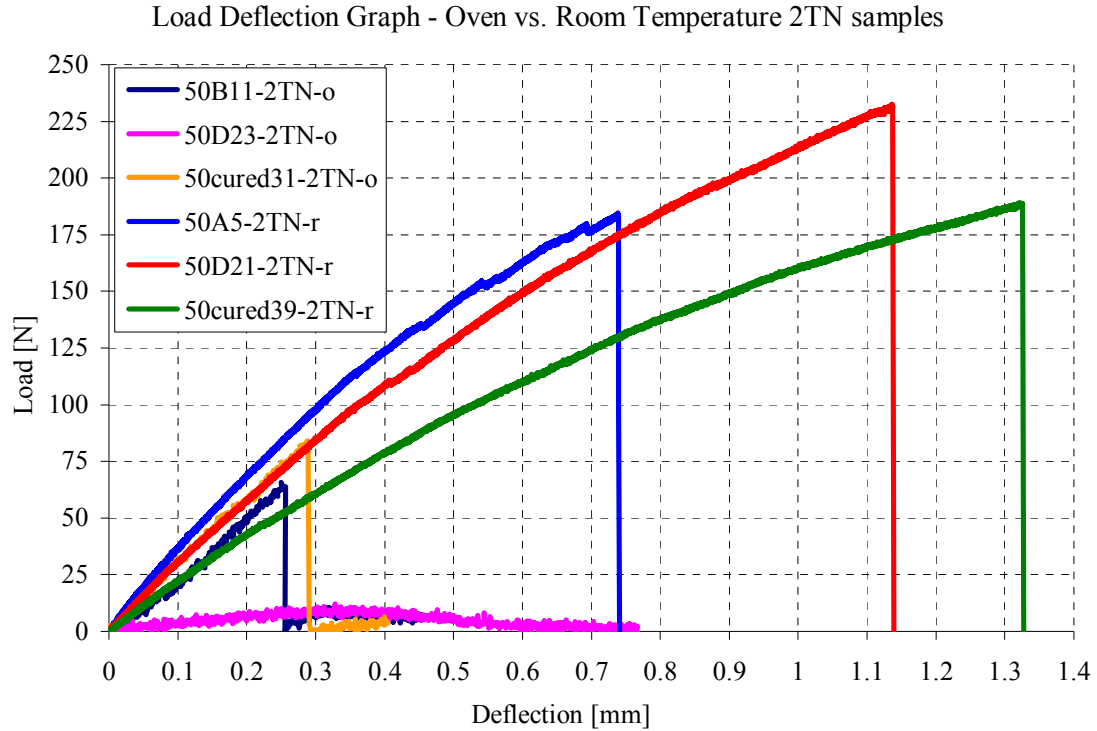
Figure 38: Load deflection for oven vs. room temperature treated 50% 2TN samples

From the presented graphs we can more precisely determine the influence of high-temperature treatment on sandwich structures. NEXTEL 610 fibers responded in a more consistent manner to the temperature treatment and presented predictable residual flexural capabilities. The reaction of DIALEAD samples to temperature cycles was inconsistent. It was noticed that high temperature conditions caused an increase in flexural toughness with two 2TC groups of 40 and 50%. The peak values of flexural force were lower, but the ability to sustain deformation before structure failure was significantly increased. In general, high temperature had a strong influence on carbon-reinforced structures; in certain areas fibers were dried out and some longitudinal delamination (between carbon fibers) was observed, though it appeared that those defects did not affect sandwich structure properties. DIALEAD-reinforced samples retained on

average 41% of their flexural force after exposure to temperature cycles. Carbon fibers gave us more erratic results, probably due to their higher modulus of elasticity (640 [MPa] for DIALEAD in comparison to 373 [MPa] for NEXTEL) and inconsistent fiber-wetting in a reinforcing layer. An unequal amount of geopolymeric glue, used for preparation of reinforcing layer, can cause significantly different flexural results from sample to sample. It was also mentioned before that geopolymeric glue swells up significantly when heated, so that property also can cause random fiber damage that will result in erratic and inconsistent results. But nonuniform wetting and adhesion of the carbon reinforcement layer provides the fiber an ability to adapt to significant core deformation by means of fiber pullout or limited fiber breaking. On the other hand, different thermal expansion of the core and reinforcing layer will probably increase levels of stress between the reinforcing skin and core and also between fibers themselves inside of the reinforcing layer. If we have all these arguments in mind, it is easy to understand obtained results and graphical data.

5.2.4 Calculations and analysis of momentum carrying capabilities

To try to eliminate the influence of different samples sizes and various cross-sectional dimensions, "equivalent" or standardized flexural stress will be calculated:

$$\sigma_i = \frac{6M_{Ui}}{bd^2}$$

Where:

- σ_i is the equivalent flexural moment of certain sample.

- M_{Ui} is the maximal flexural moment obtained from the tests.

This "equivalent" flexural stress σ_i does not represent the real state of stress levels inside the material, since sandwich samples are inhomogeneous. In this case, "equivalent" stress is used to reduce the influence of different sample dimensions. This is done to have a better understanding of the levels of stresses experienced with assumption that the material was homogenous. Changes in the equivalent flexural stress of the samples, caused by different types of reinforcement and temperature treatments, are presented in the following graphs - Figures 39 to 42.

Equivalent Flexural Stress

Figure 39: "Equivalent" flexural stress for reference and the 1TC group of samples

Sample number:	Reference group	1TC oven group	1TC room temperature group
1	30A1	30D19	30A6
2	30D20	30D24	30D22
3	30cured4	30cured9	30cured10
4	40A1	40A6	40A4
5	40C18	40C15	40B11
6	40cured26	40cured29	40cured32
7	50C13	50B8	50A3
8	50D19	50C15	50B7
9	50cured36	50D22	50cured40

Table 4: Numeration for the 1TC samples

Figure 40: "Equivalent" flexural stress for reference and the 1TN group of samples

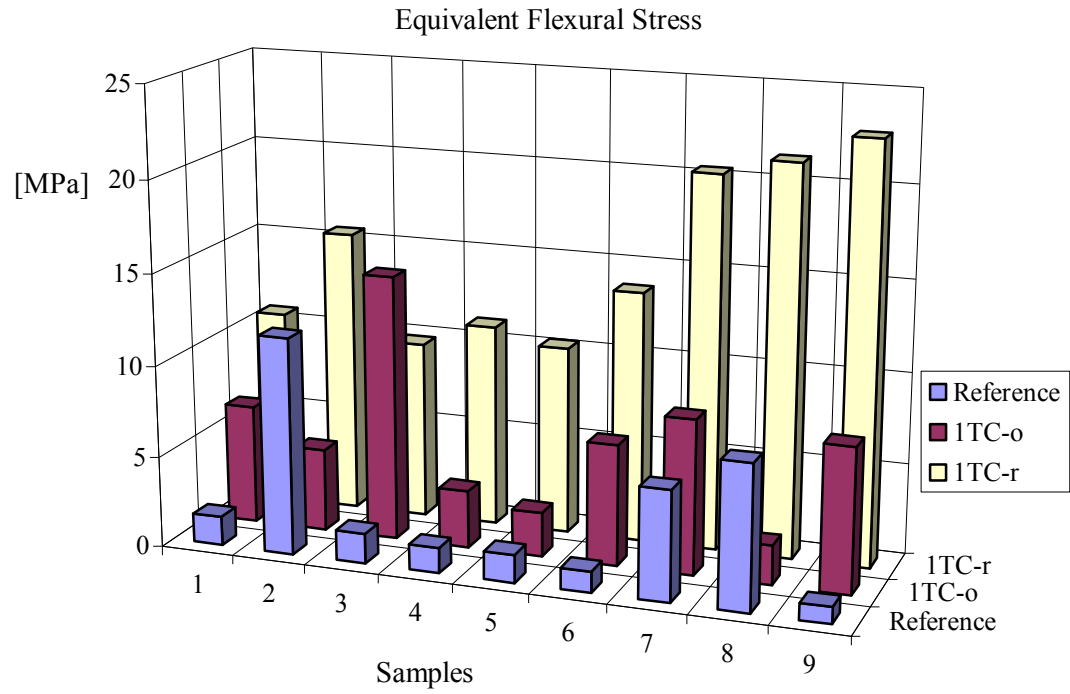| Sample number:	Reference group	1TN oven group	1TN room temperature group
1	30A1	30D21	30A4
2	30D20	30D23	30B12
3	30cured4	30cured6	30cured8
4	40A1	40E25-dmg	40B7
5	40C18	40E26	40D24
6	40cured26	40cured34	40cured31
7	50C13	50B12	50A6
8	50D19	50D24	50E26
9	50cured36	50cured32	50cured34

Table 5: Numeration for the 1TN samples

Figure 41: "Equivalent" flexural stress for reference and the 2TC group of samples

Sample number:	Reference group	2TC oven group	2TC room temperature group
1	30A1	30A3	30B9
2	30D20	30B8	30B11
3	30cured4	30cured2	30cured1
4	40A1	40A5	40A2
5	40C18	40C16	40D20
6	40cured26	40cured33	40cured36
7	50C13	50A2	50A1
8	50D19	50E30	50E27
9	50cured36	50cured35	50cured33

Table 6: Numeration for the 2TC samples
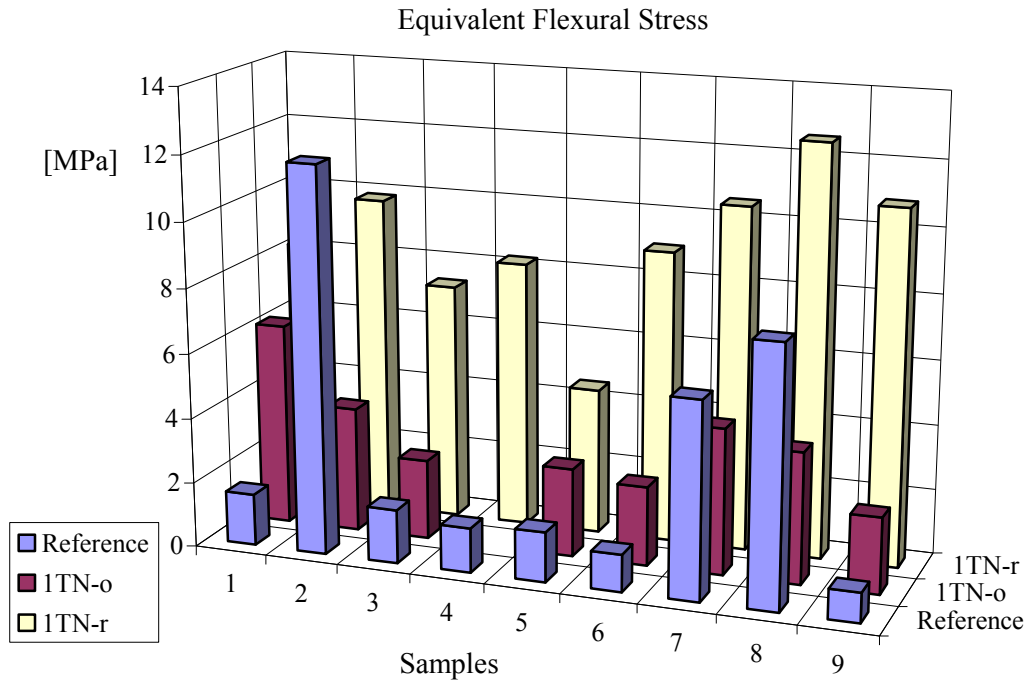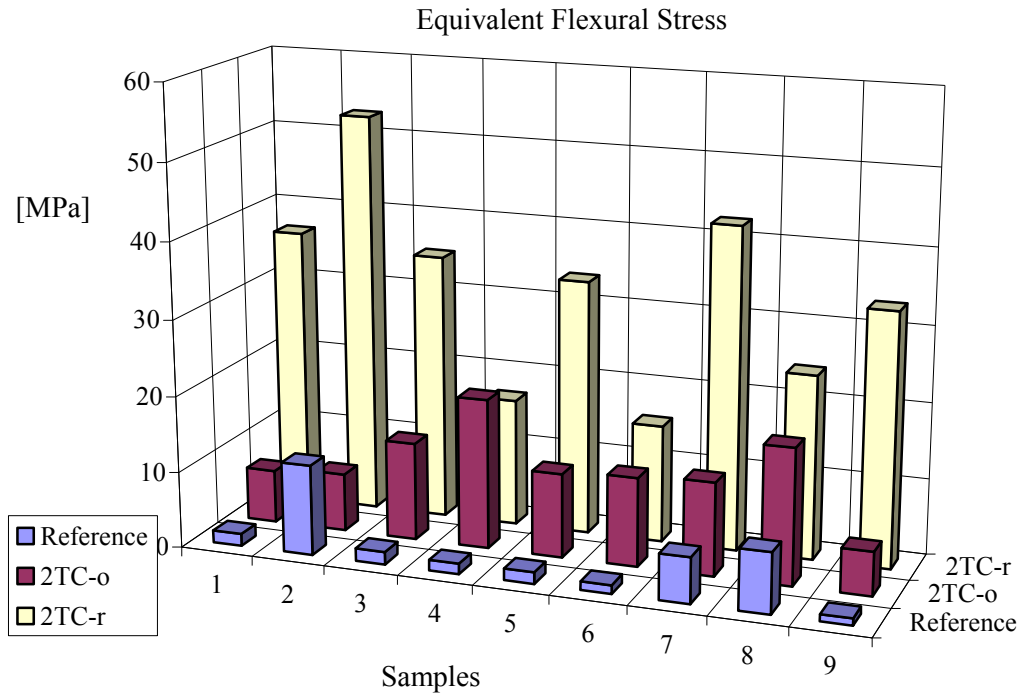
Equivalent Flexural Stress
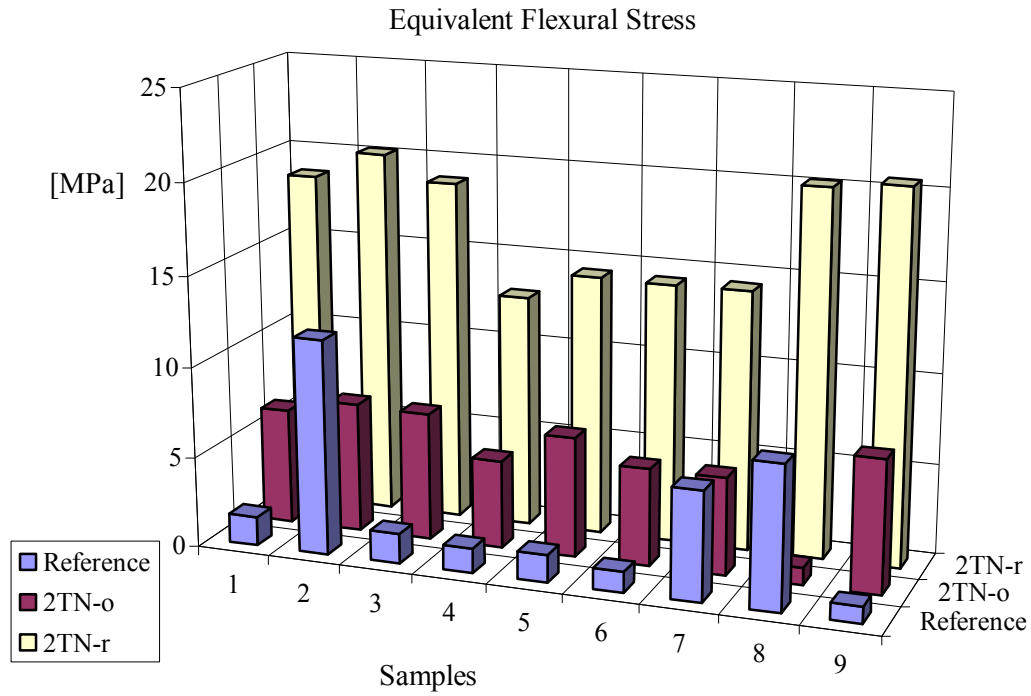
Figure 42: "Equivalent" flexural stress for reference and the 2TN group of samples

Sample number:	Reference group	2TN oven group	2TN room temperature group
1	30A1	30A2	30A5
2	30D20	30B10	30B7
3	30cured4	30cured3	30cured7
4	40A1	40C13	40B10
5	40C18	40D23	40D21
6	40cured26	40cured35	40cured25
7	50C13	50B11	50A5
8	50D19	50D23	50D21
9	50cured36	50cured31	50cured39

Table 7: Numeration for the 2TN samples

5.2.5 Flexural toughness

To incorporate the effects of measured sample deflection and to connect it to flexural force, flexural toughness was calculated. Flexural toughness was calculated as the total area under the load deflection graphs until (in our case) maximum load was achieved. Some authors used the ASTM C1018 standard and the point of first failure [56], [57], but since nature of our fibrous reinforcement does not provide a definite "first failure", the point of maximum sustained load was used. Data is presented in the following graphs - Figures 43 to 46.
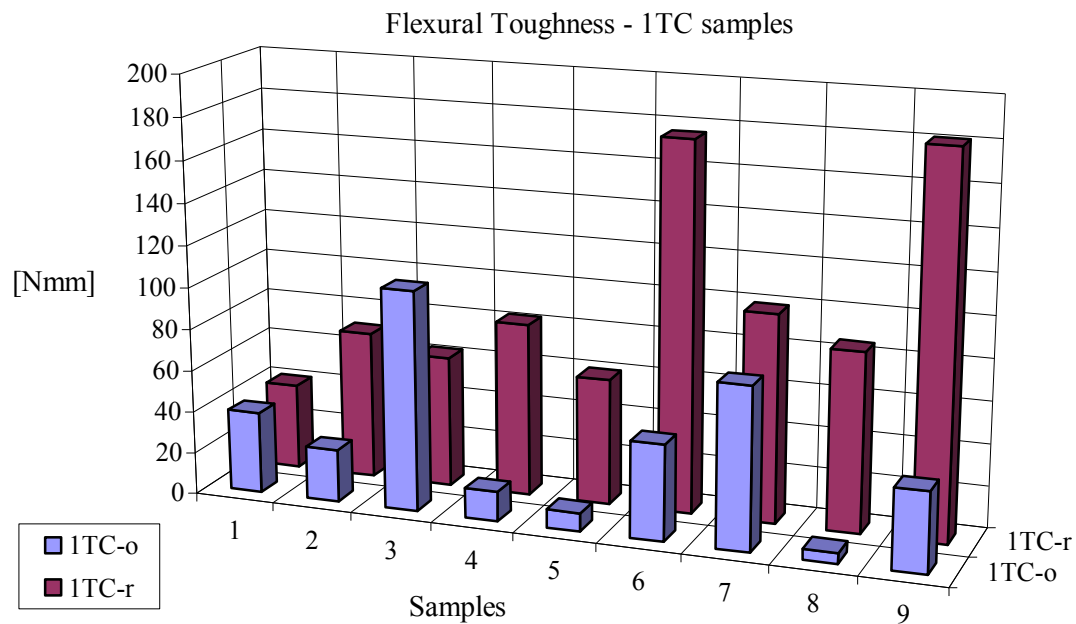

Figure 43: Flexural toughness - 1TC samples (oven and room temperature)

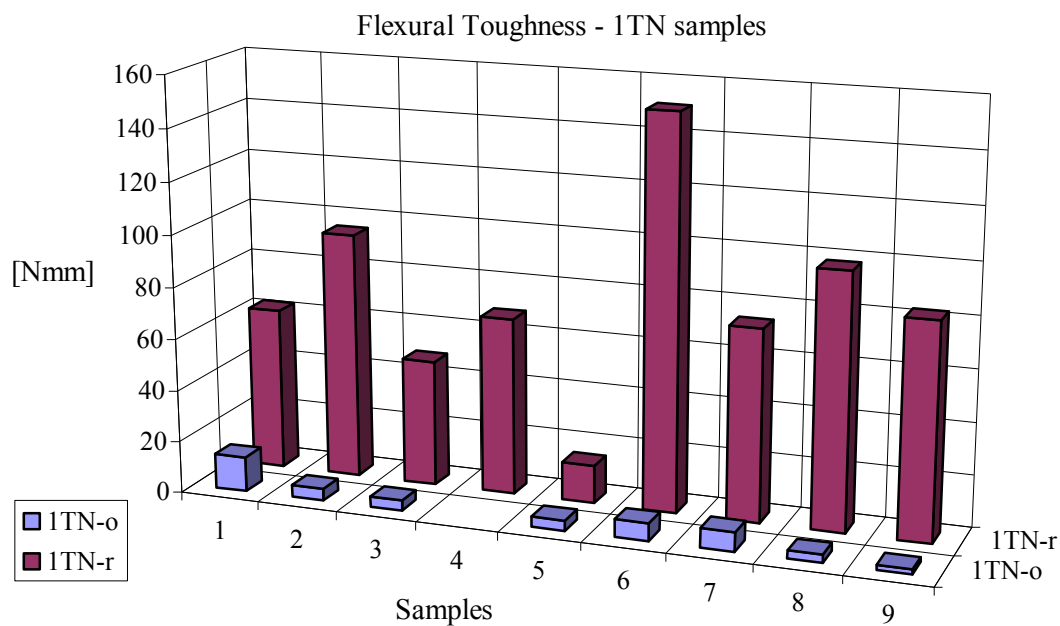For sample identification, refer to Table 4.

Figure 44: Flexural toughness - 1TN samples (oven and room temperature)

For sample identification, refer to Table 5.
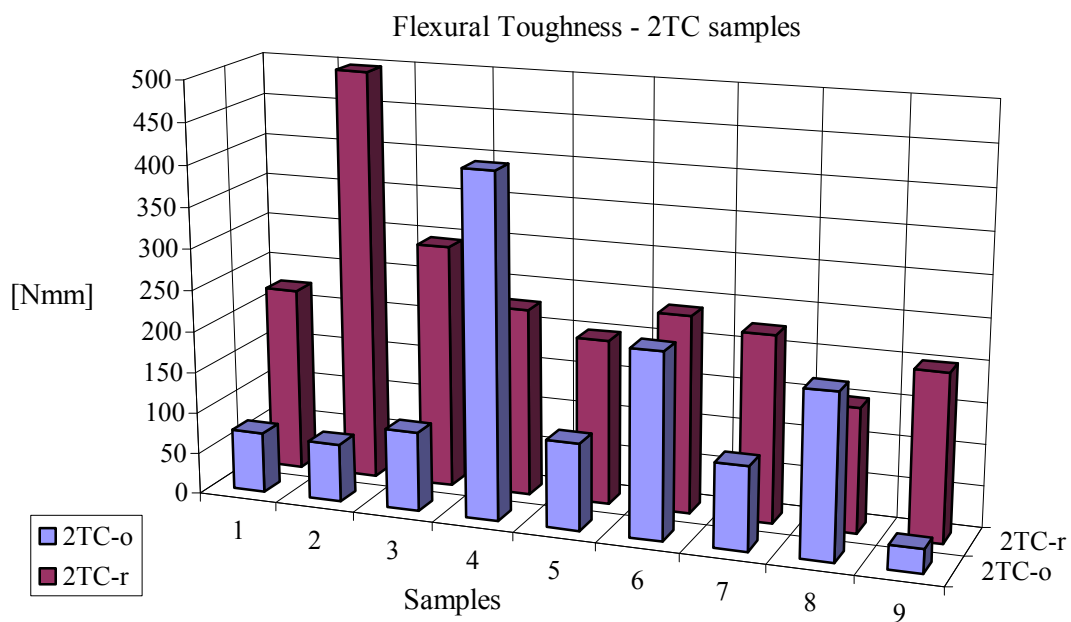
Figure 45: Flexural toughness - 2TC samples (oven and room temperature)

For sample identification, refer to Table 6.

Flexural Toughness - 2TN samples
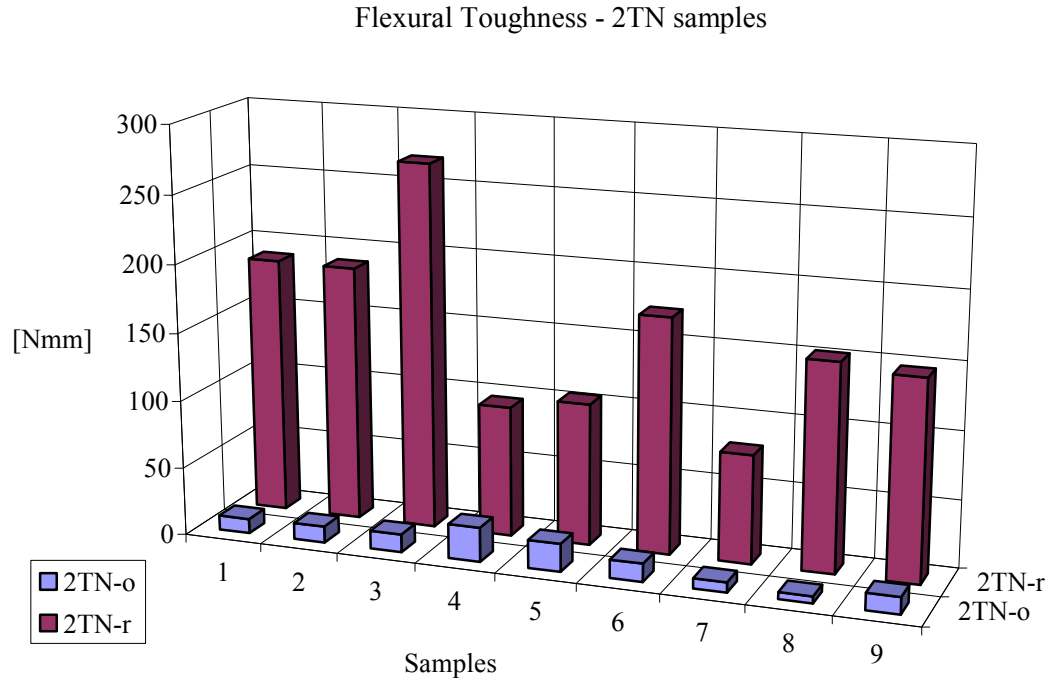
Figure 46: Flexural toughness of 2TN samples (oven and room temperature).

For samples identification, refer to Table 7.

Due to inconsistent results, it was difficult to perform relevant statistical analysis of the obtained results, but general trends could be observed:

- Flexural toughness is severely diminished by thermal treatment.

- Structures reinforced with DIALEAD fibers experienced 20-30% higher stress than NEXTEL-reinforced ones (which can be explained by the larger cross section of total DIALEAD fibers used, comparing to NEXTEL 610).

- After temperature treatment all structures lost between 60-80% of their strength, comparing to samples that were not exposed to high temperature cycles.

- Temperature-treated samples reinforced with DIALEAD fibers had a tendency to keep reinforcing trend after temperature cycles in contrast to NEXTEL 610 fibers which showed almost a total loss of their flexural and toughness properties.

- In several cases with temperature-untreated samples, it was noticed that "cured" samples possessed flexural toughness equal to or higher than that of other samples.

- NEXTEL 610 reinforced samples produced generally more consistent response, with or without temperature treatment.

5.3 Sandwich structure analysis

Testing samples used in this experiment were not homogenous, thus the regular approach for the calculation of stress, strain and modulus of elasticity for homogenous body could not be used. Our samples could have been treated as composites but since we have a thick, relatively weak core and two layers of fibrous reinforcing skin, it was best to treat and evaluate our samples as sandwich structures. To test and analyze the flexural properties of sandwich structures, the ASTM C393 [58] standard was used.

5.3.1 Core shear stress for sandwich structures:

$$\tau = \frac{P}{(d+c)b}$$

τ - Core shear stress [MPa]

P - Load [N]

d - Sandwich thickness [mm]

c - Core thickness [mm]

b - Sandwich width [mm]

Core shear stress values are presented in correlation with geopolymer mass ratio. It can be noticed that there is no specific behavior that is connected to cenosphere mass ratio percentage that is used for different sample groups. Samples reacted in a similar manner and the only obvious change in sample reaction was usage of different types of fibrous reinforcements. The highest levels of core shear stress were generated with two tow reinforcements, both carbon and aluminum. Core shear stress values go from 0.019 to 1.1588 [MPa]. In this case, it is important to show possible correlation between shear stress values and cenosphere mass ratio, so particular core shear values for each tested sample are not presented - Figure 47; for sample identification refer to Table 8.

Group	1, 2, 3	4, 5, 6	7, 8, 9
Cenosphere mass ratio	30%	40%	50%

Table 8: Sample numeration (connected to Figure 47).

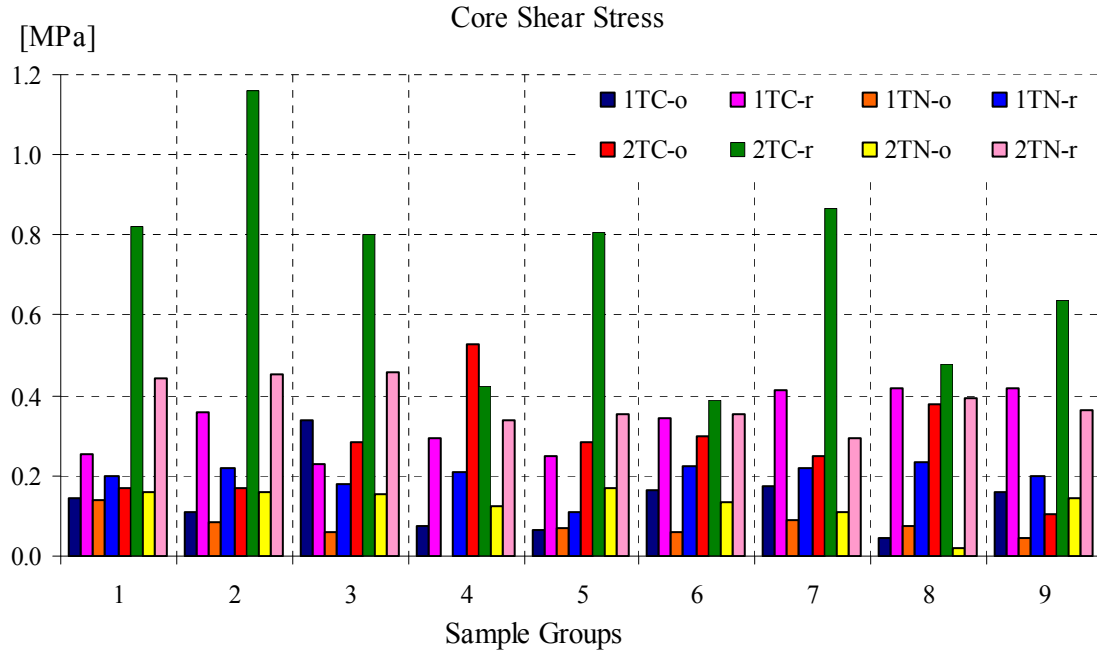Figure 47: Core shear stress for sandwich structures - all tested samples.

5.3.2 Facing bending stress for sandwich structures:

$$\sigma = \frac{PL}{2t(d+c)b}$$

σ - Facing bending stress [MPa]

t - Facing thickness [mm]

L - Testing span length [mm]

Facing bending stress depends not only on loading force but also on reinforcement thickness. Reinforcement thickness is similar inside sample groups made

with the same material and number of tows. From the graph we can conclude that NEXTEL-reinforced samples, which have a smaller total thickness of reinforcing layers than DIALEAD, have generated highest stress rates. NEXTEL 610 fibers usually failed on average of 2002 [MPa] and after oven treatment on average of 732 [MPa]. NEXTEL fibers should have retained about 80% of their primary strength, but in reality they retained on average 37%. This huge discrepancy can probably be explained by the inconsistent properties of the geopolymeric core material and high thermal expansion that could have caused stress concentrations, fiber damage and premature failure. A similar response happened with DIALEAD-reinforced samples; they failed on average of 745 [MPa] and after temperature treatment at 305 [MPa] and that shows only about 41% of strength retention. On the following graph sample density and facing bending stress are presented, but after analyzing the results no significant correlation between these two properties has been determined - Figure 48.
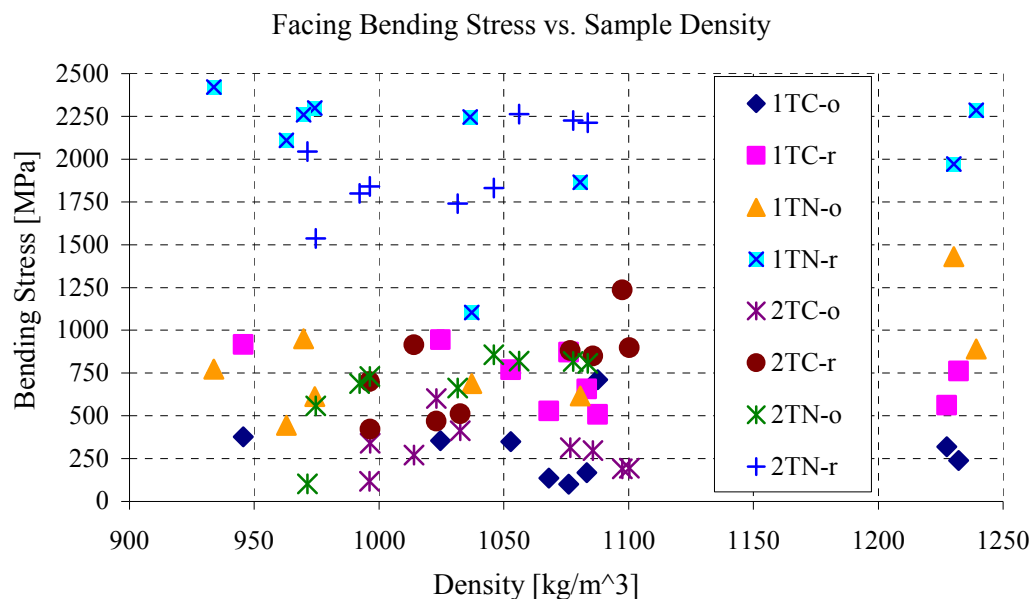

Figure 48: Facing bending stress vs. sample density - all tested samples.

5.3.3 Sandwich beam deflection:

The first element of the equation represents deflection caused by bending. The second element of the equation represents deflection caused by shear.

$$\Delta = \frac{PL^3}{48D} + \frac{PL}{4U}$$

Δ - Total beam midspan deflection [mm]

D - Panel bending stiffness [N mm^2]

$$D = \frac{E(d^3 - c^3)b}{12}$$

E - Facing modulus of elasticity [MPa]

U - Panel shear rigidity [N]

Panel bending stiffness depends only on samples' physical properties (such as width, thickness and type of reinforcement) and not on values of measured force and deflection. Representing measured deflection and panel bending stiffness on the same graph can help to determine possible correlation between these two properties. After analyzing this graph, due to inconsistent values of deflection, no correlation was determined - Figure 49.
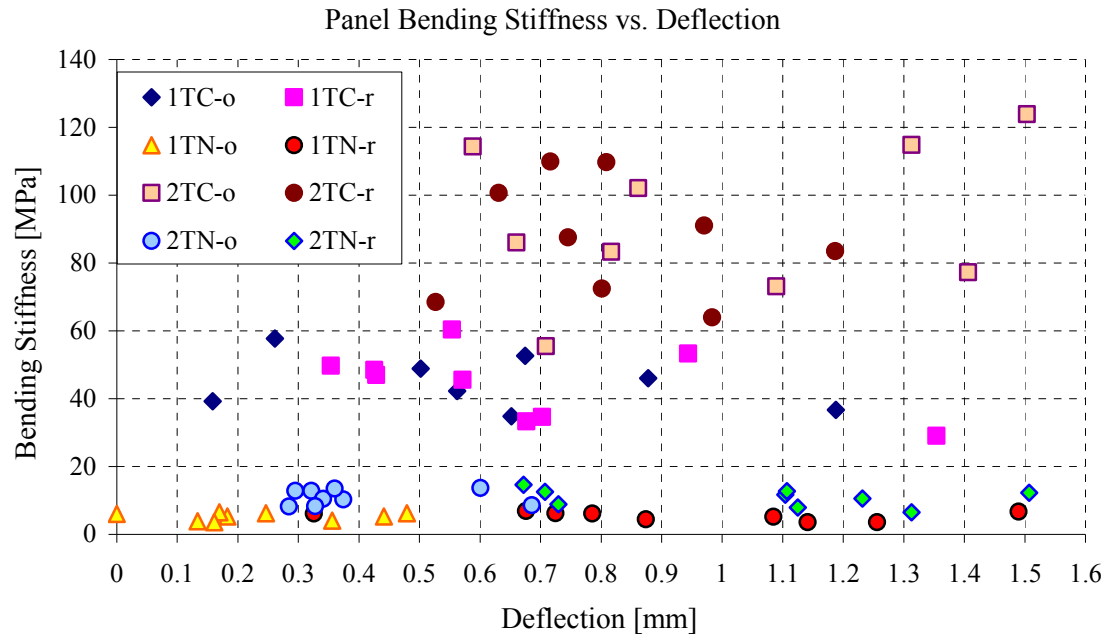
Figure 49: Panel bending stiffness vs. deflection

CHAPTER 6 - SEM ANALYSIS

To analyze material microstructure, interaction between the reinforcing fibers and core and temperature effects, several samples were examined by a Scanning Electron Microscope. Following criterions for choosing the SEM sample donors were applied:

- Samples donors had to be good representatives of properties that were analyzed (flame and temperature cycle effects; interaction among the fibers, core and geopolymer bonding agent; micro structural changes caused by flexural loading).

- Samples were picked to show possible differences between specific sample groups (different cenosphere mass ratios and fiber reinforcement influences).

Several good donor samples were chosen and a fine rotating blade cut the desired parts of material from the donor samples. The material parts were obtained from the bottom, tensile-loaded side so that they would in best way represent the cracking surface, thermal damage and micro structural changes in specific areas and the material in general. Each SEM sample had an approximate size of 5x5x5 [mm]. A total of 7 samples was inspected.

6.1 General structure SEM

Figure 50 presents the micro structure of an average sample made of donor that was tested in flexure and had no temperature treatment. Certain elements can be recognized:

- Cenospheres are scattered across the scan area. There is no evidence of aggregating, mixing is good, and different cenosphere sizes can be noticed.

- Different types of voids are present. Some are products of geopolymerization and are formed as cenospheres are dissolved. Others can be explained as residues of trapped air.

- Three whole perlite grains.

- Two areas of crushed perlite crystals (upper left and lower right).

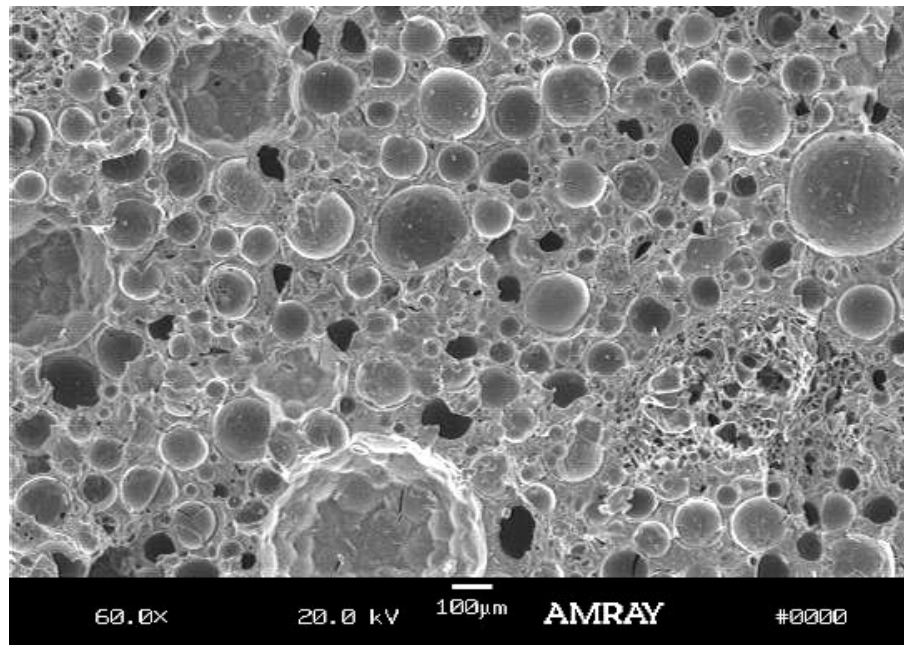Figure 50: General SEM of geopolymeric sandwich core, no heating effects 50A3-1TC

After analysis of all SEM photographs, it was concluded that the majority of samples have problems with homogeneity, voids, bubbles and crevices that are captured in the material. It is possible that if a different, more precise manufacturing process was used, some of those defects could be avoided and their influence cut to a minimum. In

several places, big chunks of perlite crystal disturbed the material core structure. In connection with that, it was noticed that in several cases material failure cracks usually went through perlite particles but did not cause debonding between slurry and perlite. Adhesion between highly alkaline slurry and perlite crystals is very good, since perlite dissolves in highly alkaline solutions [55]. This property provides excellent cohesion between slurry and crystals, and it is even stronger than the tensile capacity of crystal itself. Also we can look at the perlite particles (which are larger than other elements of the mixture) as stress concentrations and crack generators that could diminish the mechanical properties of the material. During this SEM scan, we could not find any proof that cracks begin in perlite particles or that they are a major cause of sample failures. To avoid the mentioned problems, finer-grade, or pulverized perlite could be used [59]. That will diminish the negative influence generated by big particles, but the other good properties that perlite provides as a filler will be preserved.

6.2 Cenosphere dissolving problem

When used during the geopolymer preparation, hollow cenospheres were fully or partially dissolved and fused with alkaline solution (in this case they will react with K and Al_2O_3) and would later form geopolymeric crystals. Figure 51 shows a semi dissolved cenosphere with some gas bubbles trapped in the rim. We have to be aware that geopolymerization is a very sensitive chemical reaction and that slight changes in molar ratios of reacting agents can totally change the properties of the produced material [60]. Different ratios of active agents strongly influence the cenosphere dissolving level

and other material properties [61]. As we can see the level of cenosphere dissolution is higher in the 30% group and lower in the 50% group - Figure 52.
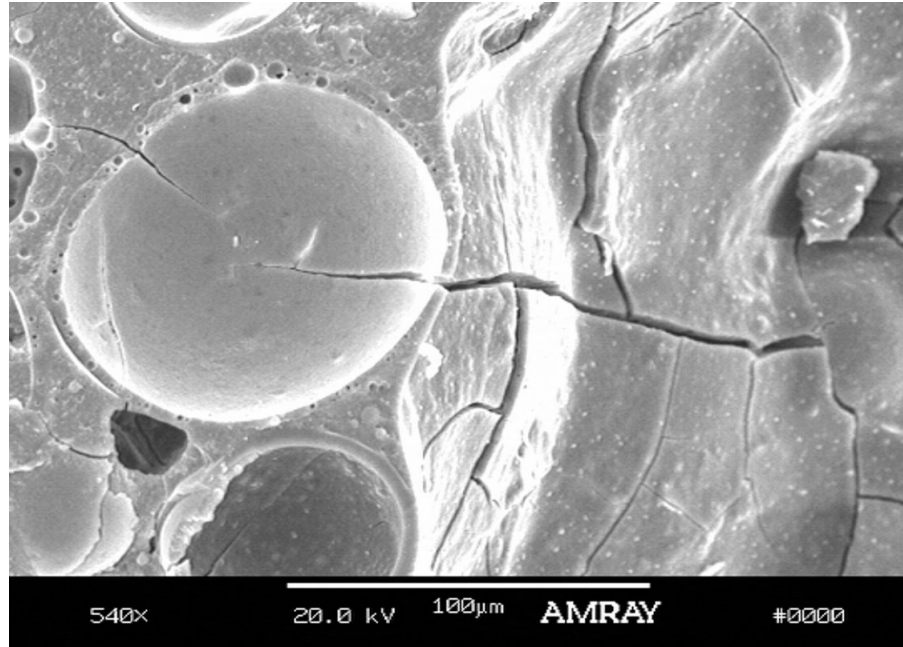

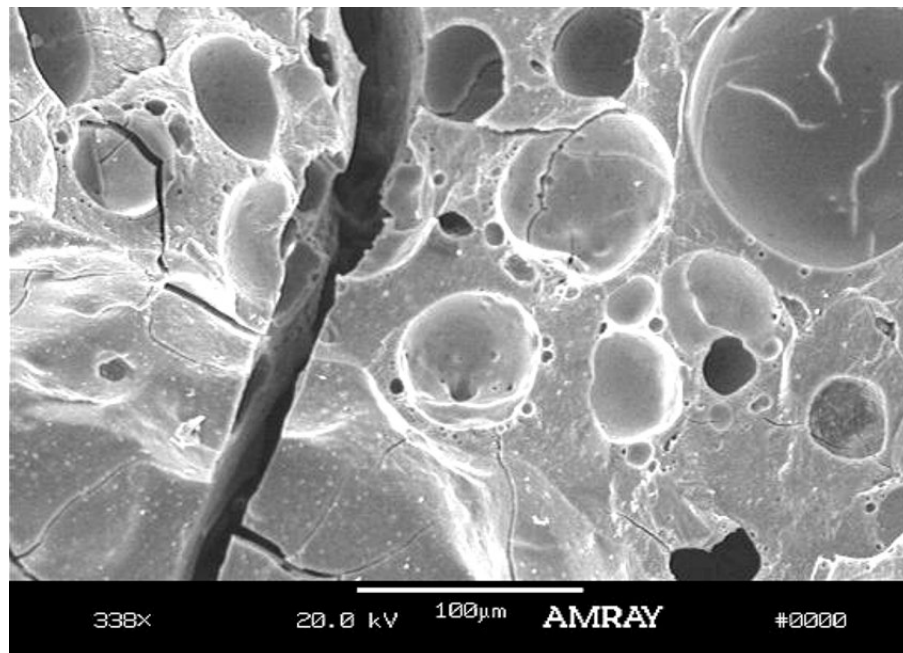Figure 51: Cenosphere contact with geopolymer core - 30A5-2TN

Figure 52: Perlite particle and surrounding material - crack progression - 30A5-2TN

In addition, it is evident that not all of the cenospheres were dissolved and "geopolymerized" and we have to be aware that during geopolimerization some spheres will be fused or "incorporated" into the surrounding material, but a spherical void will take its place. These voids can decrease material properties, by decreasing material homogeneity or by acting as point failures that will cause stress concentrations and premature cracking. Also, we can see that contact between the spheres and geopolymer is generally very good, though after exposure to high temperature some borderline cracking tends to appear - Figure 52 and Figure 53.
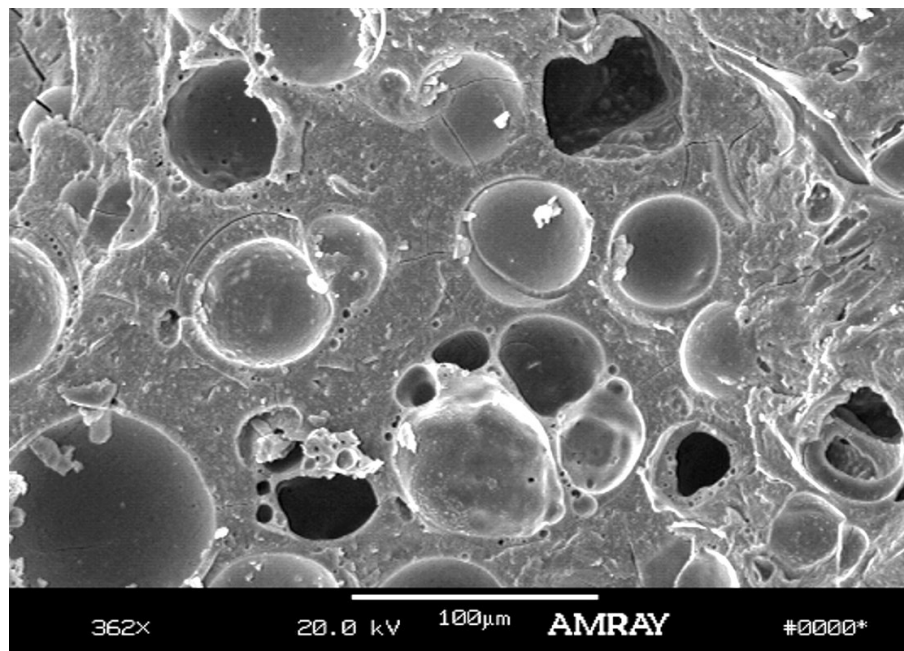

Figure 53: Dissolved cenospheres 30A5-2TN

6.3 High temperature influence on material microstructure

High temperatures significantly affect material microstructure. After exposure, cenospheres tend to break or melt; the material is swells and develops a more sponge like

structure. The level of material swelling and volume change was not measured directly, but it was significant. The observed debris and voids were formed probably by several different mechanisms:

- Thermal degradation and high thermal expansion of the geopolymer material.

- Increased pore pressure and water evaporation [62].

- Degradation and melting of glass spheres.

- Expansion and interconnection of voids that were already trapped in the material.

The average void size in samples that were not temperature-treated (if we exclude serious defects) was in a range of 10-20 [μm], but after exposure to 750°C the material became more porous and large voids were formed from connected bubbles or burned spheres. The size of newly formed voids was generally in a range of 100-200 [μm] and they became the dominating element of the core matrix. Material porosity change was not measured, but it can be done by using the mercury porosimetry method. These types of defects significantly diminish the flexural properties and strength of sandwich structures - Figure 54, 55 represent regions before and after temperature/flame exposure.

When comparing samples with different cenosphere mass ratio percentages, we noticed that the amount of structurally sound spheres was higher with higher mass ratios (the number of dissolved particles was lower with the 50% group and higher with 30%), which was expected since lower volumes of spheres can react better with larger amounts of active agents. But to understand how this affects samples' mechanical properties, we have to be aware of sample density and how density change can affect material or structural properties. It was noticed that all sample groups have problems with homogeneity and this was not connected to any group in particular.
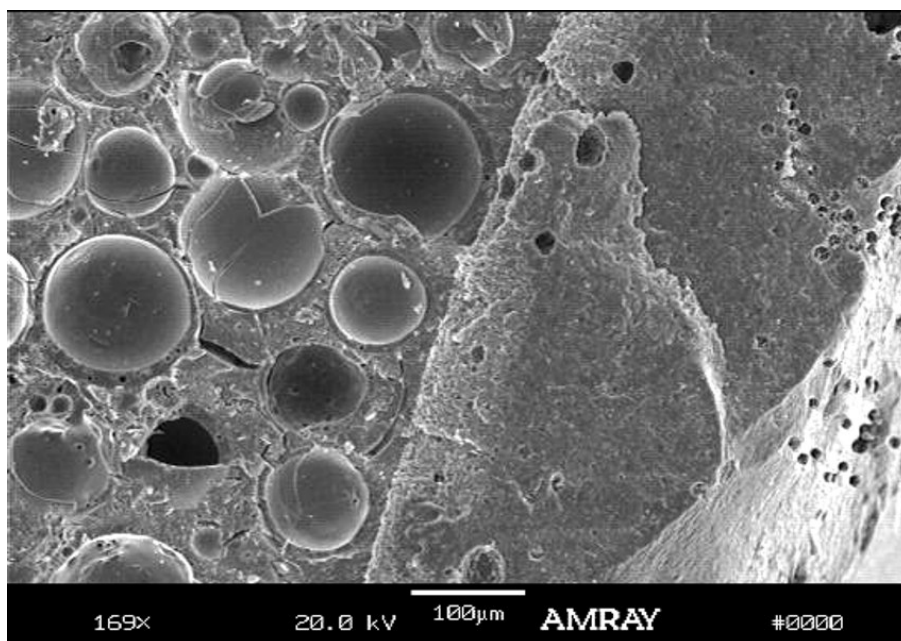
Figure 54: Contact region before high temperature exposure 50A3 1TC
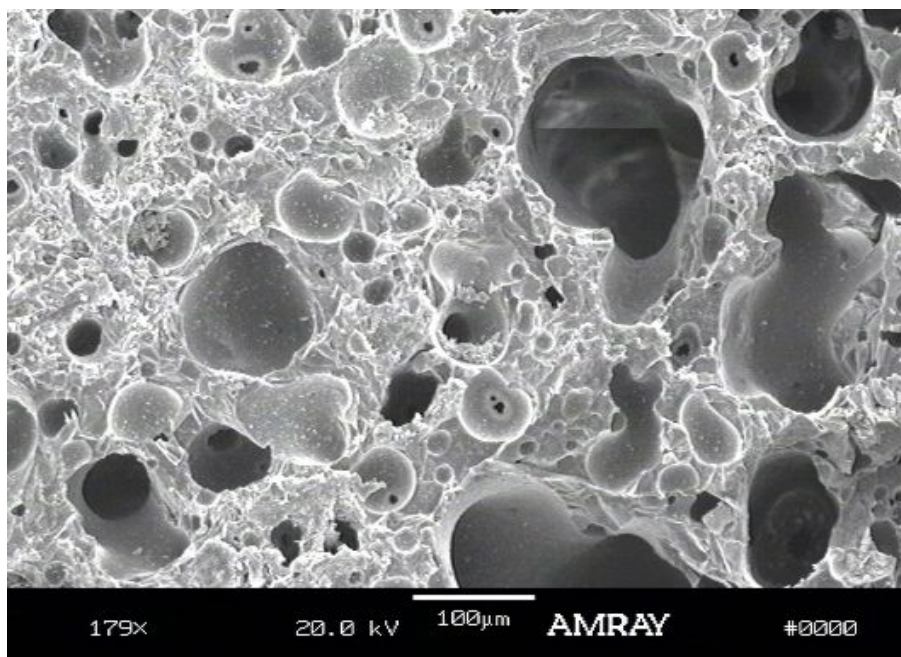
Figure 55: High temperature effect on general material microstructure 40cured25 2TN

6.4 Fiber to geopolymer adhesion

One of the possible issues was bonding and adhesion between the reinforcing fibers and geopolymer core; we were not sure if the fiber would be saturated enough and if the bonding between the fibers and geopolymer glue would be sufficient. After analyzing SEM scans of different areas of the reinforcing skin, we concluded that bonding between the fibers, both NEXTEL 610 and DIALEAD, and geopolymer was very good. NEXTEL 610 fibers have chemical structure (99% AL_2O_3) that is compatible with geopolymer based (rich with SiO_2) highly alkaline solution. The saturation and bond was very good, but some trapped voids could be observed at several places beneath the reinforcing layer - Figure 56.

Figure 56: NEXTEL reinforcing layer (after flexure test) - 40D21 2TN

DIALEAD fibers had also very good adhesion to the geopolymeric core; wetting of fibers was also very good. A more careful chec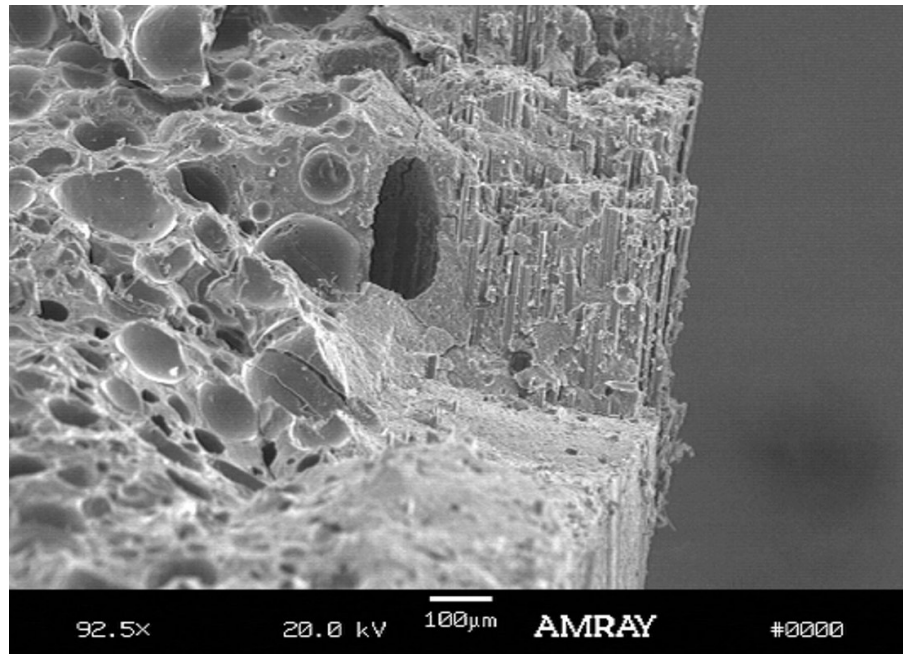k had shown traces of fiber pullout (SEM scans are mostly done on bottom tensile surface that was also exposed to the flame or high temperature). After checking the load deflection graphs, we concluded that SEM findings support graphical data, that material failed more gradually and that fiber pullout was one of the mechanisms for stress relief - Figure 57 and 58. It should be noted that DIALEAD fibers did not have any sizing.

High temperature exposure severely affected both types of reinforcements. The reinforcing layer expanded voids and cracks developed; in addition, deterioration of the contact layer between the core and reinforcement was also noticed. Decreased material homogeneity increased the possibility of premature reinforcement failure since fibers lost some of their bonding contact and support - Figure 59. Increase in number and volume of voids between the skin and the core increased the possibility of delamination and premature structural failure - Figure 60 (compare to Figure 54).
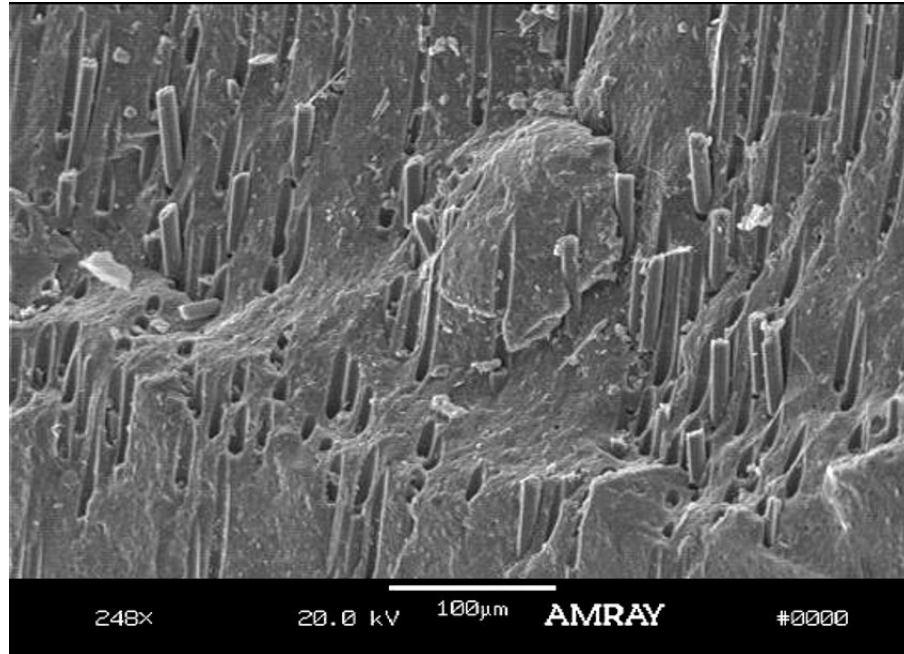
Figure 57: Carbon fibers pullout, 2TC-reinforcement
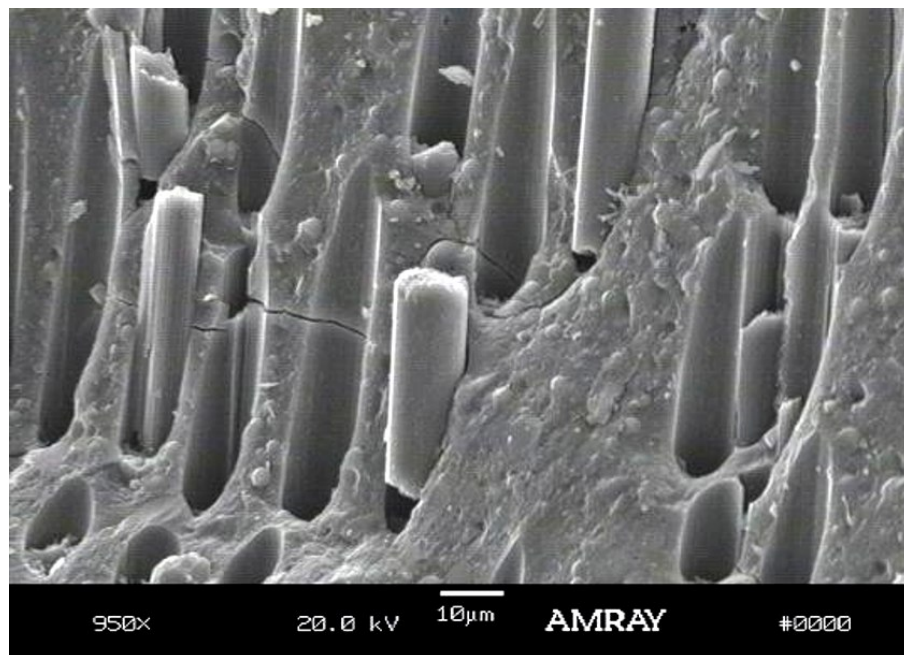
Figure 58: Carbon fibers pullout (detail), 2TC reinforcement
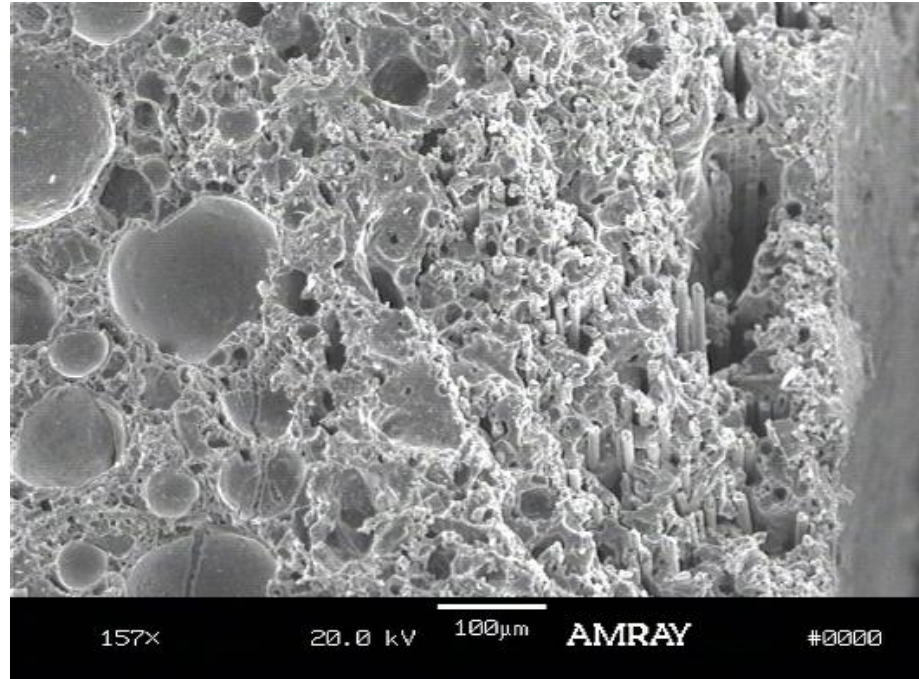
Figure 59: Reinforcing layer and contact zone affected by high temperature 50A3-1TC
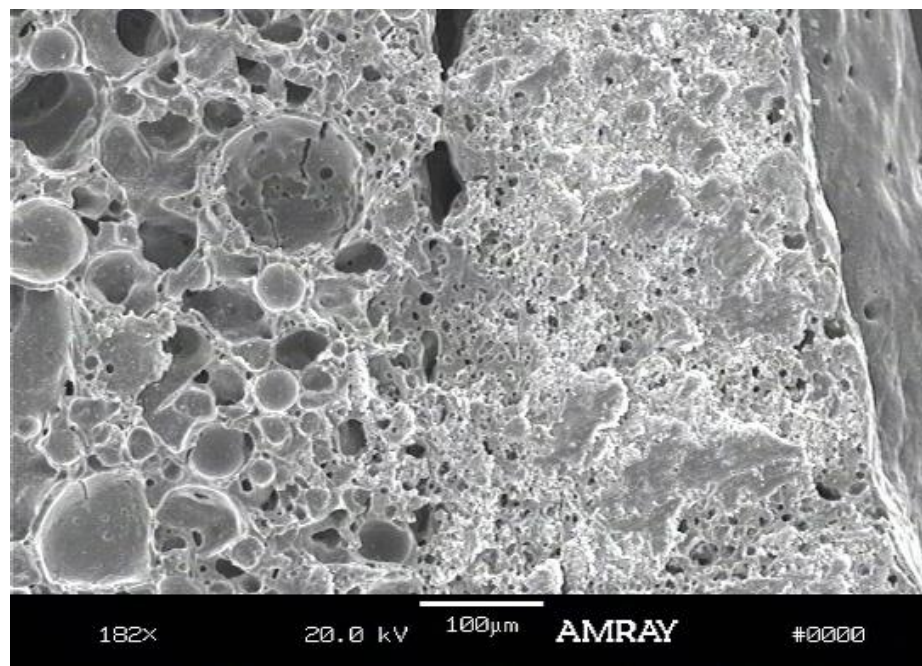
Figure 60: Voids caused by high temperature in contact zone 40cured25-2TN

6.5 Age influence on material microstructure

On certain SEM scans, a slight difference in microstructure was noticed between younger and older samples: with younger samples the process of geopolymerization was evidently incomplete, since we could observe developing crystal formations in the sample structure. Those younger crystal formations were usually positioned inside one of the broken or dissolved glass spheres or in the gaps between them - Figure 61. These nano-porous structures are a residue of dissolution that happened before polycondensation began [63]. In Figure 62, we can also see the level of micro sphere dissolution in highly alkaline slurry. Age influence on the mechanical properties of samples is outside the scope of this thesis and it was not investigated.
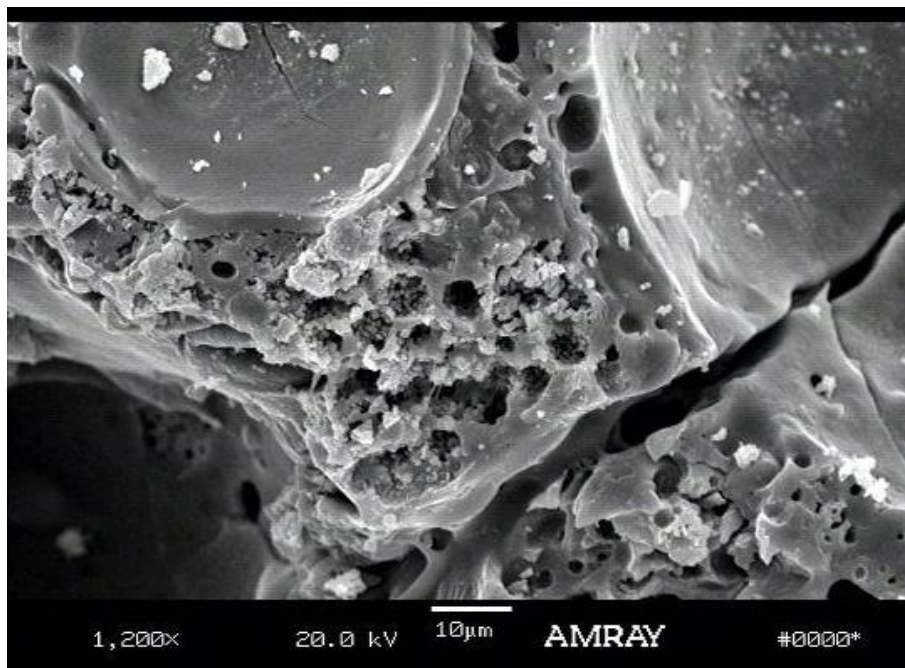
Figure 61: Micro structural residues of polycondensation
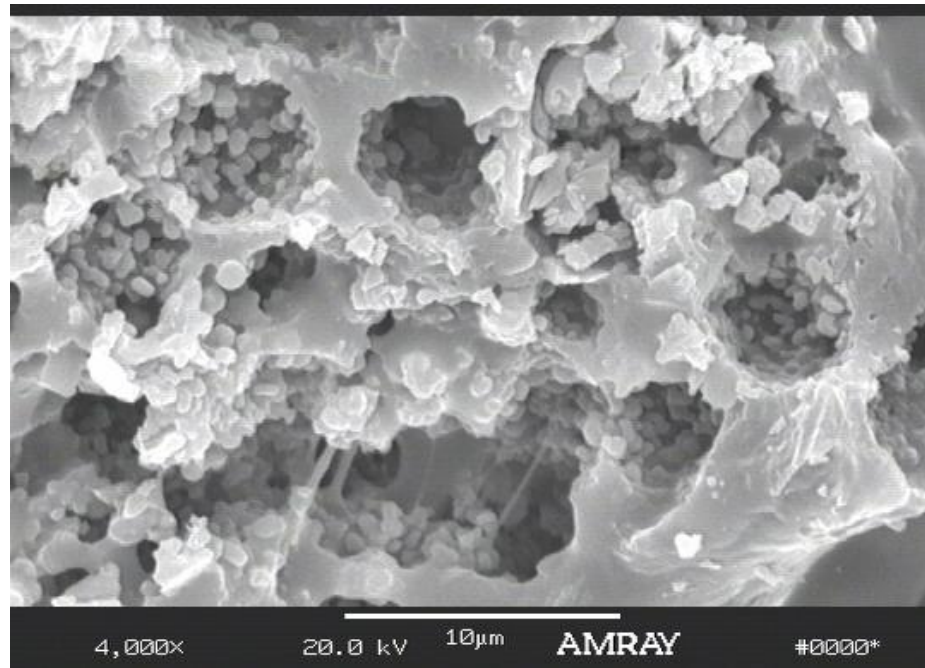
Figure 62: Detailed SEM of silica mineral structures

6.6 Crushed perlite crystals

Almost in all SEM scans it was noticed that crushed perlite crystals were scattered across the specimen area. Crushed perlite crystal is a honeycomb (lettuce) like structure with voids of approximately 10 to 50 [μm] in diameter. These structures were probably formed during material preparation (crushed during mixing) or flexural loading (perlite crystal was broken by stress). It was noticed that adhesion between the matrix and perlite crystals was excellent, but the structure was too large, so there was no mixing between the matrix, spheres or other smaller elements with this perlite crystal - Figure 63. This structure is affected by temperature to an extent equal to that of the other elements of the geopolymer core. When exposed to flame, it starts to melt and it is deformed under thermal stress from surrounding material - Figure 64. It is questionable how this crushed perlite would influence material and structural properties.
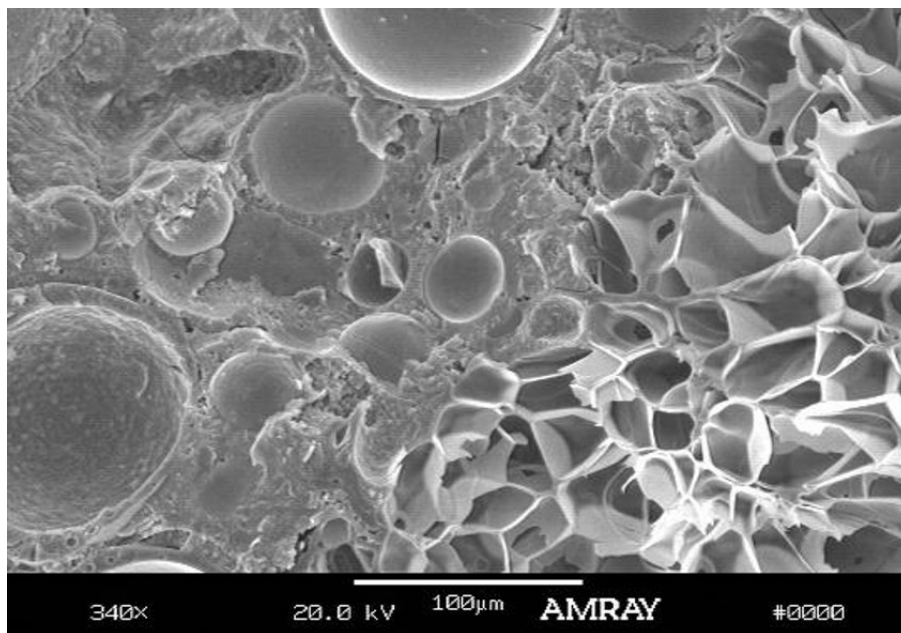
Figure 63: Crushed perlite crystal
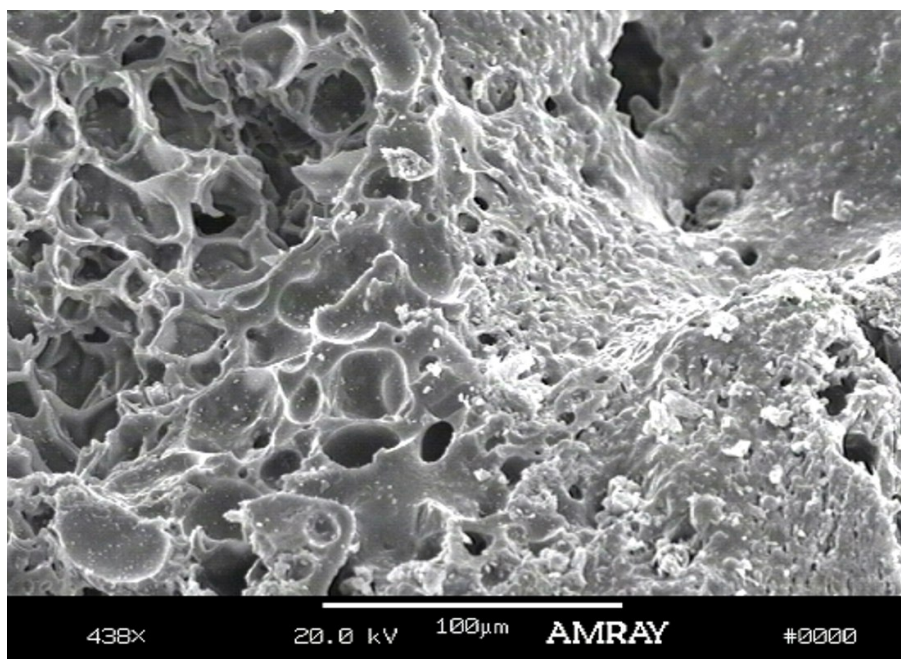
Figure 64: Crushed Perlite crystal after exposure to flame

CHAPTER 7 - CONCLUSION

From this research, several conclusions can be drawn about the mechanical properties of geopolymeric materials and structural and fire-retardant applications of geopolymer-based sandwich structures. If we look at the sandwich core, the most important thing is that matrix properties have to be analyzed and engineered properly from a chemical point of view. It was determined that preliminary properties of geopolymer material are tightly connected with its component molar ratios. Sensitive matrix properties were severely affected by minute changes in the molar ratios. It still has to be determined how exactly, components affect each other and what molar ratios would produce the best properties for desired envelope of application. Even if we know that SiO_2 (silica-silicon dioxide) has almost neutral coefficient of thermal expansion and excellent thermal shock resistance, in our case it appears that specific molar ratios of SiO_2 to Al_2O_3 (aluminum oxide) and K_2O (potassium oxide) to SiO_2 cause severe sample swelling when exposed to high temperatures. The relationship between SiO_2, K_2O, Na_2O (sodium oxide) and H_2O needs to be closely examined, but that goal is out of the scope of this research.

One more issue that is connected to the chemistry of the samples is the influence of the fly ash or other types of fillers. The chosen fillers can react with the highly alkaline geopolymer base but we also have to keep in mind that those reactions, wanted or not, can completely change the role of the filler and even the material itself. For example, instead of having density decrease and better insulation properties, we could get

a completely new material with a whole new set of properties. But fillers can be affected by chemical reactions with the geopolymer base, so they can change to a certain point etc. For example, cenospheres were chosen as active ingredient (and filler) because it was assumed that glass spheres would react and fuse with the geopolymer base and form a less dense yet strong structure. It was also expected that very rigid and dense geopolymer-potassium aluminosilicate (or polysialate-siloxo) would become less dense and more flexible but keep its mechanical and thermal properties. However, after examining the SEM scans it was obvious that the cenospheres had been dissolved in aluminosilicate resin; dissolving ratios were different and depending on level of geopolymerization, we got either a homogenous material or a sponge-like structure with partially dissolved spheres and voids. Different levels of cenosphere dissolution could have lead to different material properties. Similar things happened with perlite particles, which, due to their chemical compatibility and pozzolanic properties, adhered very well to aluminosilicate. However, stress inside the matrix was too high for the perlite crystal structure and we noticed several cracks that were progressing through the perlite particles rather than going around them or pulling them out and forming cracks between the matrix and the particle. This shows that proper selection of fillers is crucial to the properties of the final material. These specific fillers were chosen to improve applicability of the geopolymer-based matrix and if chosen properly they can do that; otherwise, they can have a negative influence on material properties.

If we analyze skin properties, we can see that both types of the reinforcing fiber showed compatibility with the geopolymeric material and that bonding between the fibers and geopolymer base was very good. The reinforcing fibers were imbedded in a thin

layer of geopolymer binder that at the same time protected them against oxidation at high temperatures or during flame exposure. No significant contact problems or effects like debonding, buckling, indentation or others were noticed during testing. Such good adhesion between the fibers and geopolymer can be explained by the chemical composition of the fibers. NEXTEL 610 fibers (Al_2O_3) were an excellent choice because they reacted with the geopolymer and produced a very strong connection. But we also have to keep in mind that the purpose of using fiber reinforcements was to improve material strength, toughness and flexibility. The goal was to avoid unpredictable brittle performance and by using adequate structural reinforcement, introduce a mechanism for stress release (like fiber pullout or matrix-to-fiber debonding). In our case, some effects of fiber pullout were noticed with both sets of fibers and material toughness was seriously increased after reinforcements were applied, but the sandwich structures still had brittle and unpredictable behavior. The used DIALEAD fibers were without any sizing, so that can explain the very good bonding between the matrix and fibers. But some small wetting problems probably increased levels of fiber motion (sliding against each other) and by that also increased material toughness.

Curing cycles and temperature-exposure seriously affected material structure and mechanical properties. The high temperature curing cycle made samples very dry and flaky and inner structure was definitely affected by changes in pore pressure and water evaporation [65]. Samples cured on higher temperatures in some cases experienced an increase in flexural toughness; they could sustain higher deflections before failing. In general, samples from the "cured" group generated lower flexural forces.

When we look at the sandwich structure in general and have in mind that this sandwich structures was built to test the possibility of structural applications at high temperature (flame) conditions, we can conclude that the core material (with these chemical ratios) does not provide good, stable support for reinforcing fibers. It was noticed that the core expanded intensely when exposed to high temperatures and this severely affected the core itself, by development of various types of cracks; fiber reinforcements, which were affected by stress concentrations or even fiber breaking (as a result of severe local geopolymer expansion). Temperature-caused deformations developed quickly and they will have to be treated as a heat transfer problem, but the exact thermal properties of this composite geopolymer material are yet to be determined. Fibers, which have a lower (neutral) coefficient of thermal expansion, were severely stressed during high temperature cycles and they failed under stress or caused severe cracking and stress concentration in the core material. It was also noticed (though not directly measured) that the core material (geopolymer material mix) has pretty good thermal insulating properties, but on the other hand, one-sided temperature or flame exposure caused severe thermal stresses and material damage [34], [64]. Samples were tested in flexure before and after temperature exposure and after high temperature cycles; flexural toughness properties were generally decreased by 55 to 68 percent. In some cases, sandwich structures failed during high temperature treatments (they were not loaded at that time).

Having all these properties in mind, we concluded that this type of sandwich structure cannot be used as a structural carrying element. Though the material has some good flame-retardant capabilities, severe thermal effects like swelling, loss of strength,

deformation and stress concentrations, make this material unfit for structural use in high temperature or fire conditions and fire-retardant applications would probably be limited.

7.1 Recommendations for future research

1. Molar ratios of chemical elements used in geopolymer preparation have to be determined very carefully and full chemical analysis of possible interactions among active components, fillers and reinforcing fibers has to be done before sample production.

2. Special research has to be done to manufacture material that will have a neutral coefficient of thermal expansion at the desired temperature envelope. Also, the properties of reinforcing fibers have to be chosen to be chemically and thermally compatible with the core material. Problems with the material's extensive volume increase and deformation at high temperatures have to be explained and solved.

3. Detailed micro structural analysis should be performed to try to explain how the level of dissolution of spherical filler affects material strength and porosity. A theoretical model should be made to try to explain the connection of porosity level, voids shape and size to material mechanical properties.

4. By using statistical methods, make a model that will correlate and explain the chemical interaction among active elements, filler materials, porosity and material strength.

5. Analyze the possible application of reinforcing material in the form of short chopped aluminum-based fibers mixed with a geopolymer base.

6. Analyze and solve manufacturing problems like aggregating, bubbles, uneven component mixture, uneven curing etc.

REFERENCES

[1] M. R. E. Looyeh, K. Rados, P. Bettess, Thermochemical responses of sandwich panels to fire, Finite Elements in Analysis and Design 37 (2001) 913-927

[2] N. Doods, A. G. Gibson, D. Dewhurst, J. M. Davies, Fire behavior of composite laminates, Composites: Part A 31 (2000) 689-702

[3] J. M. Davies, Y. C. Wang, P. M. H. Wong, Polymer composites in fire, Composites: Part A 37 (2006) 1131-1141

[4] U. Sorathia, J. Ness, M. Blum, Fire safety of composites in US Navy, Composites: Part A 30 (1999) 707-713

[5] I. S. Wichman, Material flammability, combustion, toxicity and fire hazard in transportation, Progress in Energy and Combustion Science 29 (2003) 247–299

[6] V. Birman, G.A. Kardomateas, G.J. Simitses, R. Li, Response of a sandwich panel subject to fire or elevated temperature on one of the surfaces, Composites: Part A 37 (2006) 981–988

[7] A. Samanta, R. Looyeh, S. Jihan, J. McConnachie, Thermo-mechanical Assessment of Polymer Composites Subject to Fire, project report funded by Engineering and Physical Science Research Council (EPSRC GRANT NO. GR/N10271); The Robert Gordon University, United Kingdom (2004)

[8] J. Davidovits, Geopolymers: Inorganic Polymeric New Materials, Journal of Thermal Analysis, Vol. 37,PP, 1633-1656 (1991)

[9] J Davidovits, Synthetic mineral polymer compound of the silicoaluminates family and preparation process, Patent US 4472199, 1984

[10] Valeria F.F. Barbosa, Kenneth J.D. MacKenzie, Clelio Thaumaturgo, Synthesis and characterization of materials based on inorganic polymers of alumina and silica: sodium polysialate polymers, International Journal of Inorganic Materials 2 (2000) 309-317

[11] P. Duxon, J. L. Provis, G. C. Lukey, S. W. Mallicoat, W. M Kriven, J. S. J. van Deventer, Understanding the relationship between geopolymer composition, microstructure and mechanical properties, Colloids and Surfaces 269 (2005) 47-58

[12] H. Xu, J. S. J. van Deventer, The geopolymerisation of alumino-silicate minerals, International Journal of Mineral Processing, 59 (2000) 247-266

[13] A. Fernandez-Jimenez, Ramesh Vallepu, Tohru Terai, A. Palomo, Ko Ikeda, Synthesis and thermal behavior of different aluminosilicate gels, Journal of Non-Crystalline Solids 352 (2006) 2061–2066

[14] V. F.F. Barbosa, K. J.D. MacKenzie, Synthesis and thermal behaviour of potassium sialate geopolymers, Materials Letters 57 (2003) 1477-1482

[15] W.K.W. Lee, J.S.J. van Deventer, Structural reorganization of class F fly ash in alkaline silicate solutions, Colloids and Surfaces A: Physicochem. Eng. Aspects 211 (2002) 49-66

[16] A. Palomo, M.W. Grutzeck, M.T. Blanco, Alkali-activated fly ashes a cement for the future, Cement and Concrete Research 29 (1999) 1323–1329

[17] A. Fernandez-Jimenez, A. Palomo, M. Criado, Microstructure development of alkali-activated fly ash cement: a descriptive model, Cement and Concrete Research 35 (2005) 1204–1209

[18] T.W. Cheng, J.P. Chiu, Fire-resistant geopolymer produced by granulated blast furnace slag, Minerals Engineering 16 (2003) 205–210

[19] J. Davidovits, Geopolymers Man-Made Rock Geosynthesis and the Resulting Development of High Strength Cement, Materials Education, vol. 16 (2&3), (1994) 91-139

[20] R. Giere, L.E. Carleton, G. R. Lumpkin, Micro and nano chemistry of fly ash from a coal fired power plant, American Mineralogist, vol 88, pages 1853-1865 (2003)

[21] J.C. Swanepoel, C.A. Strydom, Utilisation of fly ash in a geopolymeric material, Applied Geochemistry 17 (2002) 1143–1148

[22] F. Blanco, P. Garcia, P. Mateos, J. Ayala, Characteristics and properties of lightweight concrete manufactured with cenospheres, Cement and Concrete Research 30 (2000) 1715-1722

[23] V. Tiwari, A. Shukla, A. Bose, Acoustic properties of cenosphere reinforced cement and asphalt concrete, Applied Acoustics 65 (2004) 263–275

[24] N. Barbare, A. Shukla, A. Bose, Uptake and loss of water in cenosphere-concrete composite material, Cement and Concrete Research 33 (2003) 1681-1686

[25] J.G.S. van Jaarsveld, J.S.J. van Deventer, G.C. Lukey, The characterization of source materials in fly ash-based geopolymers, Materials Letters 57 (2003) 1272–1280

[26] S. P McBride, A. Shukla, Processing and characterization of lightweight concrete using cenospheres, Journal of Material Science 37 (2002) 4217-4225

[27] T. Bakharev, Thermal behaviour of geopolymers prepared using class F fly ash and elevated temperature curing, Cement and Concrete Research, 2006

[28] V. F. F. Barbosa, K. J. D. MacKenzie, Thermal behaviour of inorganic geopolymers and composites derived from sodium polysialate, Materials Research Bulletin 38 (2003) 319-331

[29] T. Bakharev, Resistance of geopolymer materials to acid attack, Cement and Concrete Research 35 (2005) 658-670

[30] L. F. Vilches, C. Fernández-Pereira, J. Olivares del Valle, J. Vale, Recycling potential of coal fly ash and titanium waste as new fireproof products, Chemical Engineering Journal 95 (2003) 155–161

[31] T. Bakharev, Geopolymeric materials prepared using Class F fly ash and elevated temperature curing, Cement and Concrete research, 35 (2005) 1224-1232

[32] J.G.S. van Jaarsveld, J.S.J. van Deventer, G.C. Lukey, The effect of composition and temperature on the properties of fly ash and kaolinite-based geopolymers, Chemical Engineering Journal 89 (2002) 63–73

[33] J.W. Phair, J.D. Smith, J.S.J. VanDeventer, Characteristics of aluminosilicate hydrogels related to commercial Geopolymers, Material Letters 57 (2003) 4356-4367

[34] J. W. Giancasparo, Influence of reinforcements type on the mechanical behaviour and fire response of hybrid composites and sandwich structures, Ph.D. Disertation, Rutgers, The State University of New Jersey (2004)

[35] R. E. Lyon, P. N. Balaguru, A Foden, U. Sorathia, J. Davidovits, M Davidovics, Fire Resistant Aluminosilicate Composites, Fire and Materials, vol. 21, (1997) 67-73

[36] M. Schmucker, K. J. D. MacKenzie, Microstructure of sodium polysialate siloxo geopolymer, Ceramics International, 31 (2005) 433-437

[37] A. Fernandez-Jimenez, A. Palomo, Characterisation of fly ashes. Potential reactivity as alkaline cements, Fuel 82 (2003) 2259–2265

[38] P. K. Kolay, D. N. Singh, Phisical, chemical, mineralogical and thermal properties of cenospheres from an ash lagoon, Cement and Concrete Research 31 (2001) 539-542

[39] T. Matsunaga, J. K. Kim, S. Hardcastle, P. K. Rohatgi, Cristallinity and selected properties of fly ash particles, Material Science and Engineering, A325 (2002) 333-343

[40] SPHERE SERVICES INC. The Cenosphere Company, www.sphereservices.com

[41] T.K. Erdem, C. Meral, M. Tokyay, T.Y. Erdogan, Use of perlite as a pozzolanic addition in producing blended cements, Cement & Concrete Composites 29 (2007) 13–21

[42] R. Demirboga, R. Gul, Thermal conductivity and compressive strength of expanded perlite aggregate concrete with mineral admixtures, Energy and Buildings 35 (2003) 1155–1159

[43] R. Demirboga, R. Gul, The effects of expanded perlite aggregate, silica fume and fly ash on the thermal conductivity of lightweight concrete, Cement and Concrete Research 33 (2003) 723–727

[44] D. M. Wilson, New Temperature oxide fibers, 3M Corporation, St. Paul, MN (2002)

[45] 3M NEXTEL™ - Ceramic Textile Technical Notebook, 3M Ceramic Textiles and Composites, St. Paul, MN (2004) 98-0400-5870-7

[46] D. M Wilson, L. R Visser, High performance oxide fibers for metal and ceramic composites, Presented at Processing of Fibers and Composites Conference, Borga, Italy 05/02/2002

[47] Mitsubishi Chemical Corporation, http://www.yes-mks.co.jp/en/index.html (2005)

[48] The Japan Carbon Fiber Manufacturers Association, http://www.carbonfiber.gr.jp/english/index.html, (2005)

[49] A. Palomo, M.W. Grutzeck, M.T. Blanco, Alkali-activated fly ashes a cement for the future, Cement and Concrete Research 29 (1999) 1323–1329

[50] ASTM C 1341-00 Standard Test Method for Flexural Properties of Continuous Fiber-Reinforced Advanced Ceramic Composites, Annual Book of Standards (2001), Volume15.01, Refractories; Activated Carbon; Advanced Ceramics.

[51] A. J. Foden, Material properties and material characterization of polysialate structural composites, Ph. D. Disertation, Rutgers, The State University of New Jersey (1999)

[52] S.R. Kalidindi, A. Abusafie, E. El-Danaf, Accurate characterization of machine compliance for simple compression testing, Experimental Mechanics, Vol. 37, No. 2, June 1997

[53] M. Lin, C. X. Qian, W. Sei, Mechanical properties of high strength concrete after fire, Cement and Concrete Research 34 (2004) 1001-1005

[54] R. A Fletcher, K. J. D. MacKenzie, C. L. Nicholson, S. Shamada, The composition range of aluminosilicate geopolymers, Jurnal of the European Ceramics Society 25 (2005) 1471-1477

[55] A. Mladenovic, J.S. Suput, V. Ducman, A.S. Skapin, Alkali–silica reactivity of some frequently used lightweight aggregates, Cement and Concrete Research 34 (2004) 1809–1816

[56] S. F. U. Ahmed, M. Maalej, P. Paramasivam, Flexural response of hybride steel-polyethylene fiber reinforced cement composites containing high volume fly ash, Construction and Building Materials 21 (2007) 1088-1097

[57] V. Bindiganavile, N. Banthia, Fiber reinforced dry-mix shotcrete with metacaolin, Cement and Concrete Composites 23 (2001) 503-514

[58] ASTM C 393-00 Standard Test Method for Flexural Properties of Sandwich Constructions, Annual Book of Standards (2002), Volume 15.03, Standards Relating to Space Simulation; Aerospace and Aircraft Composite Materials

[59] L.H. Yu, H. Ou, L.L. Lee, Investigation on pozzolanic effect of perlite powder in concrete, Cement and Concrete Research 33 (2003) 73–76

[60] A. Fernandez-Jimenez, A. Palomo, Composition and microstructure of alkali activated fly ash binder: Effect of the activator, Cement and Concrete Research 35 (2005) 1984 – 1992

[61] P. Duxon, J. L. Provis, G. C. Lukey, S. W. Mallicoat, W. M Kriven, J. S. J. van Deventer, Understanding the relationship between geopolymer composition, microstructure and mechanical properties, Colloids and Surfaces 269 (2005) 47-58

[62] B. Zhang, N. Bicanic, C. J. Pearce, D. V. Phillips, Relationship between brittleness and moisture loss of concrete exposed to high temperatures, Cement and Concrete Research 32 (2002) 363–371

[63] J. P. Hos, P. G. McCormick, L. T. Byrne, Investigation of a synthetic aluminosilicate inorganic polymer, Journal of Materials Science 37 (2002) 2311-2316

[64] C. G. Papakonstantinou, High temperature sandwich panels, Ph.D. Disertation, Rutgers, The State University of New Jersey (2003)

[65] N. Barbare, A. Shukla, A. Bose, Uptake and loss of water in cenosphere-concrete composite material, Cement and Concrete Research 33 (2003) 1681-1686